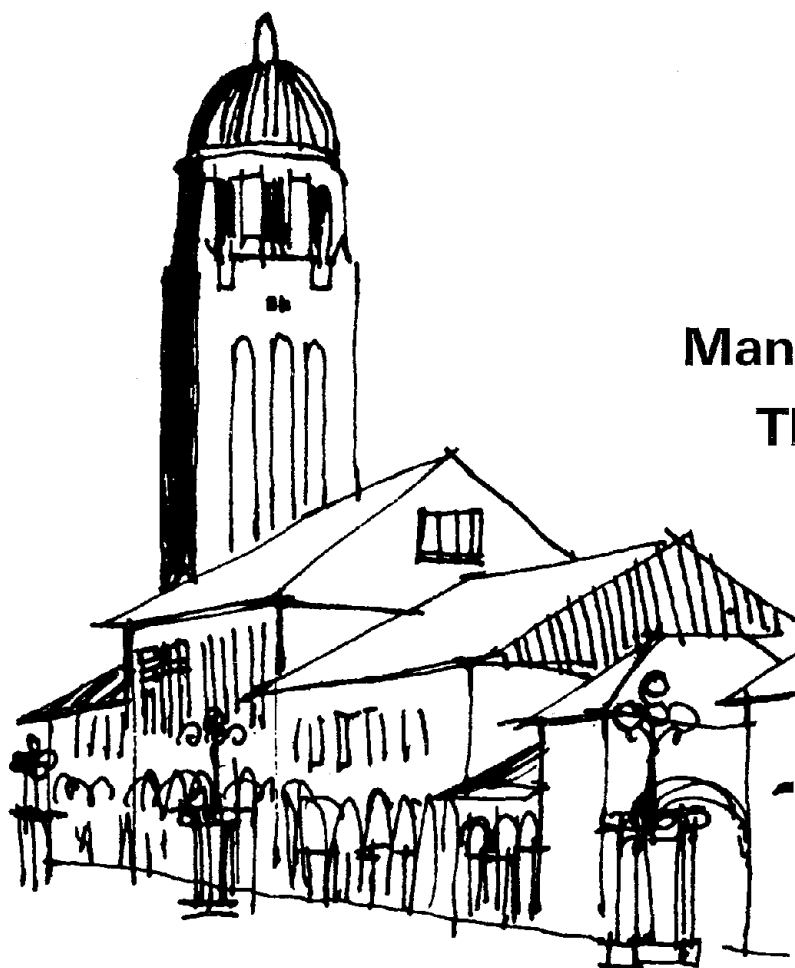


PB 297571

The John A. Blume Earthquake Engineering Center

Department of Civil Engineering
Stanford University

**SEISMIC RISK ANALYSIS FOR
CALIFORNIA STATE WATER PROJECT
Reach C**



by

Haresh C. Shah

Manoutchehr Movassate

Theodore C. Zsutty

This research was partially
supported by the Department of
Water Resources, State of California
Grant DWR B-51478 and by the
National Science Foundation
Grant GI-39122

Report No. 22
March 1976



REPORT DOCUMENTATION PAGE	1. REPORT NO. NSF/RA-761693	2.	3. Recipient's Accession No. PB297571
4. Title and Subtitle Seismic Risk Analysis for California State Water Project, Reach C		5. Report Date March 1976	
7. Author(s) H.C. Shah, M. Movassate, T.C. Zsutty		6.	
9. Performing Organization Name and Address Stanford University The John A. Blume Earthquake Engineering Center Department of Civil Engineering Stanford, California 94305		8. Performing Organization Rept. No. 22	
12. Sponsoring Organization Name and Address Engineering and Applied Science (EAS) National Science Foundation 1800 G Street, N.W. Washington, D.C. 20550		10. Project/Task/Work Unit No.	
15. Supplementary Notes Partially supported by the Department of Water Resources, State of California, Grant DWR B-51478		11. Contract(C) or Grant(G) No. (C) (G) GI39122	
16. Abstract (Limit: 200 words) A seismic hazard map for the region described as "Reach C" for the California Water Project is developed in this report. "Reach C" for this work is defined as that portion of the California Water Project from Tehachapi Afterbay up to and including the Perris Dam and Lake. The key facilities within this reach include: (1) Tehachapi Afterbay, (2) Cottonwood Power Plant Site, (3) Pearblossom Pumping Plant, (4) Mojave Siphon, (5) Silverwood Dam and Lake, (6) San Bernardino Tunnel, (7) Devil Canyon Power Plant, (8) Santa Ana Valley Pipeline, (9) Perris Dam and Lake, and (10) Perris O & M Subcenter. The report discusses the data base, the seismic sources considered and the resulting iso-acceleration maps. Relative "risks" of various sites and their implications are presented.		13. Type of Report & Period Covered	
17. Document Analysis a. Descriptors Hazards Earthquakes b. Identifiers/Open-Ended Terms Earthquake engineering Seismic hazard map California Water Project c. COSATI Field/Group		California Earthquake resistant structures Dynamic structural analysis	
18. Availability Statement NTIS	19. Security Class (This Report)	21. No. of Pages 119	
	20. Security Class (This Page)	22. Price PCAO6/ACI	

CAPITAL SYSTEMS GROUP, INC.
6110 EXECUTIVE BOULEVARD
SUITE 250
ROCKVILLE, MARYLAND 20852

SEISMIC RISK ANALYSIS FOR
CALIFORNIA STATE WATER PROJECT

Reach C

by

Haresh C. Shah

Manoutchehr Movassate

Theodore C. Zsutty

The John A. Blume Earthquake Engineering Center
Department of Civil Engineering
Stanford University
Stanford, California

Any opinions, findings, conclusions
or recommendations expressed in this
publication are those of the author(s)
and do not necessarily reflect the views
of the National Science Foundation.

This research was partially supported by the Department
of Water Resources, State of California, Grant DWR B-51478,
and by the National Science Foundation Grant GI 39122.



ACKNOWLEDGMENTS

We wish to acknowledge the help given by Mr. Robert B. Jansen, Mr. Clifford J. Cortright and Mr. Arnold E. Eskel of the Department of Water Resources, State of California. The help of Mr. David Hoexter, Mr. C. P. Mortgat, Ms. Anne S. Kiremidjian, John O. Dizon, and Professor Helmut Krawinkler of Stanford University was invaluable.

The support provided by the Department of Water Resources under grant DWR B 51478, and the National Science Foundation under grant GI 39122 is gratefully acknowledged. The help of Ms. Nancy Weaver and Ms. Janice Bailey in typing this report is very much appreciated.



Abstract

A seismic hazard map for the region described as "Reach C" for the California Water Project is developed in this report. "Reach C" for this work is defined as that portion of the California Water Project from Tehachapi Afterbay up to and including the Perris Dam and Lake. The key facilities within this reach include,

1. Tehachapi Afterbay
2. Cottonwood Power Plant Site
3. Pearblossom Pumping Plant
4. Mojave Siphon
5. Silverwood Dam and Lake
6. San Bernardino Tunnel
7. Devil Canyon Power Plant
8. Santa Ana Valley Pipeline
9. Perris Dam and Lake
10. Perris O & M Subcenter

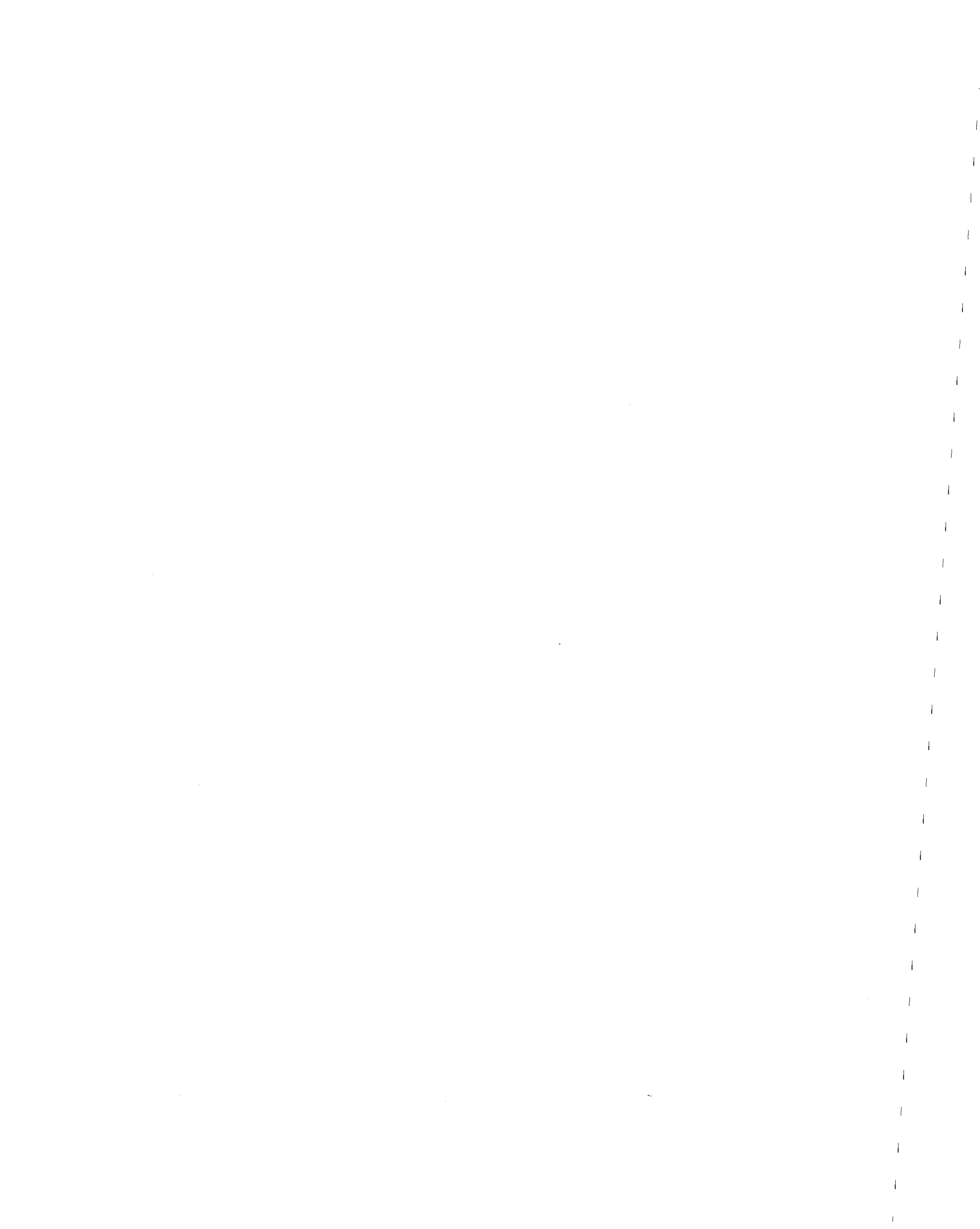
The report discusses the data base, the seismic sources considered and the resulting iso-acceleration maps. Relative "risks" of various sites and their implications are presented.

TABLE OF CONTENTS

	page
ACKNOWLEDGMENTS	ii
ABSTRACT	iii
Chapter 1. INTRODUCTION	1
Chapter 2. GEOLOGIC SETTING	4
Fault Crossing Evaluation	4
Seismic Evaluation	5
Pearblossom Pumping Plant	14
Cedar Springs Dam & Silverwood Lake	18
Devil Canyon Power Plant	21
Santa Ana Pipeline	26
Perris Dam & Lake Perris	29
Landslides and Rockfalls	32
Subsidence	32
Chapter 3. SEISMIC DATA AND SOURCE MODELING	33
Seismic Sources	33
Recurrence Relationships	35
Some Observations	45
Chapter 4. SEISMIC HAZARD MAPS FOR REACH C	46
Attenuation Relationships	46
Seismic Hazard Maps for Reach C	50
Acceleration Zone Graphs (AZG)	65
Chapter 5. DISCUSSION OF SEISMIC RISK FOR REACH C	93
Chapter 6. SUMMARY, CONCLUSIONS AND RECOMMENDATIONS	102
CHARTS	



Portion of Reach C commencing approximately
18 miles upstream from Pearblossom Pumping
Plant looking south.





Aerial view of a portion of Reach C
looking south at the south portal of
Devil Canyon Power Plant and San
Bernardino Tunnel

Chapter 1

INTRODUCTION

In earthquake engineering literature, there is, in general, ambiguity regarding two words. They are: hazard and risk. Seismic hazard is regarded by many to be synonymous with seismic risk. There is some danger in this ambiguity since these two words for seismic phenomenon have different meanings. In this work, these two words are defined as follows:

Seismic hazard is defined as "the expected occurrence of a future adverse seismic event".

Seismic risk is defined as "the expected consequences of a future seismic event". Consequences may be life loss, economic loss, function loss, and/or damages.

Expected hazard and expected risk have an implication of future uncertainty. Hence, it is not surprising that principles of probabilistic forecasting and decision making are essential in any seismic hazard or seismic risk analysis.

The objective of this study is to develop a seismic hazard map for the region in which the California State Water Project, Reach C, is located. Such a map can represent the future probable seismic loadings at various sites. Together with the knowledge about the design levels of various facilities, the information on future risks can be developed by using such a seismic hazard map.

Since the State Water Project (SWP) is essentially a series system, the reliable performance of the system depends upon the reliability of the individual components. The reliability or risk level of each component must therefore be investigated and compared with the other components in order to determine if there are any weak links in the chain. Once a weak link is identified, several alternatives may be available to bring that component into a similar risk category with the total system.

The Poisson Probability Distribution model is employed in this study for the development of forecasts of future seismic events. The parameter used as a measure of the seismic hazard is peak ground acceleration. No detailed derivations and assumptions for the development of the hazard map are presented in this report since this subject has been discussed at length in previous reports (1, 2).

A brief discussion on the geologic and seismologic setting for the region is given in Chapter 2. Some detailed study of geologic reports available through the Department of Water Resources (DWR) was made.

Chapter 3 discusses the data base and the characteristics of major seismic sources. For each postulated seismic source, a recurrence relationship with a geologically consistent upper cutoff for the Richter Magnitude is presented. This information is employed to develop the mean rate of occurrence at and above various Richter Magnitudes for use in the Poisson model. Chapter 4 presents the seismic hazard maps or the iso-acceleration maps for the region under consideration. In addition to

the iso-acceleration maps, the cumulative distribution functions and the acceleration zone graphs (AZG) for the nine key sites (see Chart 1) are obtained. Several observations regarding these results are made.

In Chapter 5, discussions regarding the seismic risk for various sites are presented. Based on the information about the design levels for the pumping and power plant superstructures and the key switching yard equipment, it is shown that the seismic risk levels and the corresponding probabilities of future damage can be inferred. Chapter 6 gives some conclusions, observations, and recommendations.

As a word of caution, it should be pointed out that the hazard maps developed in this work are based mainly on historical seismological data. No detailed geological fault studies were made to arrive at the results, and the micro characteristics of each site were not included. The results represent a statistical average behavior for the given site, assuming average micro characteristics (firm site conditions). This assumption does not limit the applicability of the results since, from the geological data available through DWR reports, all the sites considered here have "firm site" characteristics. It may be concluded that, in the absence of complete geological information, the maps developed here can help engineers and planners to establish the future seismic hazards and evaluate the corresponding seismic risks. It should also be understood that the reliability of future forecasts is subject to the statistical sampling variation inherent in the limited amount of historical earthquake data.



Chapter 2

GEOLOGIC SETTING

The emphasis of this part of the study is on seismic considerations involving fault proximities and seismic activity. The main source of information was the DWR office reports, listed in references at the end of this report.

Fault Crossing Evaluation

A glance at Figure 2-1, "Geologic Fault Map", and Figure 2-2, "Fault Map of a Portion of Southern California", shows some of the many faults crossed by the California Aqueduct. Crossings are especially common from Cedar Springs Dam south to Highway 10. The Aqueduct also encounters faults near Pearblossom, and east of Riverside.

Other fault crossings occur, which are not shown on the "Fault Map of a Portion of Southern California" (see ref. 34). No attempt has been made to catalogue them. In addition, some of the faults not shown on the map to be active, could nevertheless be active ("other faults, activity not ascertained", as shown on the map). No attempt has been made to locate faults on a larger-scale map. Several DWR reports describe the Aqueduct alignment in detail and they show all fault crossings.

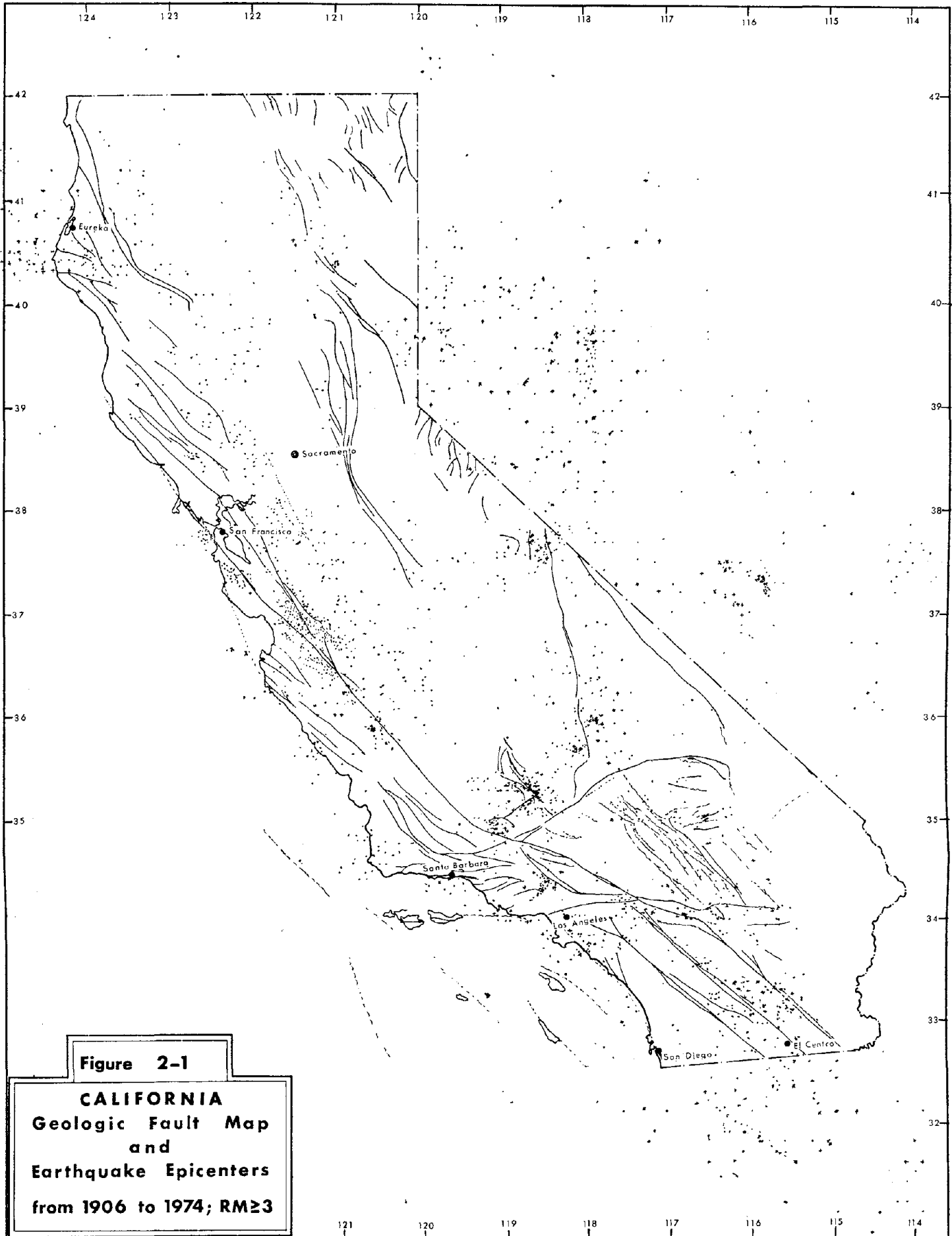
Fault crossing information is especially important on the tunnel and penstock segment of the Aqueduct, between Cedar Springs Dam and San Bernardino, due to the large gradient in this segment. At the

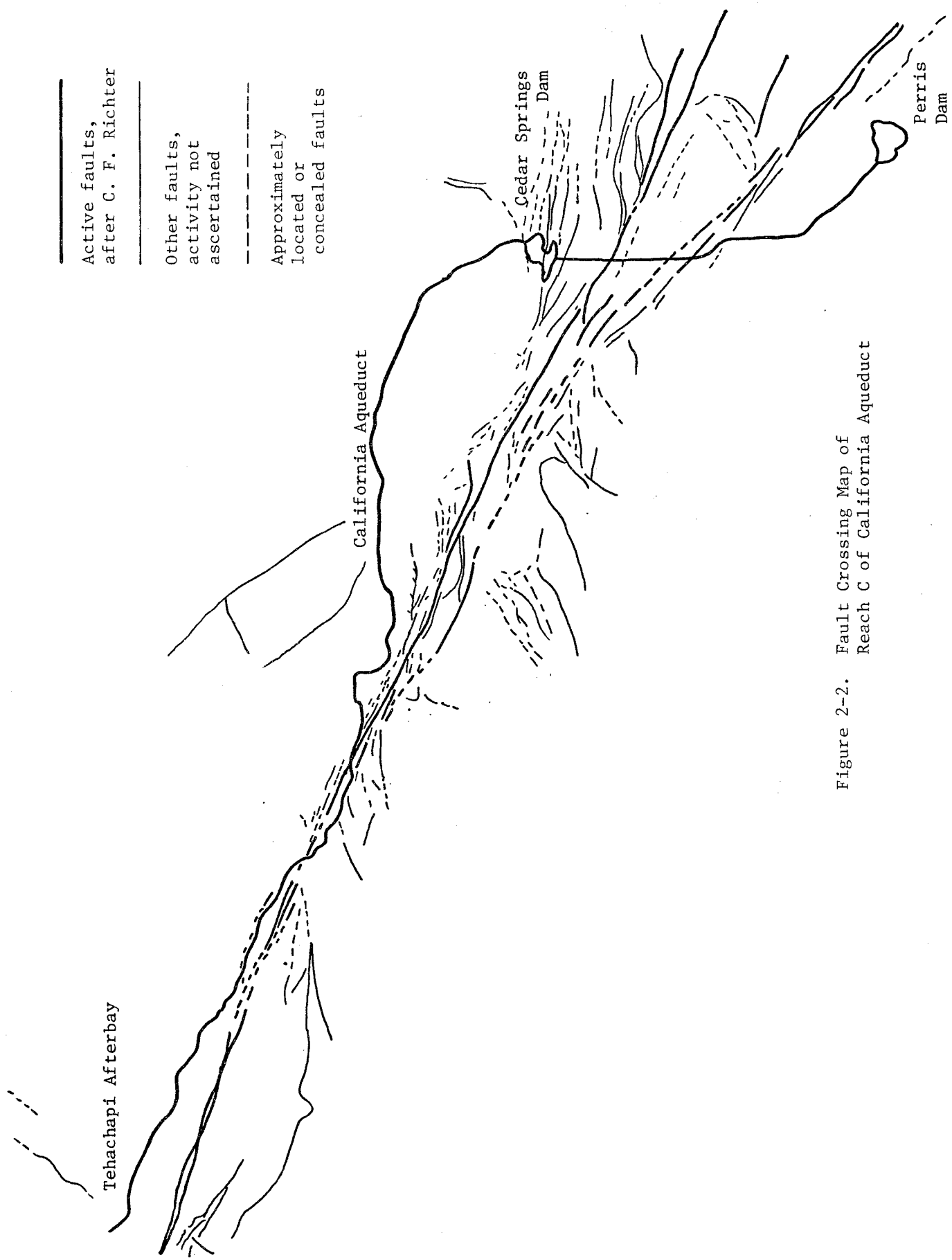
tunnel segment of the aqueduct, water flow could be impaired if rupture occurs at fault crossings. If the penstock segment (approximately 1.5 miles long) of the Aqueduct, north of Devil Canyon Power Plant, were ruptured, the consequences could be much greater. Cutoff facilities can be activated quickly in such an event by the penstock valves at the south portal of the San Bernardino Tunnel, thus averting a flash flood in Devil Canyon.

Seismic Evaluation

This is not a detailed study of the seismic setting of facilities. Such a study is beyond the scope of this report. However, the authors of this report have some thoughts on this subject which are considered to be important and which might require further consideration. Ground accelerations are emphasized.

The general geology at a site is very important in the way a structure will be affected by seismic waves. Propagation of waves will vary, depending on the transmitting material. For example, wave velocities, frequency, attenuation, and amplitude, as well as ground accelerations and velocities, are altered by ground conditions (Figure 2-3). Boore and Hill (see ref. 4) discuss differences in wave frequencies and velocities on either side of the San Andreas Fault, east of Monterey, during an earthquake. On the west side, which is composed essentially of granitic rocks, wave frequencies during the earthquake were relatively higher; Pg and Sg waves west of the fault also had higher velocities (6 and 3.5 km/sec, respectively, in comparison to 5 and 2.8 km/sec in the essentially Franciscan rocks east of the fault. Earthquake waves entering one geologic province from another, e.g.





Active faults,
after C. F. Richter

Other faults,
activity not
ascertained

Approximately
located or
concealed faults

Tehachapi Afterbay

California Aqueduct

Cedar Springs
Dam

Perris
Dam

Figure 2-2. Fault Crossing Map of Reach C of California Aqueduct

PGA. The duration employed is the time between the first and last peaks of acceleration which are at least equal to 0.05 g.

Ground motion values, as shown in Figure 2-4 correspond to average geologic site conditions, and are not the maximum possible. Schnabel and Seed also show PGA (Figure 2-5).

Data from the Parkfield Earthquake of June 28, 1966, show little attenuation of peak horizontal acceleration within about 6.2 miles of the San Andreas Fault (Figure 2-6). Regular variation of acceleration and duration with distance suggest that the Parkfield data is free from anomalous local amplification of ground motion. Maximum accelerations within 7 miles of the San Andreas Fault can probably be expected at Pearblossom and Devil Canyon, as well.

Near-Fault Horizontal Ground Motion

Magnitude	Acceleration (g) Peak absolute values				Velocity (cm/sec) Peak absolute values			Displacement (cm)	Duration ¹ (sec)
	1st	2d	5th	10th	1st	2d	3d		
8.5	1.25	1.15	1.00	0.75	150	130	110	100	90
8.0	1.20	1.10	0.95	0.70	145	125	105	85	60
7.5	1.15	1.00	0.85	0.65	135	115	100	70	40
7.0	1.05	0.90	0.75	0.55	120	100	85	55	25
6.5	0.90	0.75	0.60	0.45	100	80	70	40	17
5.5	0.45	0.30	0.20	0.15	50	40	30	15	10

¹Time interval between first and last peaks of absolute acceleration equal to or greater than 0.05 g.

Notes—1. Italic values are based on instrumental data.

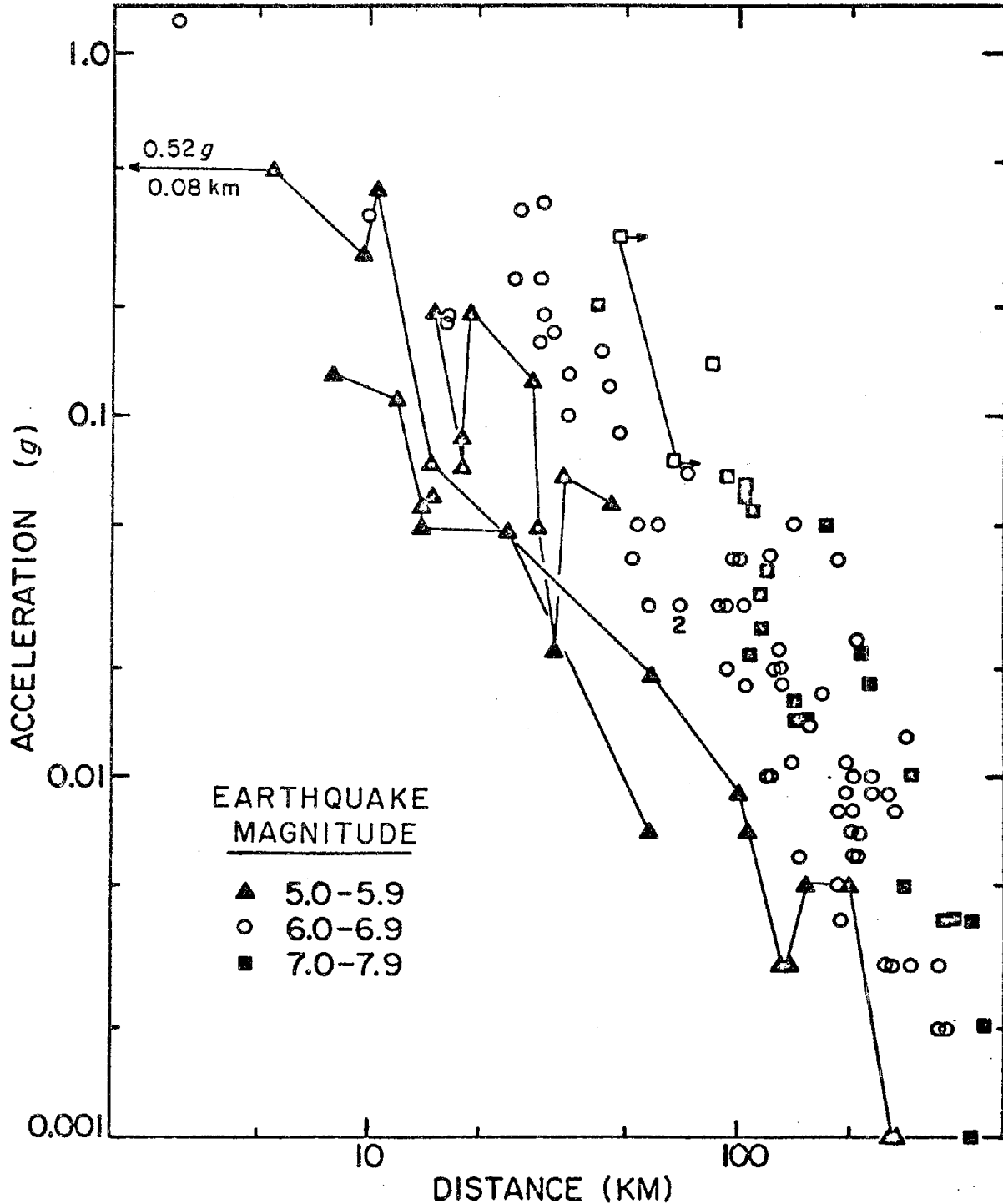
2. The values in this table are for a single horizontal component of motion at a distance of a few (3-5) km of the causative fault; are for sites at which ground motion is not strongly altered by extreme contrasts in the elastic properties within the local geologic section or by the presence of structures; and contain no factor relating to the nature or importance of the structure being designed.

3. The values of acceleration may be exceeded if there is appreciable high-frequency (higher than 8 Hz) energy.

4. The values of displacement are for dynamic ground displacements from which spectral components with periods greater than 10 to 15 seconds are removed.

Table 2-1

(Taken from ref. 18)



—Peak horizontal acceleration versus distance to slipped fault as a function of magnitude. Except for 1949 Puget Sound shock (open squares), data shown are those for which distances to fault are most accurately known (tabulated in Appendix C). Straight-line segments connect observations at different stations for an individual earthquake, for three magnitude 5 shocks and one magnitude 7 shock. From top to bottom, suites of magnitude 5 data are from 1970 Lytle Creek ($m = 5.4$), Parkfield ($m = 5.5$), and 1957 Daly City ($m = 5.3$) shocks. Closest Parkfield data point lies off plot to left at 0.08 km. For magnitude 6, most data within 100 km are from 1971 San Fernando earthquake ($m = 6.6$), and most data beyond 100 km are from 1968 Borrego Mountain earthquake ($m = 6.5$). Most magnitude 7 data are from 1952 Kern County shock ($m = 7.7$). Open squares are values from 1949 Puget Sound event ($m = 7.1$), for which distances are determined to hypocenter assuming minimum focal depth of 45 km. Arrows denote minimum values.

Figure 2-4

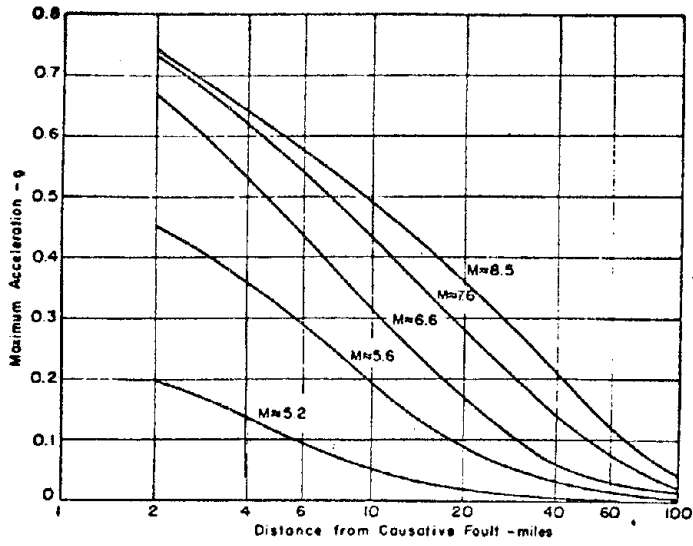


FIG. 5. Average values of maximum accelerations in rock.

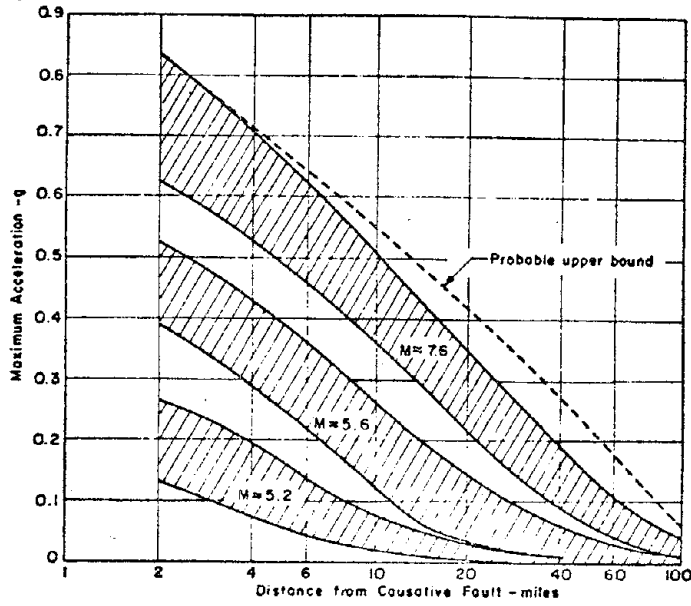
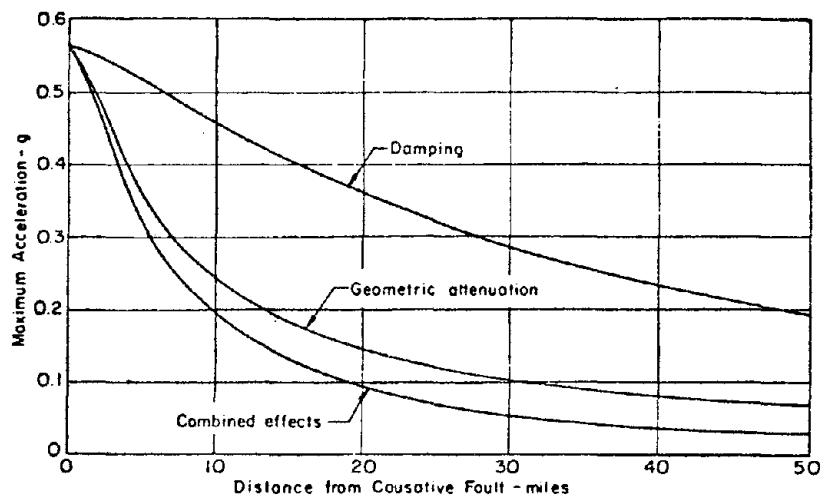


FIG. 6. Ranges of maximum accelerations in rock.

Figure 2-5
(Taken from ref. 21)



Computed effects of geometric attenuation and damping on maximum accelerations in Parkfield earthquake of 1966.

Figure 2-6
(Taken from ref. 21)

Each of the major facilities under study would be affected differently by the same earthquake, even if their epicentral distances were the same.

Cedar Springs Dam is excavated to crystalline bedrock. It overlies potentially active faults. It is subject to reverse faulting from nearby faults, and thus, to high accelerations.

Perris Dam lies athwart a relatively shallow, partially saturated alluvial deposit. The outlet tower, of particular concern to this study, is founded on crystalline bedrock. There are no immediately adjacent faults, but one of California's most active faults, perhaps the most active, the San Jacinto Fault (zone), is located approximately 16 miles away.

Devil Canyon Powerplant is also situated on crystalline bedrock, within 1000 feet of the active San Andreas Fault, and within 300 feet of the possibly active Santa Ana Fault.

The Pearblossom Pumping Plant, 2 1/2 miles north of the San Andreas Fault, is sited in an excavation dug to crystalline bedrock. The alluvium is relatively thin, and not saturated.

In the remaining portion of this chapter, a summary look at various sites, from geological and seismological point of view is presented. In particular, important sites, including and south of Pearblossom Pumping plant are included. However, it should be noted that no detailed geologic study of the Tehachapi Afterbay was available. In development

of the seismic hazard maps for the Reach C, the information presented below was implicitly included.

A. Pearblossom Pumping Plant

Introduction

The Pearblossom Pumping Plant is located 3/4 miles northwest of Pearblossom, near the southwestern edge of the Mojave Desert (see Chart 1). Water is lifted through a static head of 540 feet from the plant, then flows by gravity to Silverwood Lake. The plant site was excavated to a maximum depth of 88 ft. below a gently sloping alluvial surface.

The bulk of the material in this section is from reference 11 "Final Geologic Report of Pearblossom Pumping Plant Site Development", Project Geology Report C-30, DWR, November, 1967.

Regional Geologic Setting

The western Mojave Desert, bounded on the northwest by the Garlock Fault, and on the southwest, by the San Andreas Fault and the San Bernardino Mountains, is a relatively flat plain, with numerous isolated hills, ridges, and local mountain masses. The extreme western part of the Mojave is underlain by thicknesses of alluvium possibly as great as 2000 feet. The Tehachapi Range, to the northwest, and the San Gabriel and San Bernardino Mountains, to the southwest and the south, are composed of crystalline basement rocks, chiefly plutonic rocks, and locally, sedimentary rocks.

Geology of the Pumping Plant Site

The pumping plant is located 2 1/2 miles north of the San Andreas Fault. As discussed earlier in this report, the San Andreas Fault is a major, active fault, capable of producing a high-magnitude earthquake with surface rupture within the lifetime of the Pearblossom facility.

The bedrock material is granitic, predominantly quartz monzonite. The bedrock surface, as exposed by excavations, slopes northeast at from 27 to 85 feet below the original ground surface. It is locally highly weathered.

The bedrock has three significant features. It is cut by hydrothermal alteration zones of up to 200 feet in width. Joints occur, at spacings of from one inch to several feet. Inactive faults, especially in the bedrock, are distinguished by clay gouge zones of from less than one inch to several inches in width. Because of the numerous faults, a complex block pattern has been formed. The alteration zones, joints, and faults have created blocks of varying bearing capacity.

The bedrock is overlain by "Older Alluvium", which averages 10 feet in thickness. This alluvium is a dense, cohesive arkosic sandstone, with a slightly impervious silt and clay binder, and minor gravel.

"Recent Alluvium" at the site occurs to an average depth of 45 feet. It consists of loose, clean, well-to-poorly graded gravelly silty sands (SW, SP), interbedded with compact, gravelly-silty sand

(SM), with a maximum of 40% silt. Gravel comprises 5-25% of the alluvium, and is rarely greater than 3 inches in diameter.

Groundwater occurs at 107 feet below the ground, 25 feet below the pumping plant bowl area. The occurrence of water is essentially in fractures.

Seismic Setting

The western Mojave Desert is a seismically active region. An earthquake occurring on July 11, 1967, with its epicenter near Littlerock Dam, less than 5 miles from the plant, registered a Richter Magnitude of 3.5. No damage occurred, nor did tiltmeters or strong-motion seismographs in the area register the disturbance. Another earthquake, on February 27, 1969, with its epicenter near Palmdale Reservoir, 13 miles distant, occurred at a depth of approximately 3 miles, and had a magnitude of 4.6. Strong motion instruments at Pearblossom did not record this event, either.

The April 9, 1968 Borrego Mountain earthquake, its epicenter 140 miles distant, triggered a strong-motion seismograph at the pumping plant site. However, ground motion was insufficient to produce a meaningful record for design ("Engineering Geology of Pearblossom Pumping Plant Discharge Line", Office Report, DWR, August, 1969). Page, et al, (see ref. 18), show a Pearblossom recording of .006 g at 126 miles from this quake. From the San Fernando Earthquake of February 9, 1971, PGA's of .13 and .15 were recorded at Palmdale and Pearblossom, respectively, 22 and 27 miles from the epicenter.

Between 1934 and 1969, two earthquakes with magnitudes greater than 4.0 have occurred within 20 miles of Pearblossom. Six quakes of magnitude 3.0-3.5 have occurred within 10 miles.

The most recent surface rupture of the San Andreas Fault in the Mojave region was on January 9, 1857, as discussed in the Devil Canyon section of this report. No movement of the fault, monitored by geodimeter lines and precise quadrilateral surveying, has occurred near Pearblossom since 1964. This would suggest that this portion of the fault is "locked", i.e. stress build-up is not being relieved by creep. Many geologists believe that this would indicate that an earthquake should be expected as the stresses build up to such a level that the fault ruptures.

Conclusions

The Pearblossom Pumping Plant is situated on slightly-to-highly weathered granitic bedrock. Fault gouge zones, joints, and hydrothermal alteration zones divide the bedrock into blocks of varying size and bearing capacity. Groundwater occurs within the bedrock, 25 feet below the pumping plant bowl area.

The seismicity is high. Numerous minor and one major earthquake have occurred since 1856. This activity can be expected to continue in the future. The plant is sufficiently set back from the San Andreas Fault to preclude ground rupture at the site.

Not discussed in this section is the plant discharge line. One important point should be made. The line crosses several faults which are related to the San Andreas Fault. At least one of these faults displaces Older Alluvium.

B. Cedar Springs Dam and Silverwood Lake

Introduction

Cedar Springs Dam is located 13 miles north of San Bernardino, in the San Bernardino Mountains (see Chart 1). The dam is 2230 feet long at its crest, and lies 249 feet above the streambed. Silverwood Lake, impounded by Cedar Springs Dam, holds 74,970 acre-feet of water at a maximum elevation of 3355 feet above sea level.

The information in this section has been compiled from "Engineering Geology of Cedar Springs Dam and Reservoir", Office Report, DWR, July, 1968 and contact through DWR personnel.

Regional Geologic Setting

The San Bernardino Mountains, 55 X 30 miles in area trending east-west, are composed mainly of Mesozoic age (270-70 million years) gneissic and granitic rocks, with some pre-Cambrian (?) gneiss in the southwest part of the range. Tertiary and Quaternary age (70 million years to the present) continental sediments occupy structural troughs and valley floors within the range.

Among the sedimentary formations is the Harold formation, of Plio-Pleistocene age (less than 10 million years). The Harold formation is an indistinctly bedded to massive poorly indurated (consolidated) white to buff arkosic sandstone, containing one-inch to one-foot clay and silt lenses and some clean white sand.

The San Andreas Fault, seven miles south of Cedar Springs Dam, dominates the structure of the area. Trending N 70° W, it forms the southern border of the San Bernardino Mountains. Several high angle, normal and reverse faults, form a horst-graben structure (alternating ranges and valleys), and trend sub-parallel to, and merging west of the dam, with the San Andreas Fault.

Geology of Silverwood Lake

The reservoir is situated in three east-west trending valleys, each controlled by high-angle faults, including the Cleghorn Fault, two miles south of Cedar Springs Dam. The structure is fault-block, with the block on the north side upthrown. Recent movement is an apparent reversal of historical movement, with the Harold formation on the south displaced upwards with respect to the northern (granitic) block.

There is no major landslide hazard. A seiche could be generated from an earthquake along any of the faults in the region, but its period would be long, and much of the wave energy would be quickly dissipated in side canyons.

Geology of the Cedar Springs Dam Site

The major features of the damsite geology are several faults which must be considered active. Also of importance is the nature and thickness of the sediments and bedrock at the dam site.

The average thickness of Quaternary alluvium at the dam site is 30 feet, with a maximum of 50 feet at the base of both of the dam

abutments. The alluvium is a sandy gravel to gravelly sand, with less than 5% non-plastic fines. The Harold formation, exposed at the northeast abutment and the upstream channel, is a silty sand (see previous, more detailed description). The dam site is excavated to bedrock, which is deeply weathered granitic material, especially where cut by faults.

Several related steeply-dipping faults pass through the dam site. There is a general line of faulting along the Harold formation-granitic contact, with the vertical offset totaling more than 1000 feet. The several small faults at the dam site are part of this system. Two of these small faults show up to 5 ft. of apparent vertical offset in Quaternary sediments, considered recent (less than 10,000 years) by the DWR staff (see ref. 7). Although these faults underlie the dam, they do not underlie the dam's clay core. The faults have gouge zones 1-6 feet wide and crushed zones 10-25 feet wide, with a maximum width of 50 feet.

The spillway and inlet works also cross faults. There is no evidence of recent activity on these portions of the faults, although they are located so close to parts of the faults that do display recent movement that they must also be considered active. Both the spillway and inlet works, as well as the outlet tower, are situated on fresh, moderately fractured granite, except where they cross faults.

Seismic Setting

Between 1934 and 1962, 16 earthquakes with a Richter magnitude greater than 4 occurred with epicenters within 20 miles of Cedar Springs

Dam. The dam is designed to withstand a maximum of 50% g acceleration, and to accommodate 3 feet of lateral or vertical displacement on the Harold-granitic rock fault contact. According to the DWR, creep movement along the faults will not occur.

Based on the data available, it is not possible to state whether the 3 feet displacement designed for is adequate. It is probable that release of major strains accumulated in the area will occur on the San Andreas or San Jacinto Faults, but small local strain build-ups, or reaction to strain release on the major faults, could cause earthquakes on the smaller faults at the dam site.

Conclusions

Bedrock material at the Crystal Springs Dam site is sufficiently competent. Alluvium and weathered granitic rock has been excavated to relatively unweathered granitic rock.

Faults at the dam site are active. The site could be affected by major, distant, and by major and minor local earthquakes, including actual ground rupture.

Introduction

The Devil Canyon Power Plant is located approximately 6 1/2 miles north of San Bernardino, on the southwest edge of the San Bernardino Mountains (see Chart 1). The power plant is located approximately 6750 feet downstream of the outlet of the San Bernardino Tunnel and Penstock, which supplies water by gravity from Silverwood Lake.

The power plant complex is composed of the power plant itself and the afterbay, which is located immediately south of the plant and supplies water to the Santa Ana Pipeline.

The information in this section has been compiled from reference 15 "Geologic Data, Devil Canyon Power Plant", Project Geology Report D-108, DWR, April, 1969, and reference 14, "Geologic Data, Devil Canyon Power Plant Penstock", Project Geology Report D-118, DWR, January, 1970.

Regional Geologic Setting

The basement complex of the San Bernardino Mountains is composed of igneous and metamorphic rocks, essentially Mesozoic age (270-70 million years) granitic and gneissic rocks (see discussion of the regional geologic setting in the Cedar Springs section of this report). Immediately to the southwest of the site is the Santa Ana Valley, down-dropped along several major faults, including the San Andreas and San Jacinto Faults.

Geology of the Power Plant Site

The power plant is located at the bottom of Devil Canyon, and is approximately 800 feet wide at this point. Devil Canyon empties in a large alluvial fan into the major east-west trending Santa Ana Valley. The valley is bordered by the San Andreas and Santa Ana Faults on the north, directly adjacent to the power plant. The Santa Ana Fault, branching from the San Andreas Fault northwest of the power plant, is a zone of faulting at least 300 feet wide which cuts directly across the afterbay site.

The San Andreas Fault is active; that is, it is capable of movement within the lifetime of the power plant. The Santa Ana Fault, a branch of the San Andreas fault, has much less chance of movement, but still should be considered active. The most recent surface rupture in the immediate area occurred along the San Andreas Fault on January 9, 1857, with surface rupture occurring to some point east of San Bernardino, possibly to Whitewater, Riverside County, on the southeast, and extending past Fort Tejon as far as Cholame, San Luis Obispo County, to the northwest.

The Santa Ana Fault does not displace recent alluvium; thus, movement is older than the deposition age of the alluvium. It appears from the trench logs that the older alluvium is also not displaced. If this is the case, an age date from the older alluvium could help determine the last date of movement of the fault.

The question of extreme importance is whether faulting at some future date could affect the power plant facilities. There is a high probability that the site will be severely shaken by nearby earthquakes. In addition, surface rupture on the San Andreas Fault, and possibly the Santa Ana Fault, is very likely. It is more difficult to assess the possibility of surface rupture at the plant itself, however.

The DWR places a major trace of the Santa Ana fault 120 feet south of the inferred northern trace of the fault, which, in turn, is 125 feet from the power plant. The combined set-back of 245 feet should be sufficient if rupture occurs along the fault in the future, but this depends on an accurate location of the fault trace. A potential

problem with this location could be the presence of several gouge zones in one of the trenches under the power plant. Whether these are related to the Santa Ana Fault, or to some older, unrelated activity, is impossible to state. As the major movement on the fault has probably been in the zone 245 feet from the power plant, the setback should be adequate, as any future movement can be expected to occur along previous zones of weakness.

The Santa Ana fault is part of the San Andreas fault zone. It branches in a northeast direction from the San Andreas fault at Cable Canyon, 3 miles northwest of Devil Canyon. There are both surface and sub-surface indications of movement on the Santa Ana fault. A break in slope on older alluvium forming the terrace west of the plant coincides with the subsurface trace of the fault. The terrace south of the fault is uplifted relative to the north side.

A maximum of 20 feet right-lateral and 3 feet vertical displacement is deemed possible within the San Andreas fault zone. The DWR Consulting Board for Earthquake Analysis has stated, "Should such movement take place, the most likely place for it to occur would be along the most recent trace of the San Andreas fault . . . Presumably, such displacement could occur on the Santa Ana fault . . ." (see ref. 30).

Seven rock or soil units are exposed at the Devil Canyon site. The oldest is granite, which is moderately weathered, and varies from weak and friable to moderately strong. The second oldest is marble, a moderately strong crystalline limestone. Third is an undifferentiated complex of granitic and metamorphic rocks, predominantly a banded granite-gneiss, but locally containing marble, quartzite, and other rock

types. Each of these rock units is locally faulted into a fault gouge, with the properties of a clayey sand to soft clay.

Younger rocks, all Quaternary age (less than 1 million years), include "older", moderately consolidated stream deposits (gravel and sand with large boulders and minor silt), "younger", unconsolidated stream deposits, and last, slopewash deposits and recent soil (descriptions from DWR Report D-108, plate 3).

Considerable groundwater is present. Fifty gallons per minute (gpm) flowed into Trench 1 from the fault zone and younger alluvium, and 200 gpm flowed from the alluvium into Trench 2 (see ref. 15).

Seismic Setting

The Devil Canyon Power plant is located in a highly seismic region. It is probable that at least one high-magnitude earthquake will occur within the lifetime of the structure. Surface rupture at-or-near the plant site, as discussed, could occur during future earthquakes.

Conclusions

The power plant site consists of a granite and gneiss bedrock complex, overlain by stream deposits, to maximum depths of approximately 63 feet. The power plant excavation reaches bedrock. This bedrock, however, is weathered to an unknown depth, and contains soft gouge zones.

The power plant appears to be set-back sufficiently from the Santa Ana Fault to preclude damage from fault rupture. The probability of a "major" earthquake within the lifetime of the plant is high, either

along the San Andreas Fault, or along one of the other numerous faults in the area.

D. Santa Ana Pipeline

The major concern with the Santa Ana Pipeline is with several crossings of active or potentially active faults within a heavily populated area. The capacity of the pipeline is 469 cubic feet per second; the water velocity is 7.36 feet per second. Four geologic maps have been examined for this evaluation. Although of differing scales, each shows the pipeline, so locations of the faults and fault crossings may be determined with reasonable accuracy.

The first fault crossing is the Loma Linda fault, which is crossed by the pipeline at the intersection of Highland Ave. and State Street, in San Bernardino. The topography at this location is nearly flat. There are a number of occupied houses, stores, and empty lots nearby. The fault is shown on the General Plan and Profile, Santa Ana Pipeline (see ref. 27), from which the pipeline crossing location has been taken. The fault is not shown in Jennings (see ref. 28), "State of California, Preliminary Fault and Geologic Map". Rogers (see ref. 19), "Geologic Map of California, San Bernardino Sheet", shows the fault to the southeast, and another fault, the Glen Helen fault, to the northwest, with their continuations across San Bernardino questioned. If connected, these two faults appear to be the same fault as in the General Plan Profile. Finally, Hill (see ref. 4), "Earthquake Epicenter and Fault Map of California, Southern Area", shows the Loma Linda fault, and

considers it active. As Hill's map is a DWR publication it appears that the DWR considers this fault active, and its proximity to the San Jacinto fault reinforces this conclusion.

The second fault crossing is the main trace of the San Jacinto fault, at the intersection of Foothill Blvd., 4th and 5th Streets. There are some homes, shops, and industry nearby, as well as the Lytle and Cajon Creek Floodway. The exact fault crossing is based on the General Plan and Profile map (see ref. 27). The fault is shown on each of the other publications cited above. The fault is active. Jennings (see ref. 28) shows fault creep along this segment of the fault. It is reasonable to assume that any water escaping from a rupture of the pipeline would run off through the floodway.

The third fault crossing, to the southwest, also involves the San Jacinto fault. This crossing is on Colton Ave. between Crest and Harber Streets, at the Colton-San Bernardino city boundary. There is a definite change in slope at this location, which could be attributed to faulting. Spillage from a rupture on this segment of the pipeline could enter the Lytle Creek Flood Control Channel, but could also cause damage to a nearby residential area (single-family homes).

The fourth crossing is difficult to locate exactly, but could be at Washington Street, between Mt. Vernon Ave. and Barton Road, in Colton. This is the Colton-Rialto fault. There is a definite slope at this location, and a low pass through the adjacent hills that could be attributed to faulting. The General Plan and Profile map does not show this fault, but each of the other maps does, although it is unnamed in T. H. Rogers (see ref. 19). Hill (see ref. 34) does not ascertain the

recency of movement on this fault. Jennings (see ref. 28) shows the fault as being active during the Quaternary (2 million years), but not historically active. It is possible that the General Plan and Profile map does not show this fault because DWR does not consider the fault to be potentially active. Some homes, service stations, and other structures could be damaged by rupture of the pipeline, although flow is directed towards the Santa Ana River channel.

There is one additional fault crossing, located north-northeast of the intersection of Kendall Drive and College Parkway, adjacent to the California State College, San Bernardino campus. This unnamed fault is shown on the DWR General Plan and Profile, in Jennings (see ref. 28), and in Rogers, (see ref. 19). A low range of hills appears to have been uplifted along the fault. As the fault crossing is directly adjacent to a flood control channel, and only a short distance from cut-off facilities at Devil Canyon Power plant, there is probably little likelihood of flooding even if the pipeline is ruptured here.

According to available information, there is no cut-off facility on the Santa Ana Pipeline between Devil Canyon Power plant and Perris Dam. Rupture could occur at any of the 5 fault crossings, allowing flow of a large volume of water under a high head from at least any of the 4 southerly crossings. This would occur until shut-off of the pipeline at Devil Canyon, 5 to 11 miles to the north, depending on the location of the fault crossing, is accomplished and damage to residential areas could occur.

E. Perris Dam and Reservoir

Introduction

Perris Dam is located 17 miles southeast of Riverside and 4 miles northeast of Perris (see chart 1). The dam, with a crest length of 11,600 feet, impounds 131,452 acre-feet of water. Perris Reservoir is the terminus of the California Aqueduct.

The information in this section has been compiled from "Engineering Geology, Perris Dam and Lake", Office Report, DWR, August, 1970 and contact with DWR personnel.

Regional Geologic Setting

The Perris Dam and Reservoir are located on the Perris Block, located between the San Jacinto and Elsinore Fault zones. The Perris Block is composed essentially of massive Cretaceous (130-70 million years) granitic rocks, with inclusions of schist and gneiss. The block was downdropped at least 3000 feet during the Pliocene and Pleistocene (10 million to 10,000 years), and covered with sediments. Subsequently, the block has been uplifted, and most of the sediments eroded.

There is some evidence that part of the block east of the dam and lake is again subsiding. This evidence includes large open cracks and sinkholes, especially along the Casa Loma and San Jacinto Faults.

Seven major faults, the San Andreas, San Jacinto, Elsinore, Agua Caliente, Casa Loma, Loma Linda, and Hot Springs Faults, are located within 20 miles of the dam. Each of these faults, especially the San Jacinto, is active, and must be considered capable of movement, including surface rupture, within the anticipated lifetime of the dam and reservoir.

Geology of the Perris Dam Site

Perris Dam is situated at the head of a shallow, two-mile wide valley, opening to the southwest. The valley floor is alluvial, with scattered low protruding granitic knobs.

The rocks at the dam abutments and underlying the alluvial valley are predominantly granodiorite, diorite and tonalite, allequigranular medium to coarse grained igneous rocks of the Southern California Batholith (granitic rock complex). Contacts within the basement rocks and the locally-occurring metamorphic rocks are intrusive. The rocks are jointed at spacings of greater than 4 feet, in 3 sets: 1) northwest and 2) northeast-striking joints, with steep dips, and 3) randomly oriented joints, with shallow dips (exfoliation). Weathering along the joints has caused the formation of many large blocks.

Alluvium in the valley is a generally silty sand (SM), with lenses of clean sand (SP), gravel (GP), and silt (ML), with minor clayey sand and clay. Groundwater levels vary. At the left abutment, groundwater was penetrated in some borings. Across the valley, water levels lie within the decomposed granitic rock, parallel to the ground surface, with flow to the southwest. There is one major exception to this in the form of a large subsurface channel. Its maximum depth is 300 feet; the maximum width is 1400 feet. Here, groundwater saturates the lower 100 feet of alluvium.

Engineering Geology of the Inlet and Outlet Works

The inlet channel lies atop rock decomposed to depths of 44 feet and atop alluvium of variable thicknesses. Thus, foundation conditions vary considerably. The alluvium is silty sand, with in-place densities

of 115 pcf, and bearing capacities estimated at 3 ton/foot² after stripping. The weathered rock has a bearing capacity of less than 5 ton/foot², and the fresh rock greater than 8 ton/foot².

The outlet facilities are situated upon both alluvium, to a maximum depth of 45 feet at station 15 + 00, and decomposed, weathered to fresh granitic rock. Depths to fresh rock are highly variable. The outlet structure's foundations will be in fresh granitic rock, with a bearing capacity of more than 10 t/foot² (see ref. 9 & 13.) Some water is encountered in joints in these rocks. Some shear zones bisect the outlet tunnel, but there is no evidence that these are related to active faulting.

Seismic Setting

The Perris Dam and Reservoir sites are located in the most seismic area of California. Four earthquakes of magnitude greater than 6 have occurred nearby in the last 50 years. Since 1918, 93 earthquakes of $M = 4.0-6.9$ have occurred within 50 miles. Since 1935, 2 earthquakes of $M = 6.0-6.9$ occurred within 20 miles, 31 earthquakes of $M = 3.0-3.9$ within 10 miles, and 15 earthquakes of M greater than 4.0 have occurred within 30 miles.

Conclusions

The Perris Dam and Reservoir will probably be subjected to strong seismic shaking during the next 50 years. There is no evidence of faulting at the dam site itself. The alluvium and decomposed granitic rock at the site, partially saturated, could amplify earthquake waves. Potentially liquefiable lenses of sand could present a problem.

Landslides and Rockfalls

Landslides and rockfalls are only a minor problem in Reach C.

At Cedar Springs dam and reservoir, DWR geologists have judged landslide potential to be small. Some rock falls could occur, but will not be significant. Failure of the dam abutments is unlikely.

At Devil Canyon, sliding and rockfalls are expected from the hills east of the plant during earthquakes (DWR, Earthquake Hazard Report #32 (see ref. 33)). It appears that rockfalls and minor slumping between the San Bernardino Tunnel portal and the power plant could occur but that these pose no threat to vital facilities.

Subsidence

Subsidence does not seem to be a problem in Reach C. No special studies were made of landslides or subsidence on the reach from Pearblossom to Perris.

Based on these observations and the relative seismicity of various faults, a seismic hazard map for the region under consideration is developed in the next two chapters. Again, it is emphasized that no micro studies (or detailed site studies) are included in this work. That would be beyond the scope of this report.

Chapter 3

SEISMIC DATA AND SOURCE MODELING

There are twenty-two seismic line sources and five seismic area sources which could generate a future seismic event affecting reach C. See chart 2 for location of these sources. Table 3.1 shows the names of these sources and the seismic data base for each of these sources. Appendix I gives a listing of all the seismic events considered in this study. The earthquake data from April 1906 to December 1970 was obtained through the National Earthquake Information Center at Boulder, Colorado. In addition, the data from January 1971 to September 1974 was taken from the Bulletin of the Seismological Society of America. A total of approximately 6,000 seismic events during the past 67 years were considered in developing future seismicity for the region.

In reference 2, the reliability of the available information and its effect on the forecast of future seismicity is discussed in detail.

In figure 2.1, the fault location and the epicenter map of California was presented. Knowledge on the existence and the activity of all the faults in Southern California is not complete. Thus, only those faults that have shown recent activity are considered. Most of the faults considered are classified by geologists as quarternary faults. Prequarternary faults are considered in cases where earthquakes have been recorded.

Seismic Sources

As mentioned above, the location of faults and other seismic sources - where faults have not been identified - has been modeled by means of lines or areas. Chart 2 at the end of this report shows the location of

Table 3-1

Source Number	Name of Source	Number of Records	RM _{max} (Assigned)	RM _{max} (Recorded)
<u>Line Sources:</u>				
1	San Andreas	103	7.5	6.5
2	" "	68	6.1	5.1
3	" "	47	6.6	5.1
4	" "	507	7.3	6.5
5	Garlock	83	6.7	5.5
6	San Gabriel	133	6.2	4.9
7	Helendale	155	6.3	5.5
8	Pinto Mountain	415	7.1	5.9
9	San Jacinto	1029	8.0	7.1
10	Aqua Caliente	458	7.5	6.5
11	San Gabriel	59	7.1	5.1
12	" "	220	7.3	7.1
13	Newport-Inglewood	358	7.1	5.9
14	Santa Ynez	176	6.8	6.1
15	" "	58	6.0	4.9
16	" "	45	6.6	5.3
17	Big Pine	53	7.4	6.3
18	" "	67	6.5	5.7
19	Nacimiento	163	6.8	5.7
20	Garlock	100	5.7	5.1
21	San Andreas	294	7.1	5.7
22	Elsinore	132	7.0	6.3
<u>Area Sources:</u>				
23		301	8.0	7.7
24		501	7.5	6.1
25		311	7.2	6.3
26		8	4.3	3.7
27		195	7.1	6.3

these modeled sources. In some cases, several line segments are used to model a single fault. This is to represent variable seismicity of a fault along its length. Earthquakes corresponding to each source were sorted using a standard sorting computer program. The number of events corresponding to each source are listed in table 3-1. This table also shows the largest Richter Magnitude recorded for each source and the largest Richter Magnitude assigned. The maximum Richter Magnitude assigned is obtained from Greensfelder (see ref. 35).

For all the sources, a focal depth of 25 kms is considered. This assumption of constant focal depth for all the sources may introduce some errors. However, in ref. 2, it has been shown that error in focal depth assumption does not result in appreciable error in the final iso-acceleration mapping. That is, resulting peak ground acceleration at a site, predicted by using the models presented in this report are insensitive to variations in focal depth.

Recurrence Relationships

The log-linear recurrence relationships discussed in Shah et al (ref. 1) is used to represent the frequency of occurrence of seismic events for each source. This relationship is given by equation 3-1.

$$\ln N(M) = \alpha + \beta M \quad 3-1$$

where $N(M)$ = Number of events above Richter Magnitude M .

M = Richter Magnitude

α and β are regression constants.

Equation 3-1 represents the frequency of occurrence of seismic events for a given source whose total length (or area) is L (or A) and for which the data base is for a time period t . This equation can be normalized with respect to length or area of each source and for the time period of the

data. Thus

$$\ln N'(M) = \alpha' + \beta M \quad 3-2$$

represents normalized recurrence relationship. In equation 3-2,

$$\begin{aligned} N'(M) &= N(M)/Lt && \text{for line source} \\ &= N(M)/At && \text{for area source.} \end{aligned} \quad 3-3$$

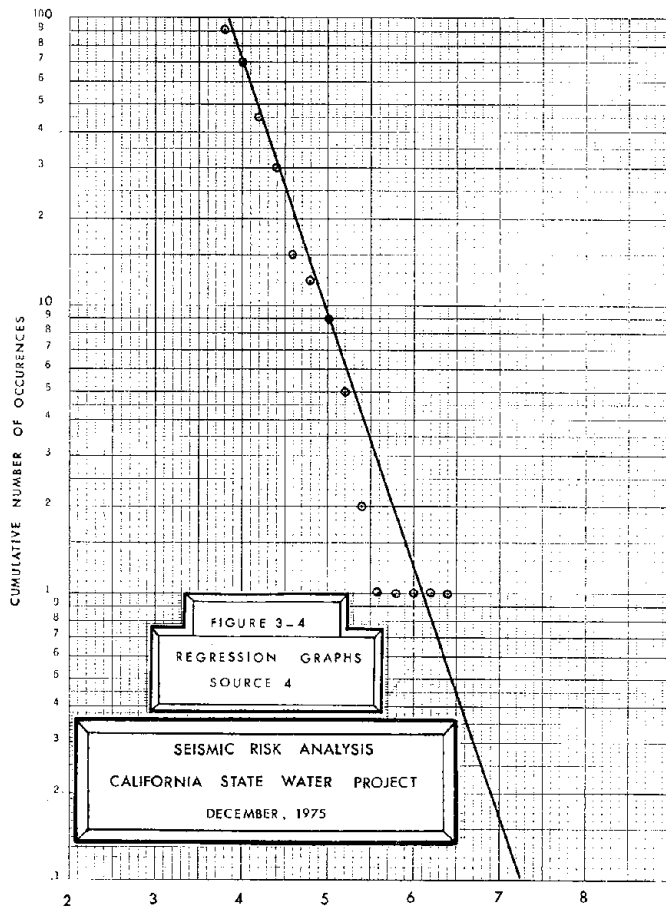
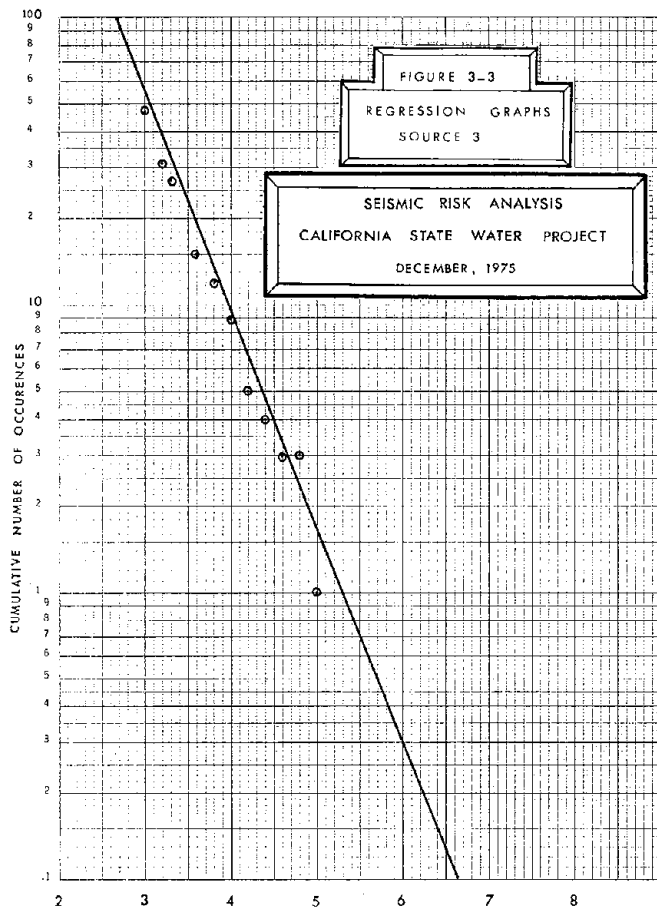
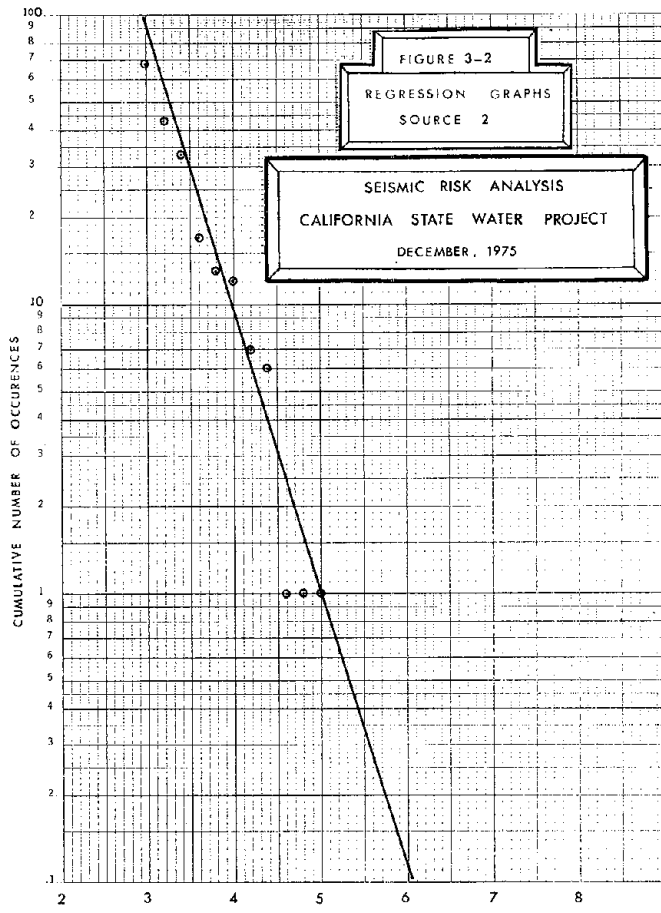
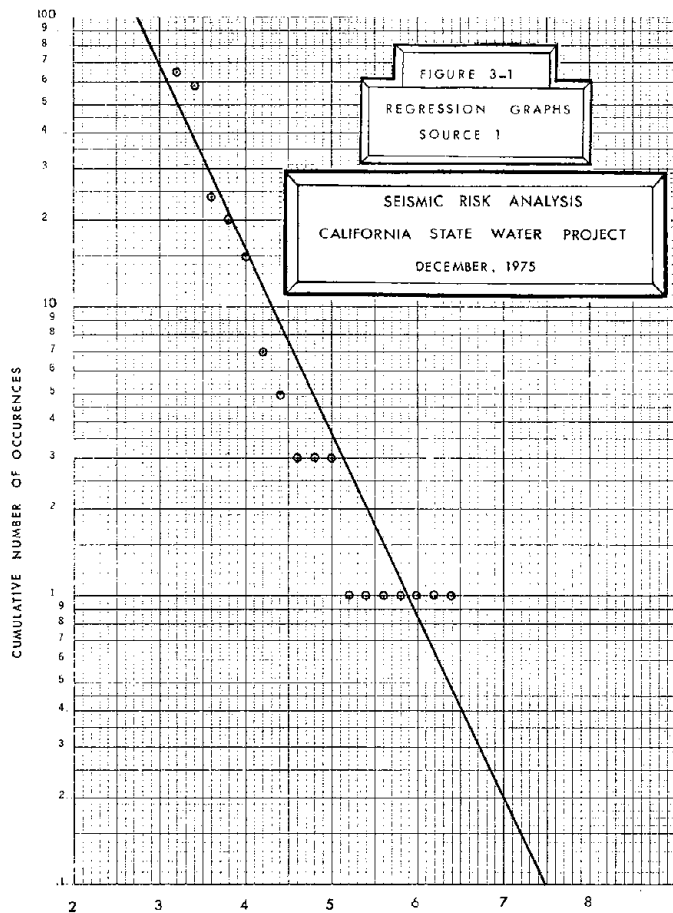
L is length of the line source

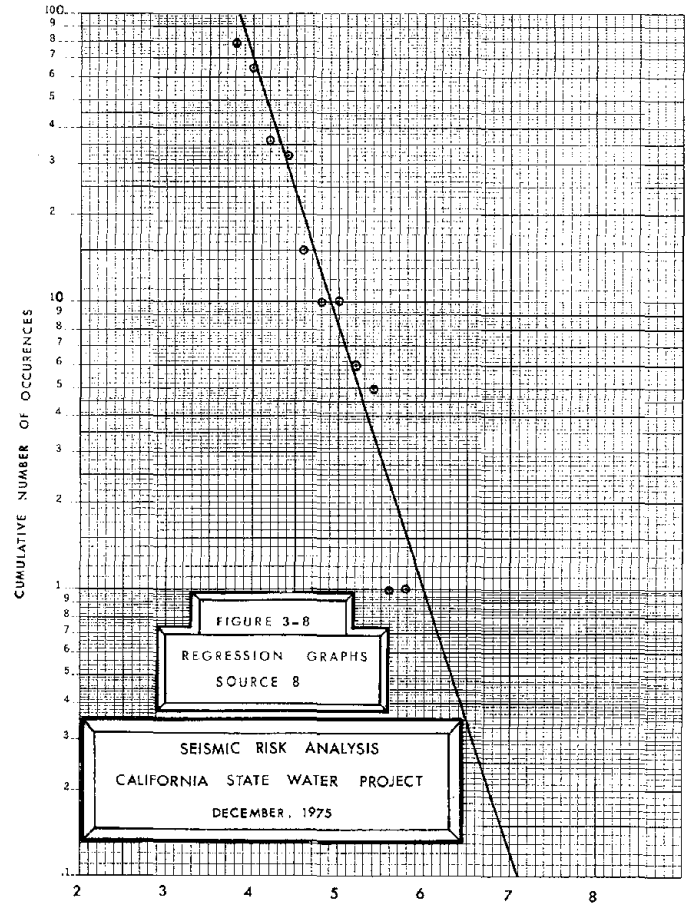
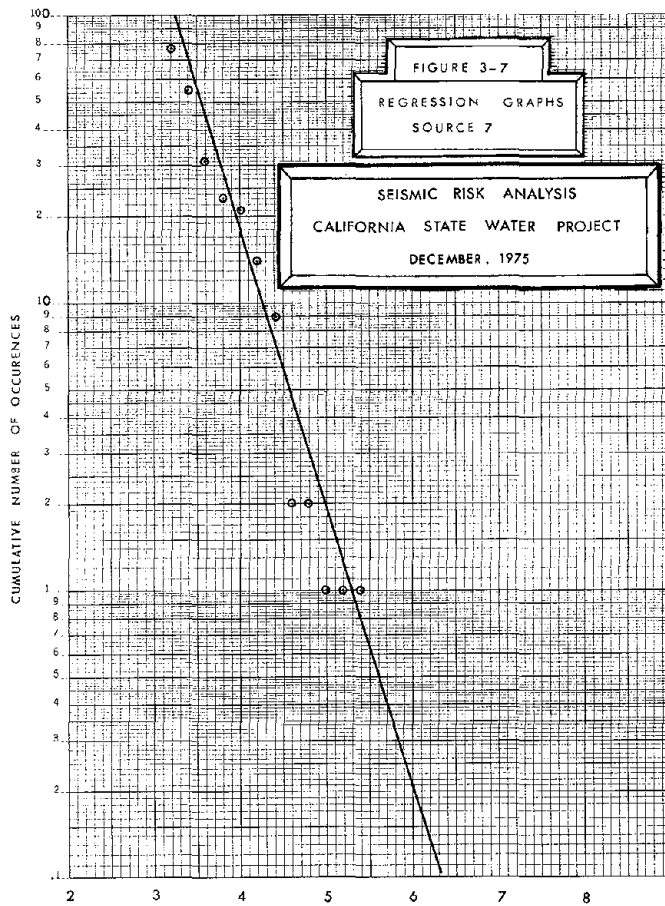
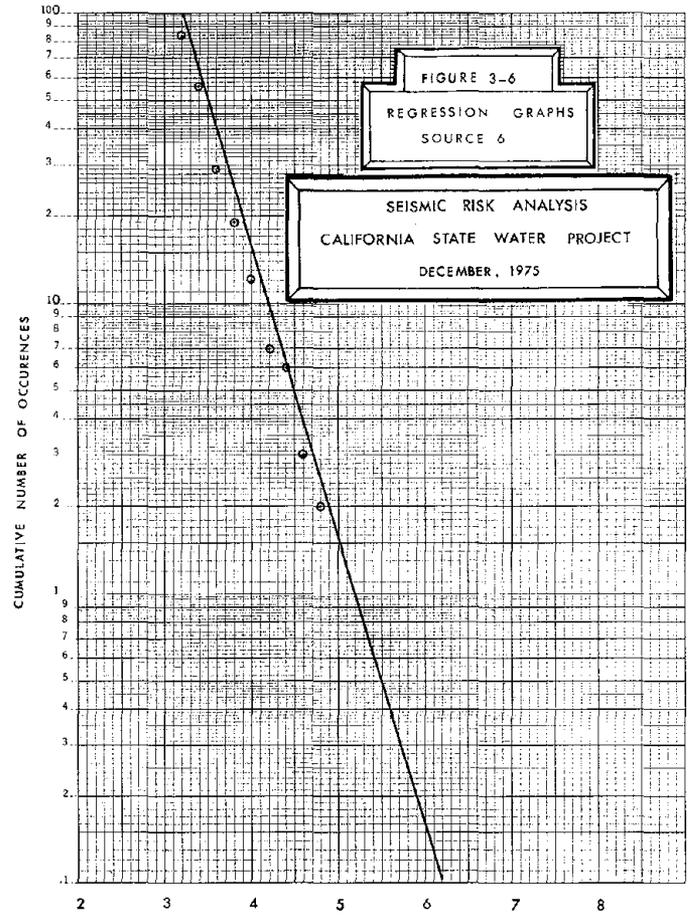
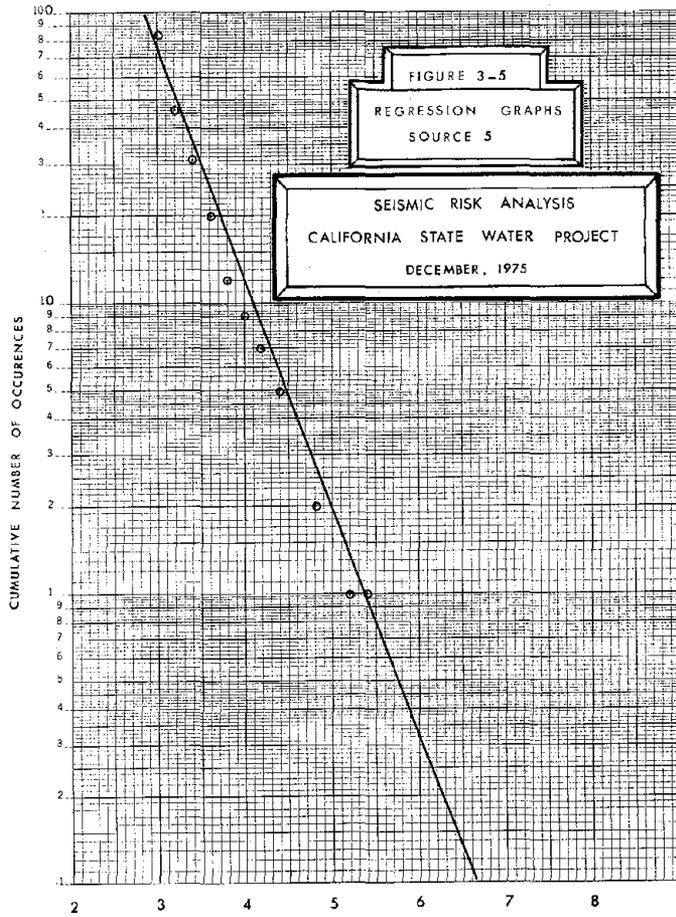
A is area of the area source

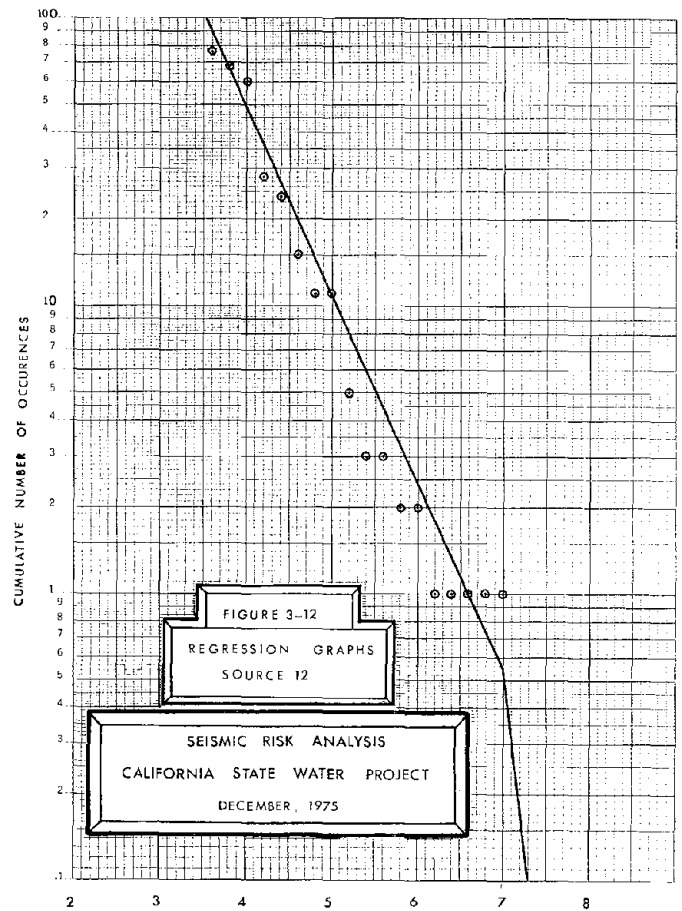
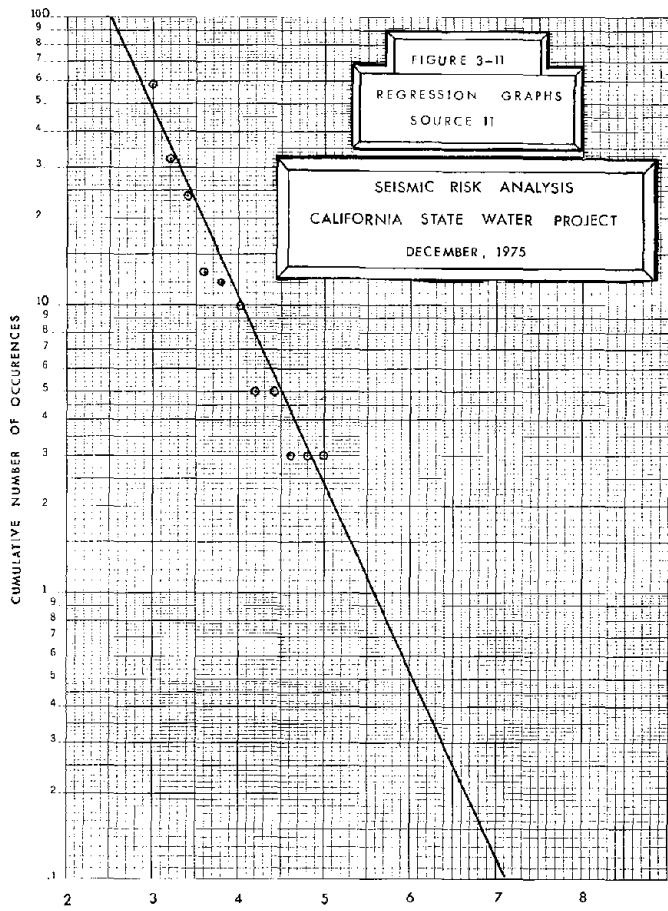
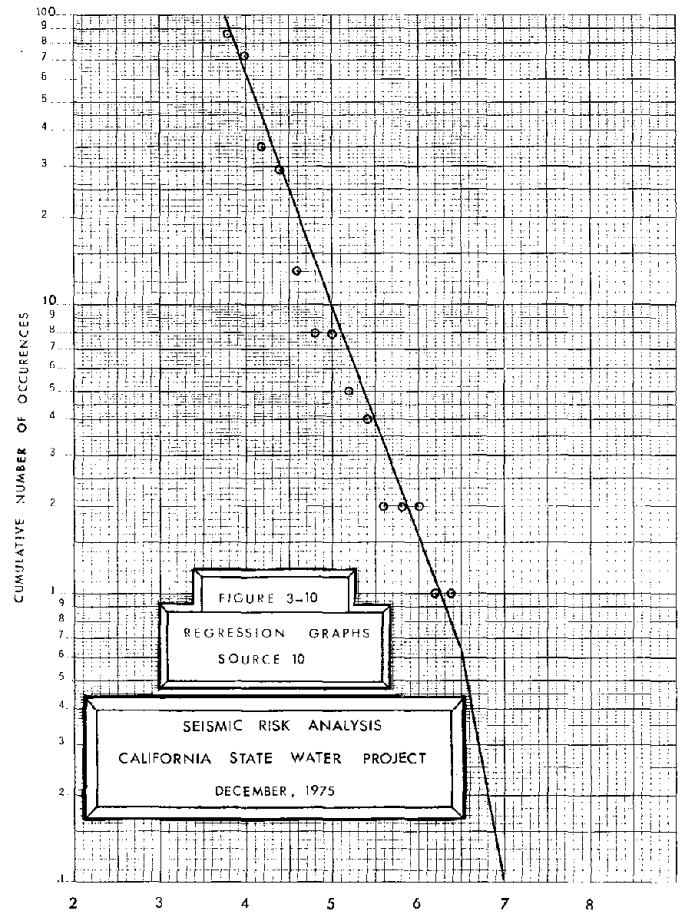
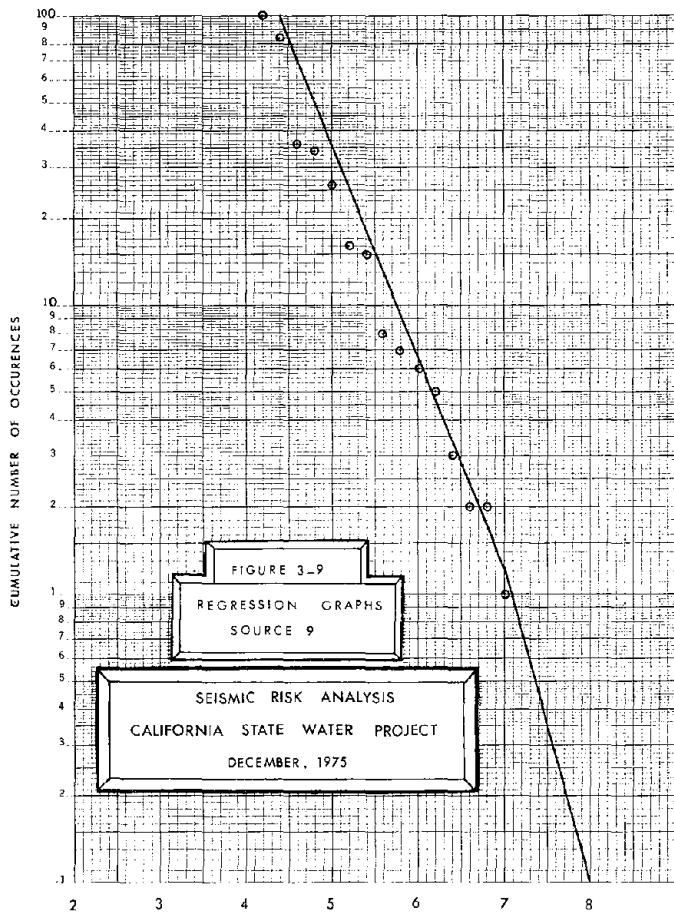
t is the time period of the data (67-1/2 years)

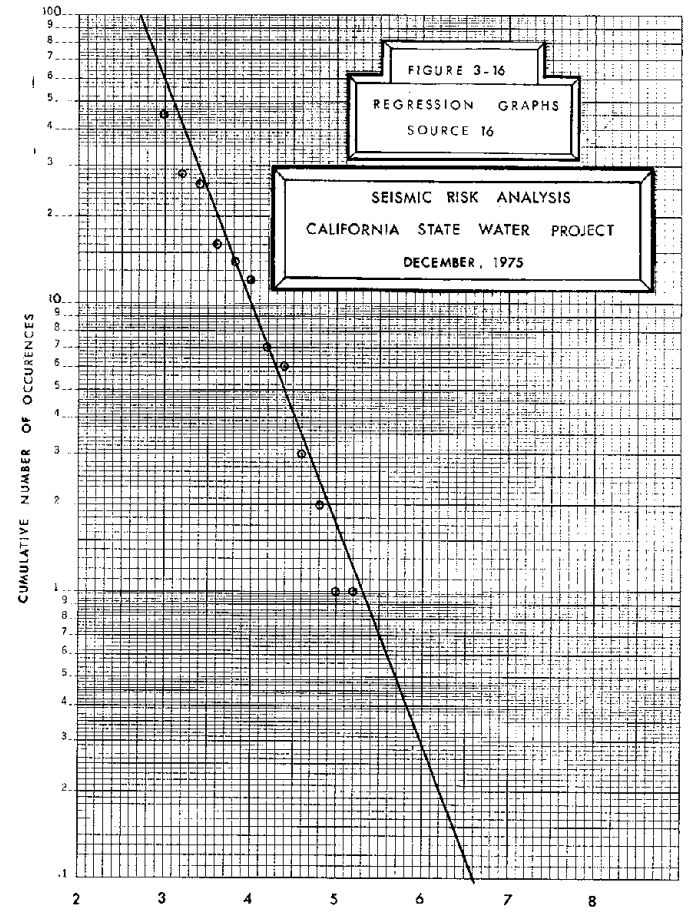
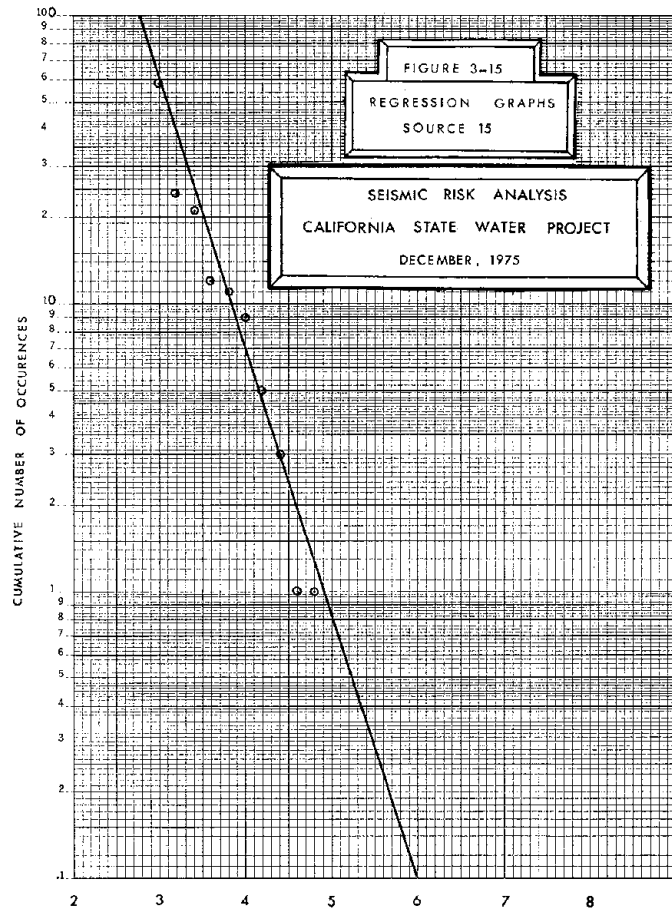
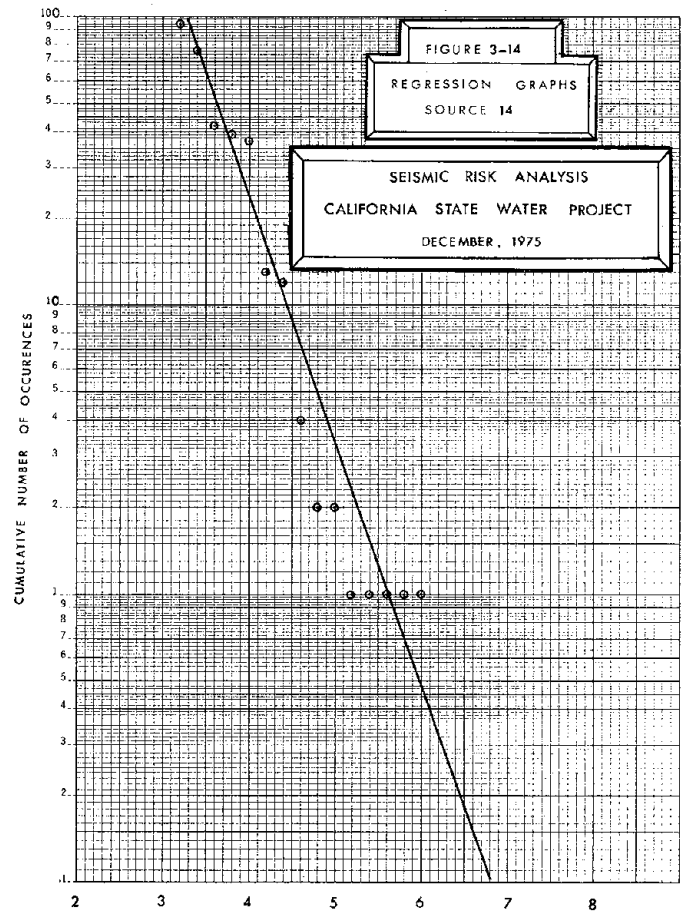
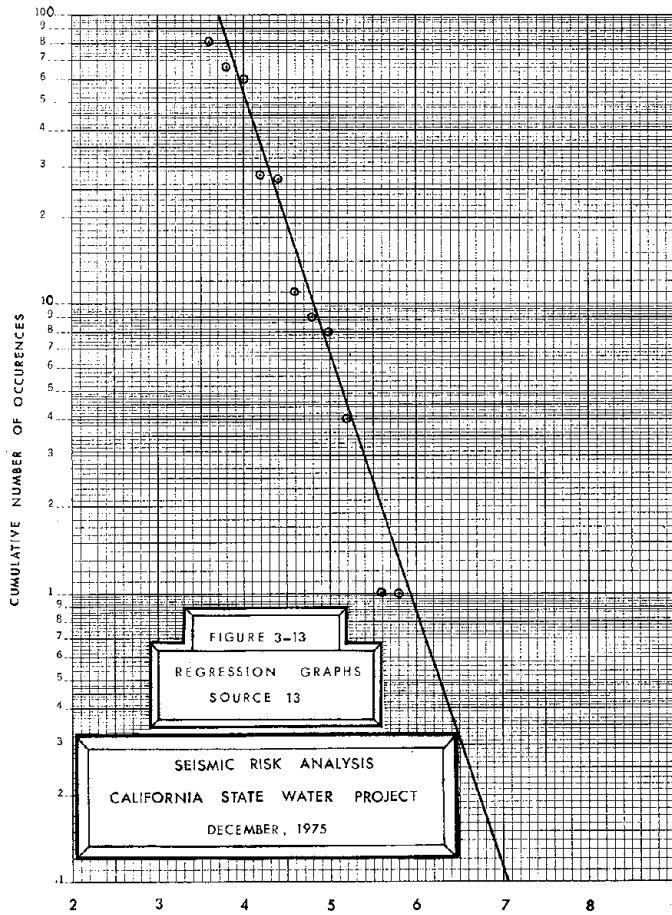
$$\begin{aligned} \alpha' &= \alpha - \ln(Lt) && \text{for line source} \\ &= \alpha - \ln(At) && \text{for area source.} \end{aligned} \quad 3-4$$

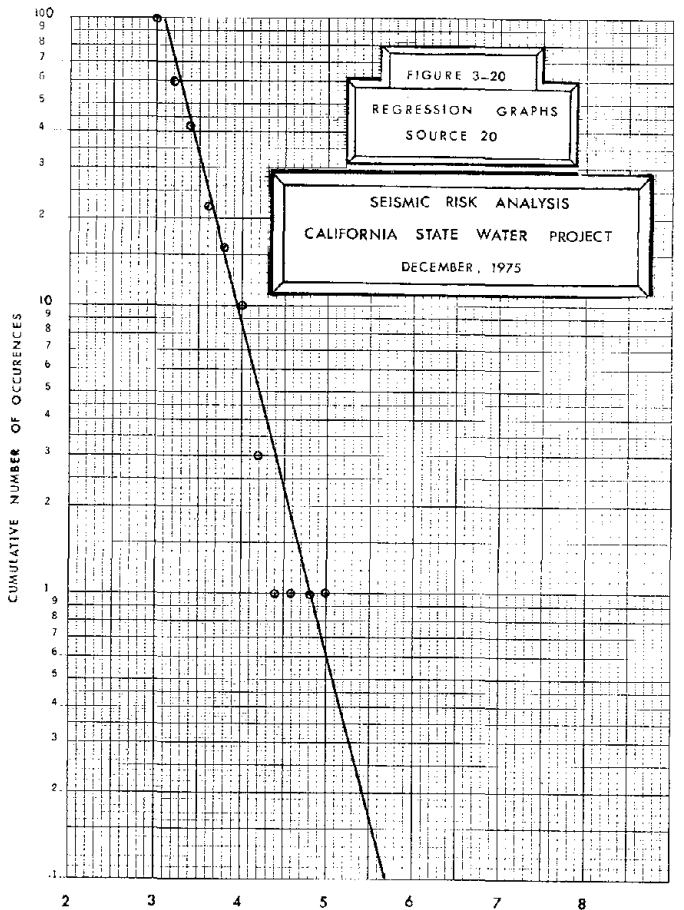
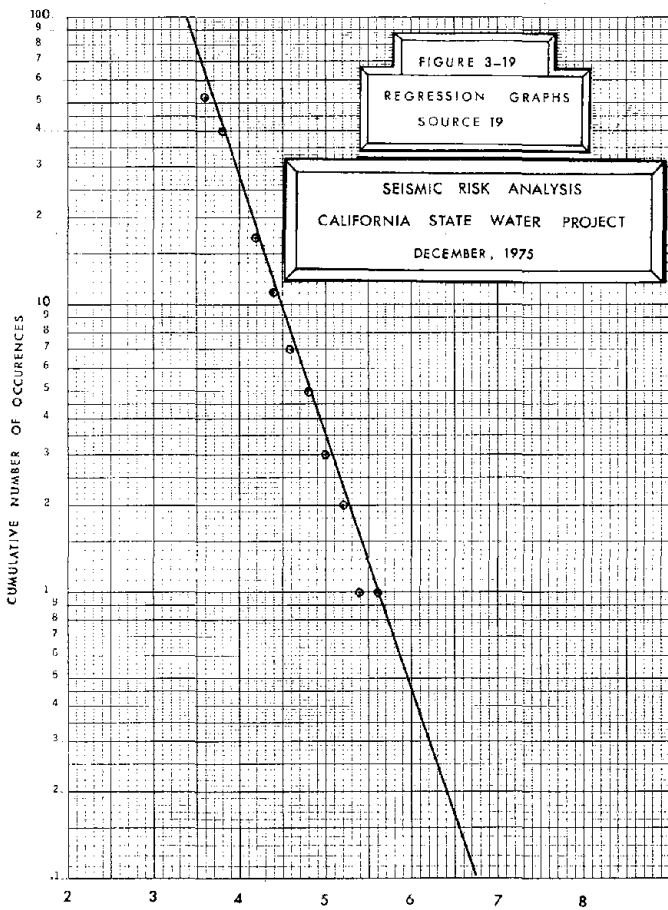
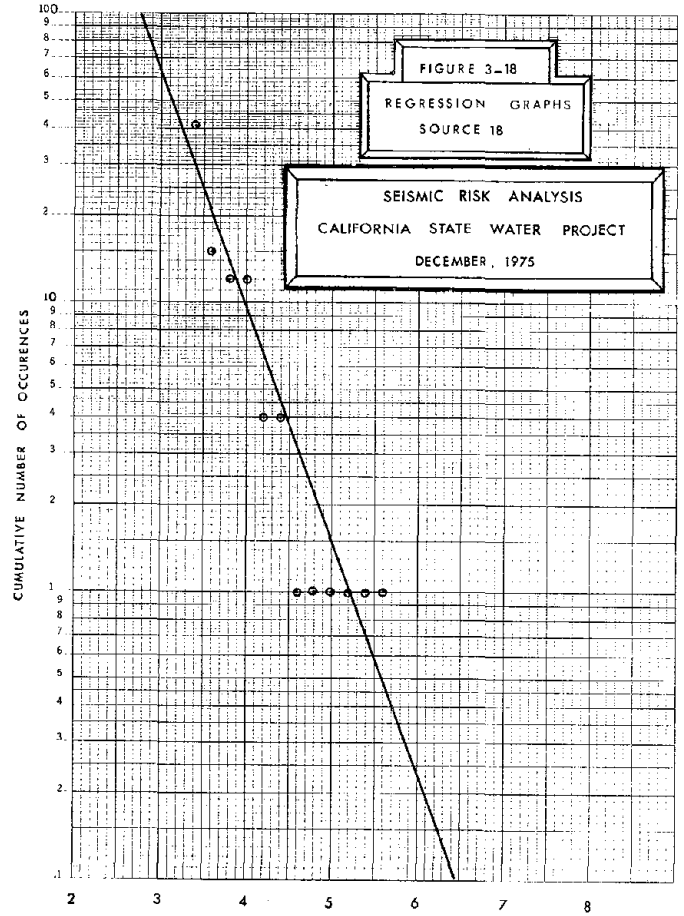
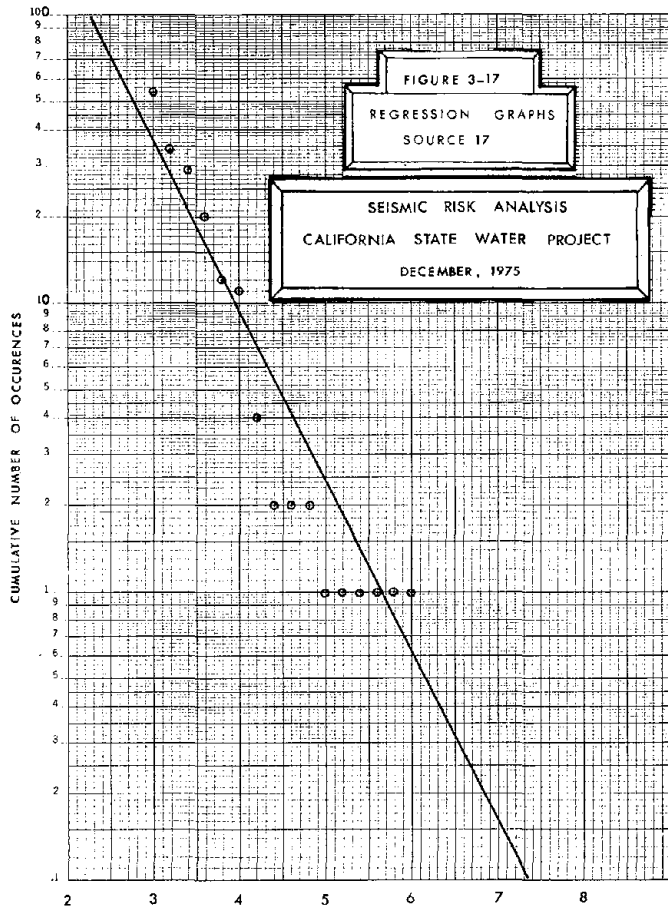
For some seismic sources, a single line represented by equation 3-1 did not fit the data. In such cases, a second line was fitted to obtain bilinear recurrence relationship. Table 3-2 shows normalized values of the regression constants. These values of $|\beta|$ are consistent with the values obtained by other researchers (36, 37). It can be seen that for most of the sources, only one recurrence line is needed to describe their "seismicity." Four sources 9 (San Jacinto), 10 (Aqua Caliente), 12 (San Gabriel), 22 (Elsinore), 23 (Area source) and 24 (Area source), a bilinear recurrence relationship, represented by constants α'_1 , β_1 , α'_2 and β_2 was needed. For all the sources, a geologically consistent upper Richter Magnitude cutoff (table 3-1) was used. This cutoff is introduced to prevent unreasonably high Richter Magnitude earthquakes being forecast by the recurrence model. Figures 3-1 through 3-27 show these recurrence relationships for all the sources considered. It can be seen from these figures that the log-linear fit is quite good. For sources where the amount of data is small, the uncertainty in the fitted line is large. As more information and data are available, the reliabilities of these relationships should improve.

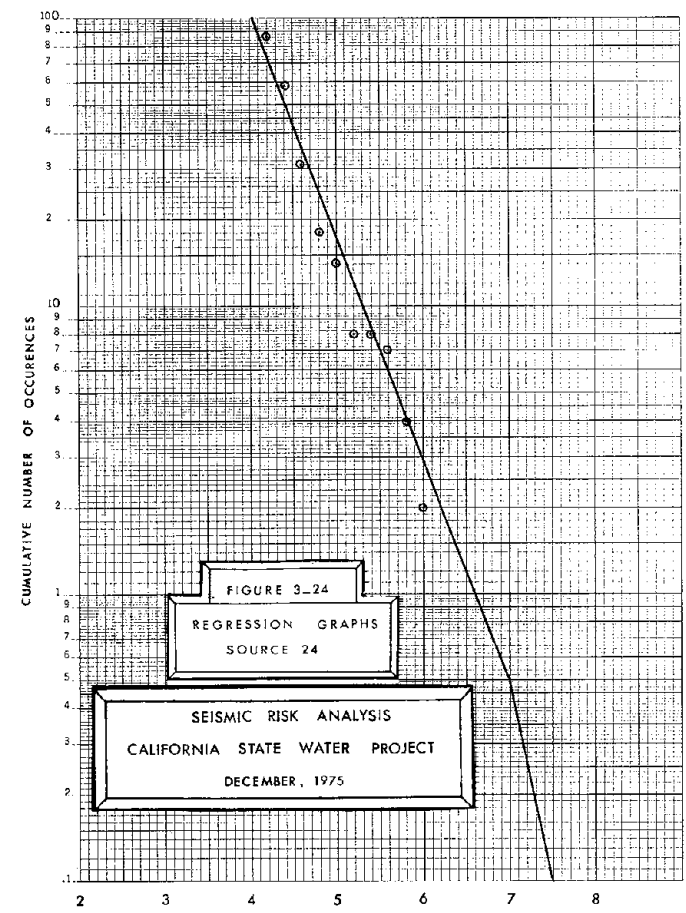
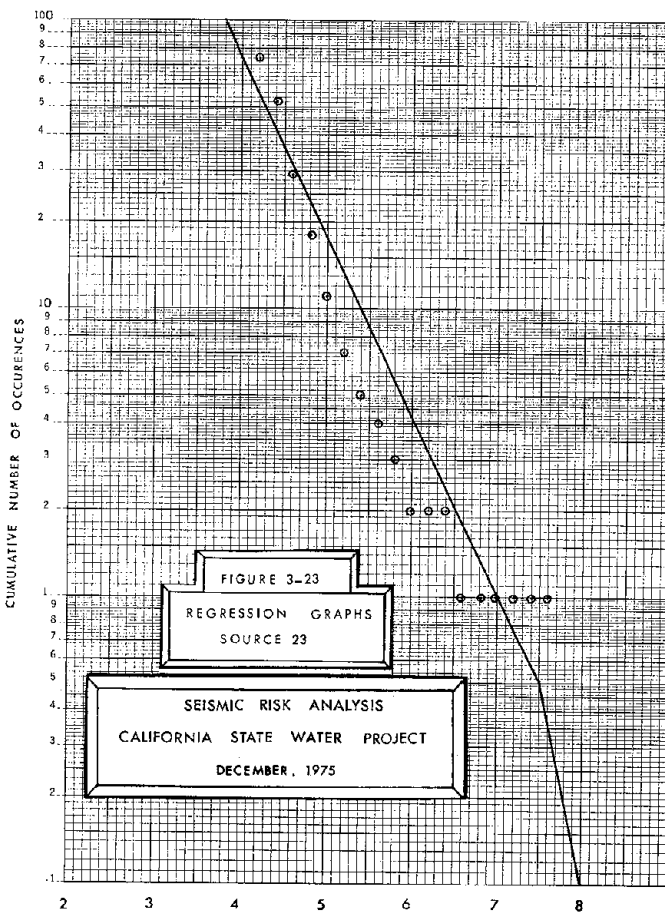
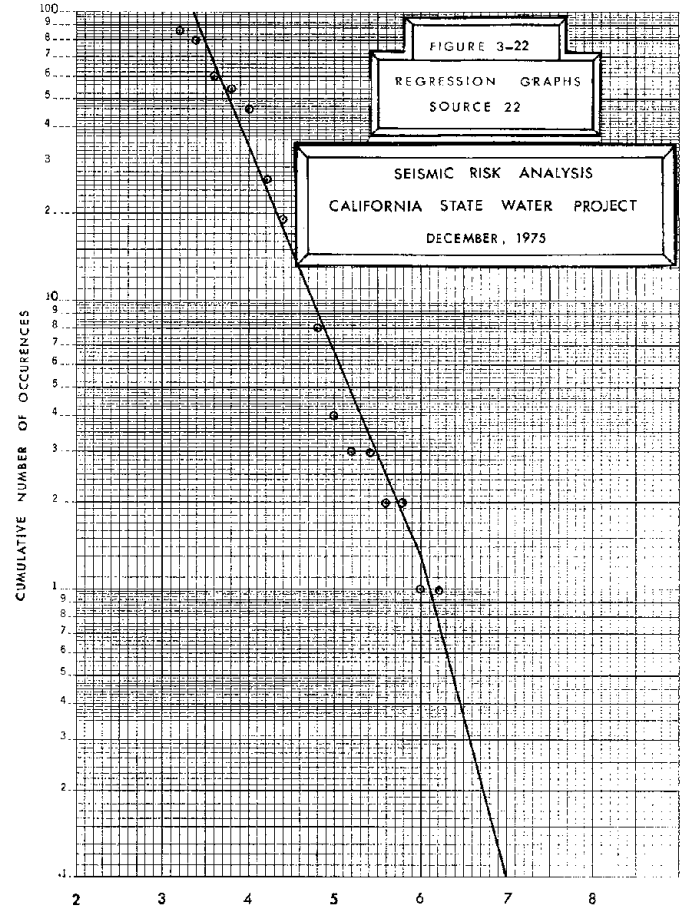
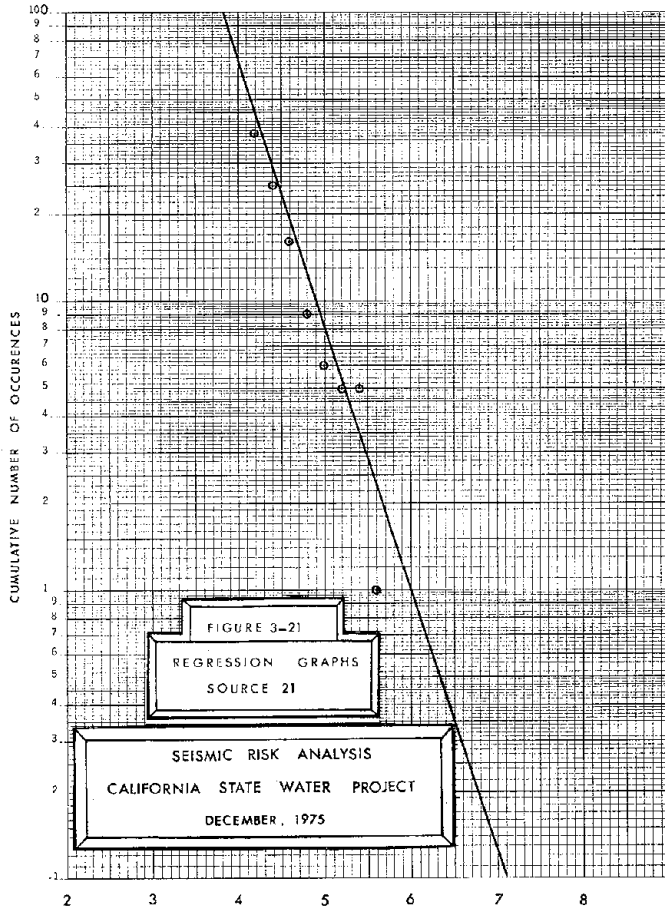












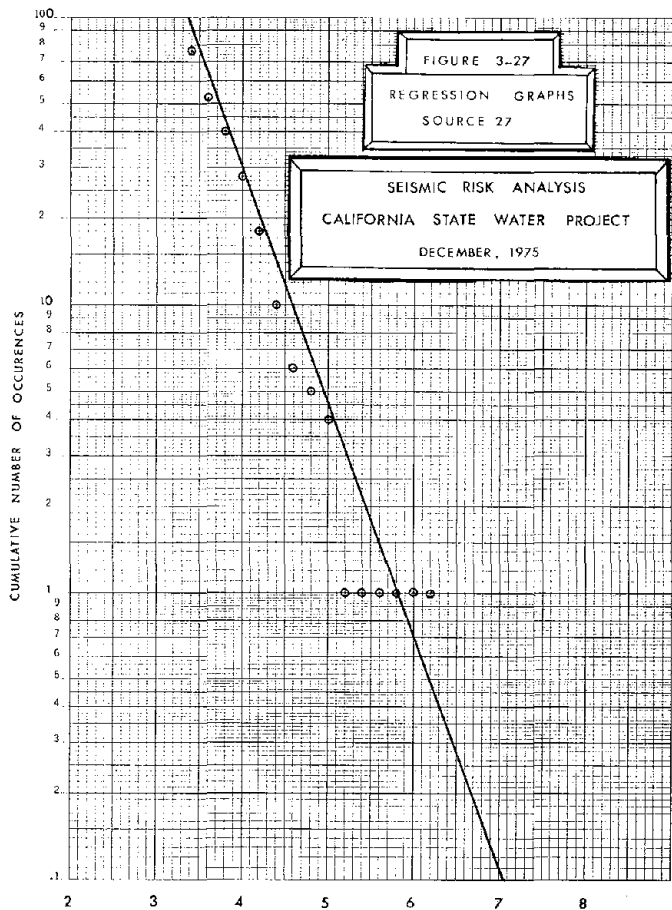
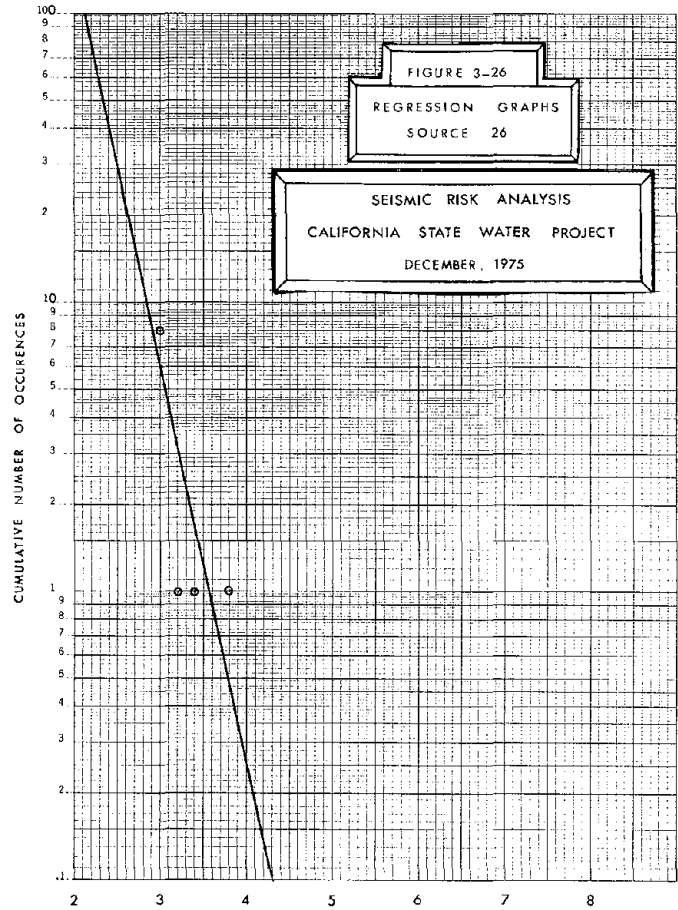
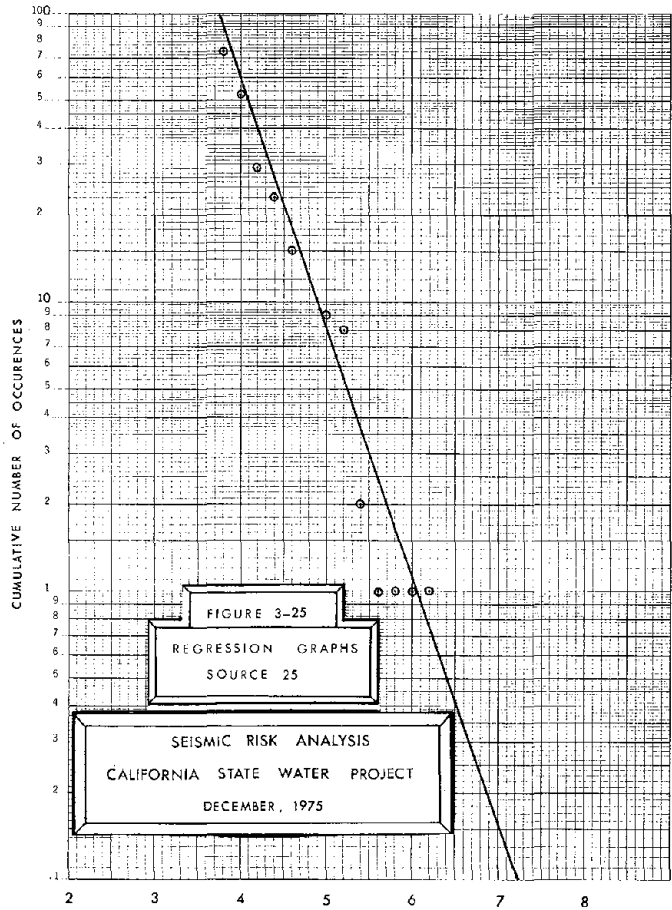


Table 3-2

Source	α'_1	β_1	α'_2	β_2	Length or Area
1	4.86	-1.47			74 miles
2	8.31	-2.24			34 "
3	5.69	-1.76			63 "
4	8.02	-2.03			135 "
5	5.92	-1.82			83 "
6	9.23	-2.32			29 "
7	8.38	-2.25			59 "
8	8.68	-2.10			90 "
9	7.35	-1.69	12.85	-2.47	176 "
10	7.17	-1.85	19.57	-3.76	147 "
11	5.82	-1.52			24 "
12	6.99	-1.50	35.82	-5.62	31 "
13	9.15	-2.06			37 "
14	7.89	-1.95			38 "
15	7.78	-2.16			30 "
16	6.80	-1.77			23 "
17	5.25	-1.37			20 "
18	6.70	-1.85			35 "
19	7.71	-2.07			90 "
20	9.57	-2.65			45 "
21	8.59	-2.06			79 "
22	6.76	-1.64	12.50	-2.60	50 "
23	8.23	-1.42	21.67	-3.22	653 sq. miles
24	9.50	-1.78	20.09	-3.30	1132 " "
25	10.00	-1.98			871 " "
26	10.92	-3.12			131 " "
27	8.34	-1.84			1220 " "

Some Observations

Selection of a line or area source model to represent reality is at best an approximation. In this work, source modeling is essentially based on historical data. It is quite possible that the true geologic behavior of any or all sources may not be similar to the modeled behavior. Cyclicity of seismic activity in geologic time frame cannot be represented by the historically based model shown here. However, it is felt that for an engineering time frame, the forecasts based on historical records are reasonable. Thus, to model the behavior of various sources for the next fifty to hundred years, the recurrence relationships developed here are "sufficient."

Various researchers in the past have suggested other forms of recurrence relationships. Some of those suggested forms may fit the data a little better. However it is felt that a small gain in data fit at an expense of analytical complexity is not warranted. This argument is especially relevant when one considers the uncertainties introduced by other factors such as the ones discussed in previous paragraph.

Various other observations regarding the source modeling are made in reference 2 and are not repeated here. In conclusion to this chapter, it can be said that a more detailed modeling of faults and seismicity at a great cost to the region would not have increased the reliability of the results substantially.

Attenuation Relationships

The recurrence relationships developed in chapter 3 for each of the 27 seismic sources represent the mean rate of occurrence of a seismic event above Richter Magnitude M per unit time (one year) and unit length or unit area. This mean rate of occurrence, together with a Poisson occurrence model can be used to estimate the probabilities of occurrence of various Richter Magnitude seismic events for a time period t. Reference 1 gives all the detailed derivations and are not repeated here.

The use of Poisson model and the recurrence relationship for each source provides an estimate of the probabilities of various Richter Magnitude seismic events occurring at individual sources. To determine the probabilities of exceeding the peak ground accelerations at various sites due to all the sources for a future time t, an attenuation equation, giving relationship between Richter Magnitude M, epicentral distance R, the focal depth h and the peak ground acceleration a is needed. There are many such relationships available in the literature. Table 4-1 and figure 4-1 show some of these (see ref. 38) relationships. The attenuation relationship used in this work is given by equation 4-1.

$$A = \frac{5000 \exp(0.8M)}{(R_h + 40)^2} \quad 4-1$$

where A = Peak Ground Acceleration in cm/sec²

M = Richter Magnitude

R_h = Hypocentral Distance in kms.

Table 4-1

Attenuation Equations

DATA SOURCE	EQUATION	REFERENCE
1. San Fernando Earthquake February 9, 1971	$y = 186206 R^{-1.83}$	
2. California Earthquakes	$y = \frac{981 y_0}{1 + \left(\frac{R^1}{h}\right)^2}$ <p>where $\log y_0 = (\bar{b}+3) + 0.81m - 0.027m^2$ \bar{b} is a site factor</p>	Blume (1965)
3. California Earthquakes	Graphical Presentation	Housner (1965)
4. California & Japanese Earthquakes	$y = \frac{5}{\sqrt{1G}} 10^{0.61m - P \log R + Q}$ <p>where $P = 1.66 + \frac{3.60}{R}$ $Q = 0.167 - \frac{1.83}{R}$ $T_G =$ fundamental period of site</p>	Kanai (1966)
5. Cloud (1963)	$y = \frac{6.77 e^{1.64m}}{1.1 e^{1.1m} + R^2}$	Milne & Davenport (1969)
6. Cloud (1963) Housner (1962)	$y = 1230 e^{0.8m} (R+25)^{-2}$	Esteva (1970)
7. U.S.C. & G.S.	$\log_{10} y = 6.5 - 2 \log_{10} (R^1 + 80)$	Cloud & Perez (1971)
8. 11 Selected Records	Graphical Presentation	Schnabel & Seed (1973)
9. 303 Instrumental Values	$y = 1300 e^{0.67m} (R+25)^{-1.6}$	
10. Western U.S. Records	$y = 18.9 e^{0.8m} (R^2+400)^{-1}$	
<p>y is cm/sec^2 R is kilometers (distance to causative fault) R^1 is miles (epicentral distance) h is miles (focal depth) m is magnitude</p>		

(Taken from ref. 36)

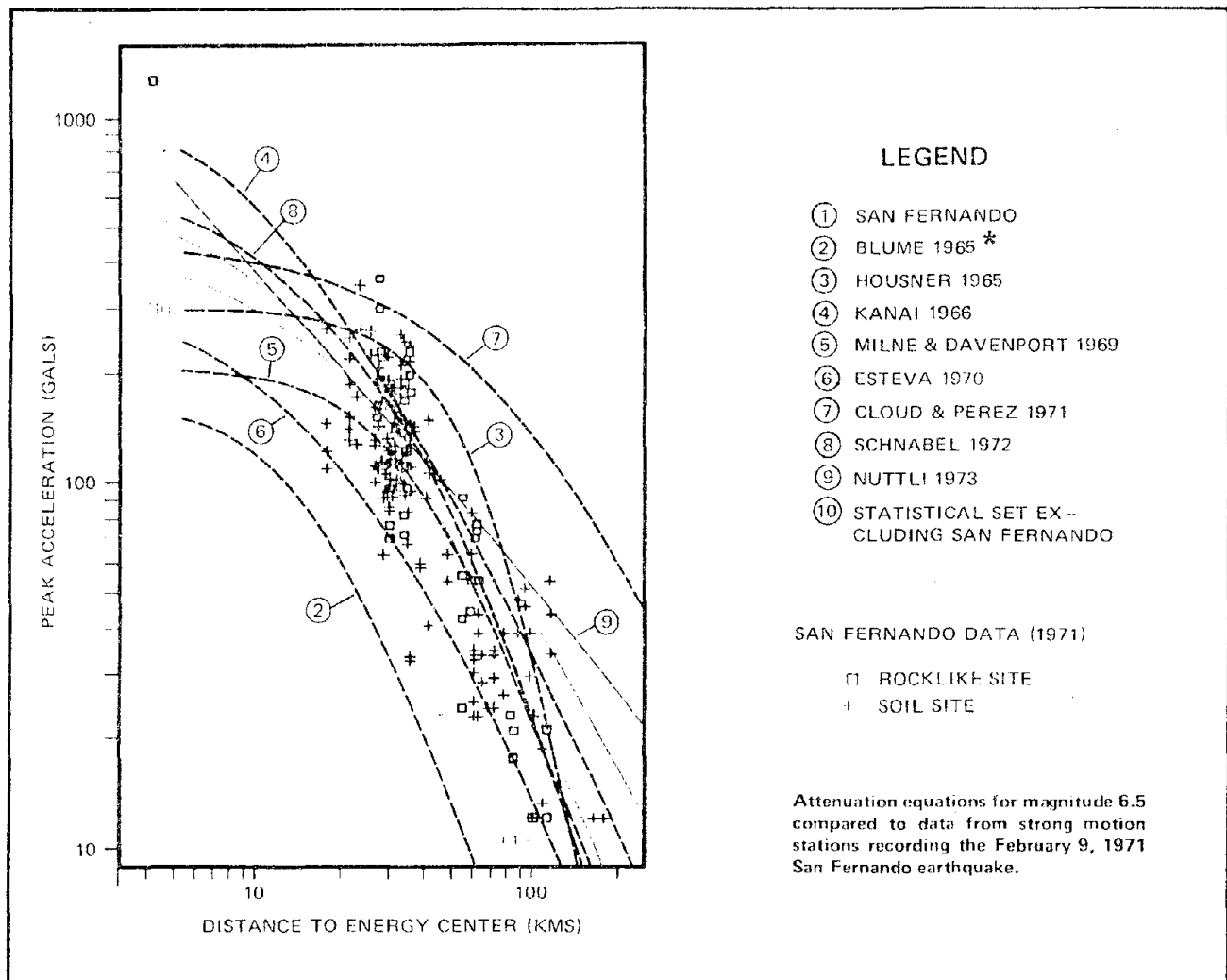
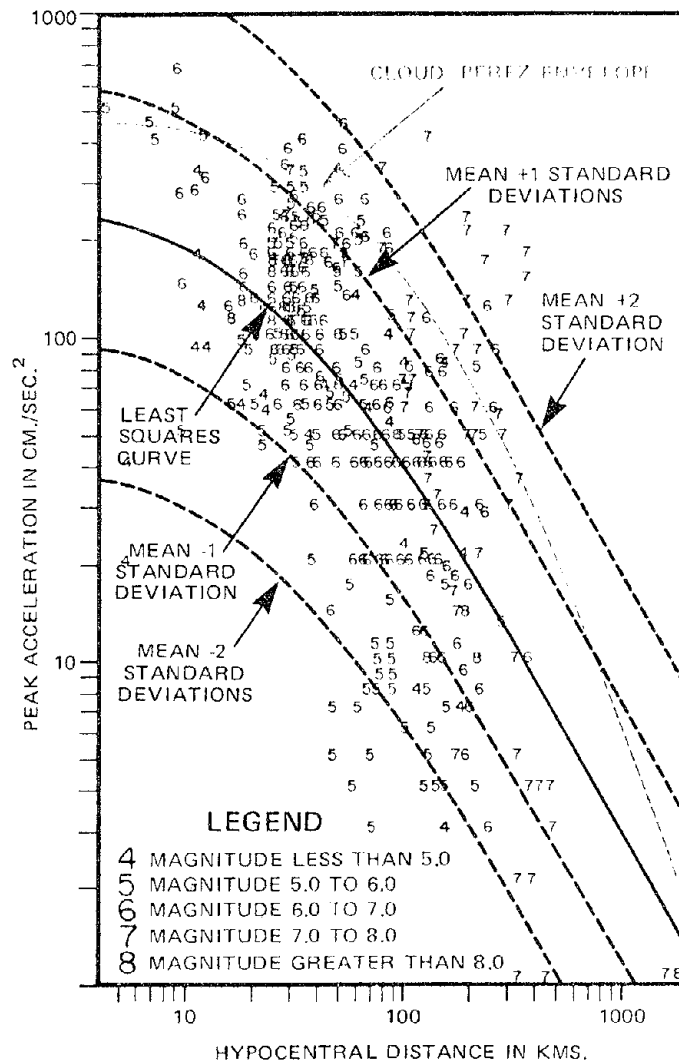


Figure 4-1
(Taken from ref. 36)

* Note: This relation can provide results which are very close to mean data behavior if the soil characteristics for the region are recognized. In all fairness it must be stated that this soil input was not used in the preparation of this figure from reference 36.



Peak ground acceleration in terms of distance from causative fault. This graph was compiled from a world-wide set of 515 strong-motion records without normalization of magnitude.

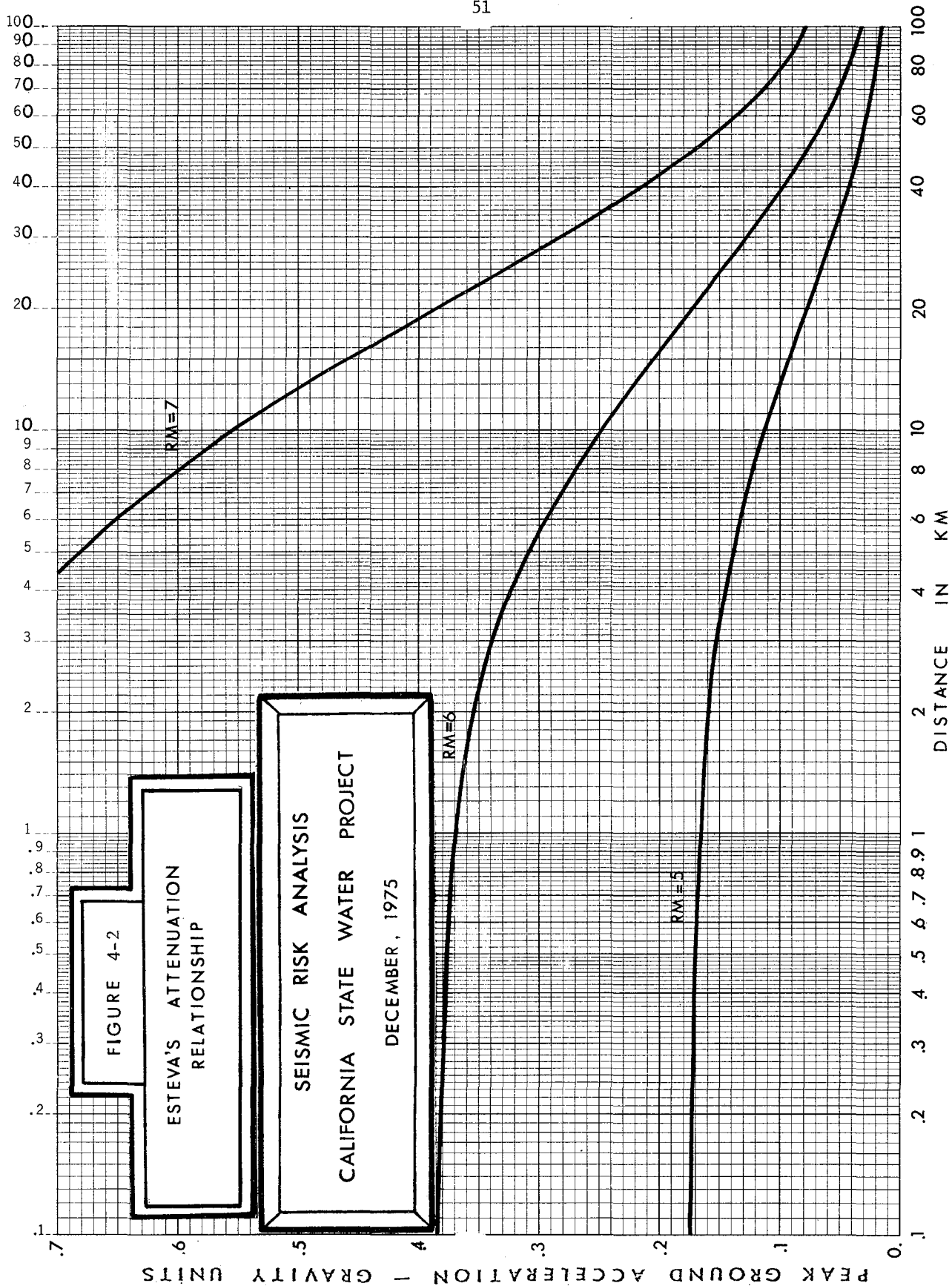
Figure 4-1 continued
(Taken from ref. 36)

In all the development of seismic hazard maps, estimation of attenuation relationship constitutes one of the greatest uncertainties. The scatter of actual data points is very large about the mean empirical relationship selected. In reference 2, the effect of uncertainty in this relationship on the final seismic hazard maps is discussed. Figure 4-2 shows the shape of the attenuation relationship used. The form of this equation was first suggested by Esteva (see ref. 36).

Seismic Hazard Maps for Reach C

The ground shaking hazard for the general region in which Reach C of the State Water Project (SWP) is located, is represented by means of iso-acceleration maps. See chart 1 for the location of Reach C. If Reach C is taken as a whole, one could determine peak ground accelerations at different locations for a specific time period t (exposure time) and a specific probability of $A < a$. Thus, for example, for a future period of 50 years and 10% chance of the peak ground acceleration A exceeding some value a , one could obtain lines of equal ground accelerations a . These lines of equal accelerations for a specific probability of exceedance and exposure time are called "iso-acceleration" lines. The maps representing iso-acceleration lines are called iso-acceleration maps. These iso-acceleration maps are seismic ground shaking hazard maps. Charts 3, 4 and 5 show these iso-acceleration maps for a time period of 20, 30 and 50 years respectively. The risk level considered for these three maps is 10%. The risk level is defined as the probability that the peak ground acceleration will be exceeded during the exposure time (or economic life) of the facility under consideration.

46 5490



In addition to the iso-acceleration maps for the Reach C, the following key facilities and locations along the aqueduct are studied in detail.

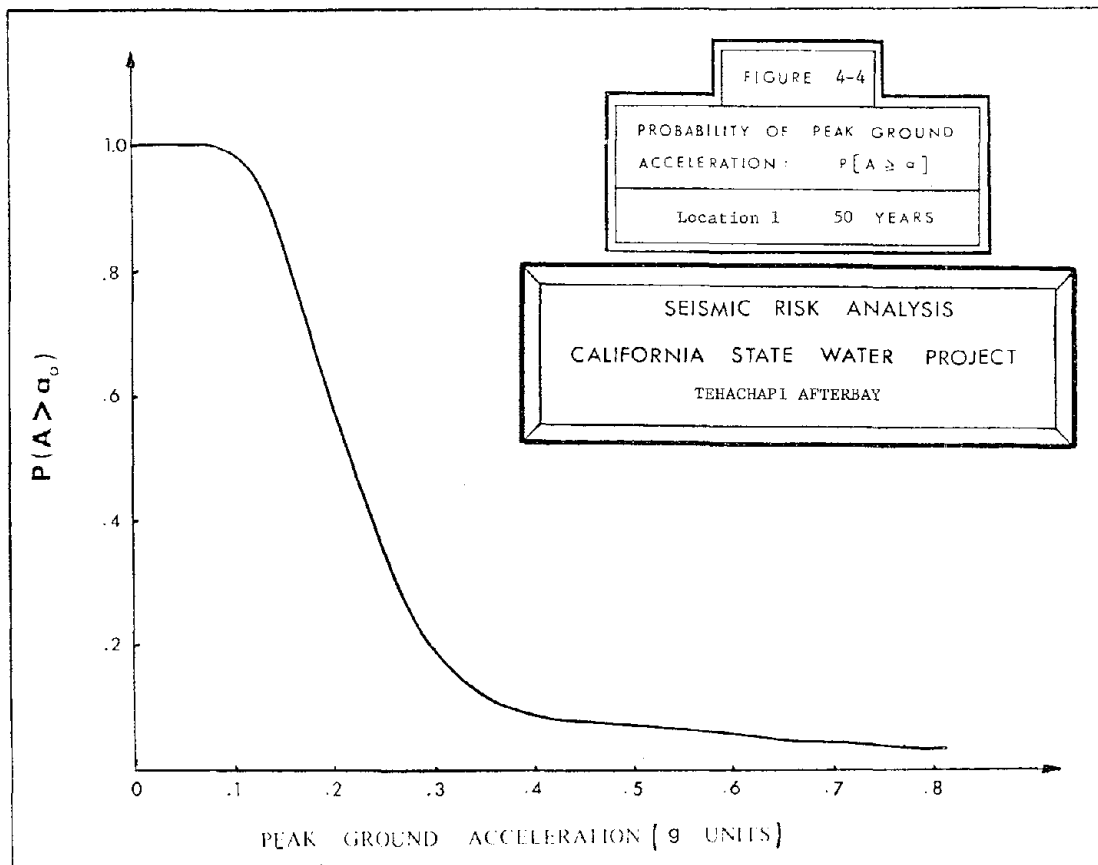
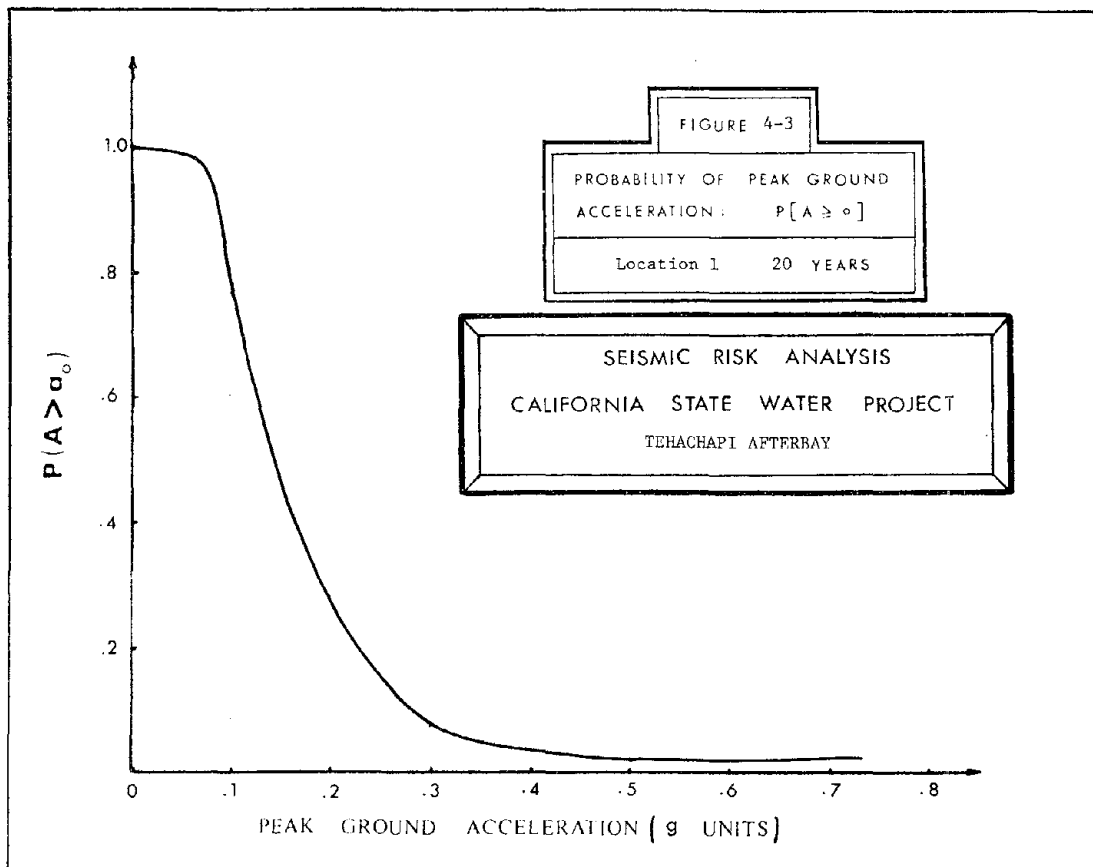
1. Tehachapi Afterbay
2. Pearblossom Pumping Plant
3. A location along the aqueduct (see chart 1 for these locations)
4. A location along the aqueduct (see chart 1)
5. Silverwood Lake and Cedar Springs Dam
6. San Bernardino Tunnel
7. " " "
8. Devil Canyon Power Plant
9. Santa Ana Pipeline (see chart 1)
10. " " " " " "
11. Perris Dam and Lake (also O and M Subcenter)

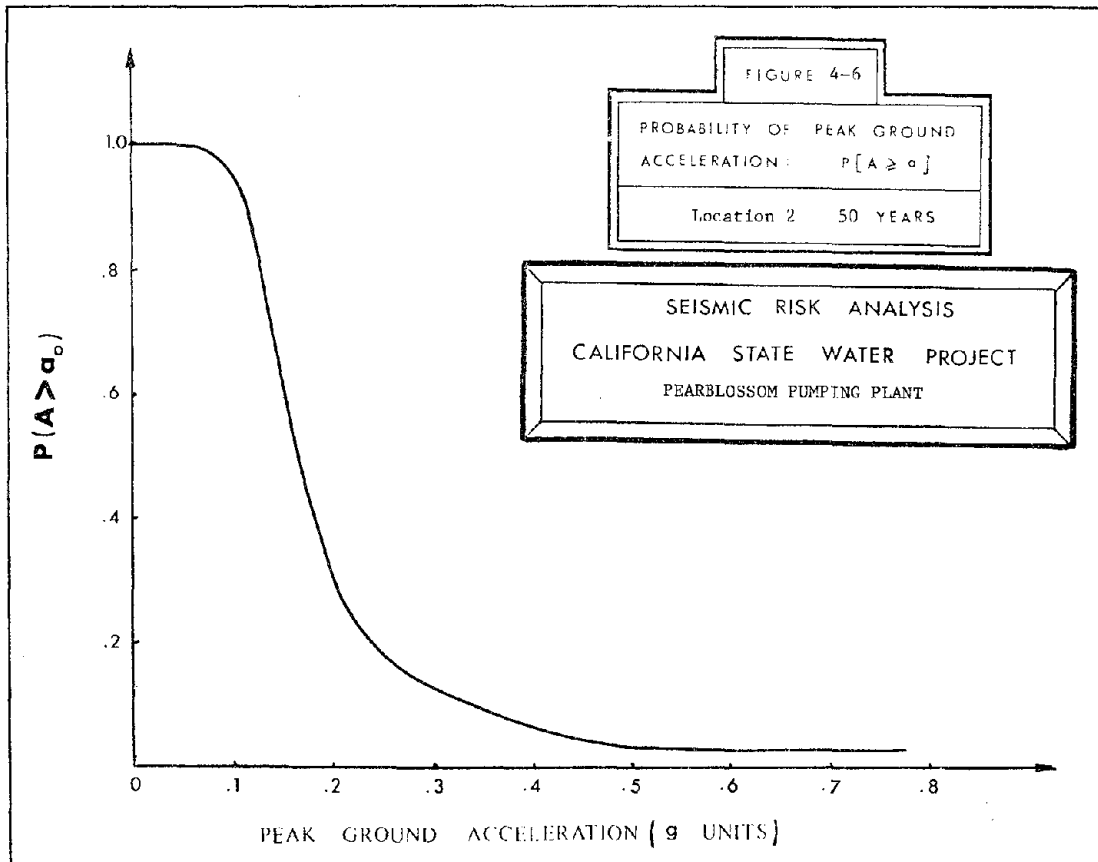
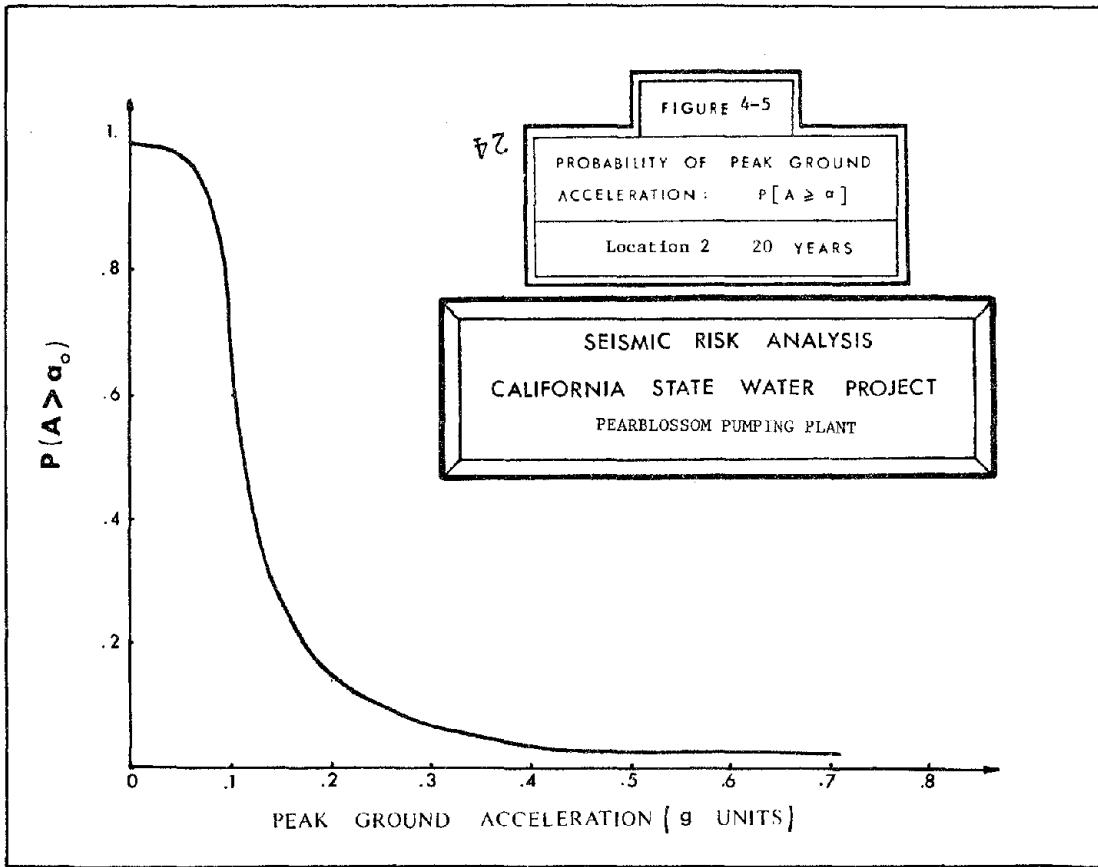
Table 4-2 shows the locations of these sites in terms of their longitudes and latitudes. Figures 4-3 through 4-24 show the cumulative distribution function of the peak ground acceleration for each site location. Results are presented for the exposure time of 20 years and 50 years.

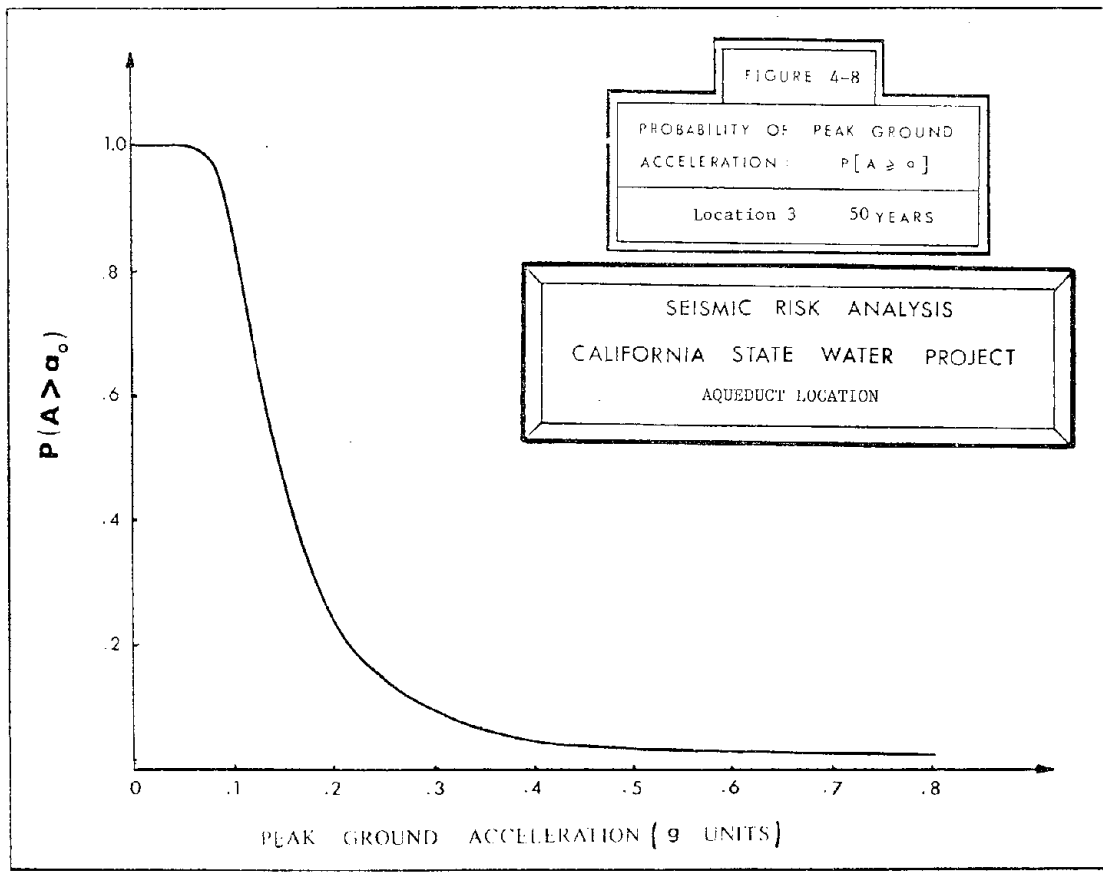
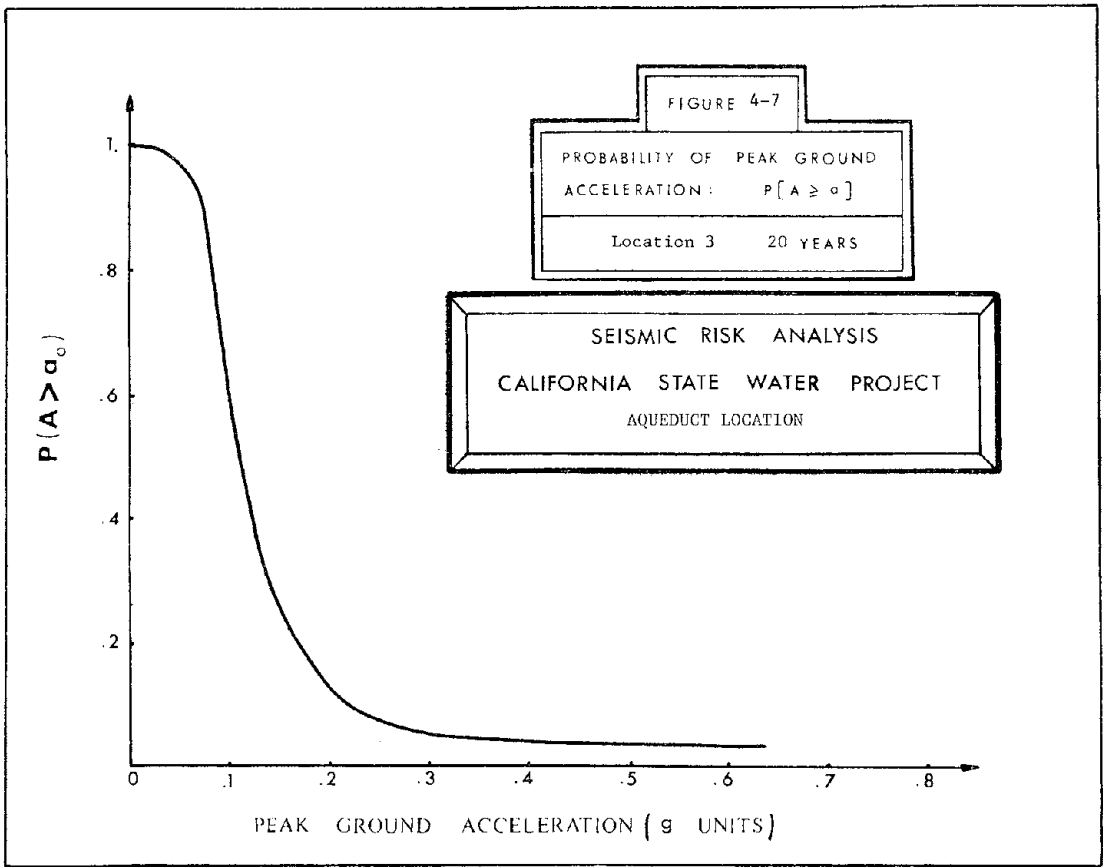
Thus, as an example (see figure 4-17) for Devil Canyon power plant, there is approximately 25% chance that the peak ground acceleration will exceed .2g in 20 years. The corresponding risk of exceeding .2g in 50 years is approximately given by 52% (see figure 4-18). The implications of these probability values and the corresponding PGA values will be discussed in Chapter 5. However, one observation to keep in mind is that the probabilities of exceeding a given peak ground acceleration for a given site increases with the increase in exposure time.

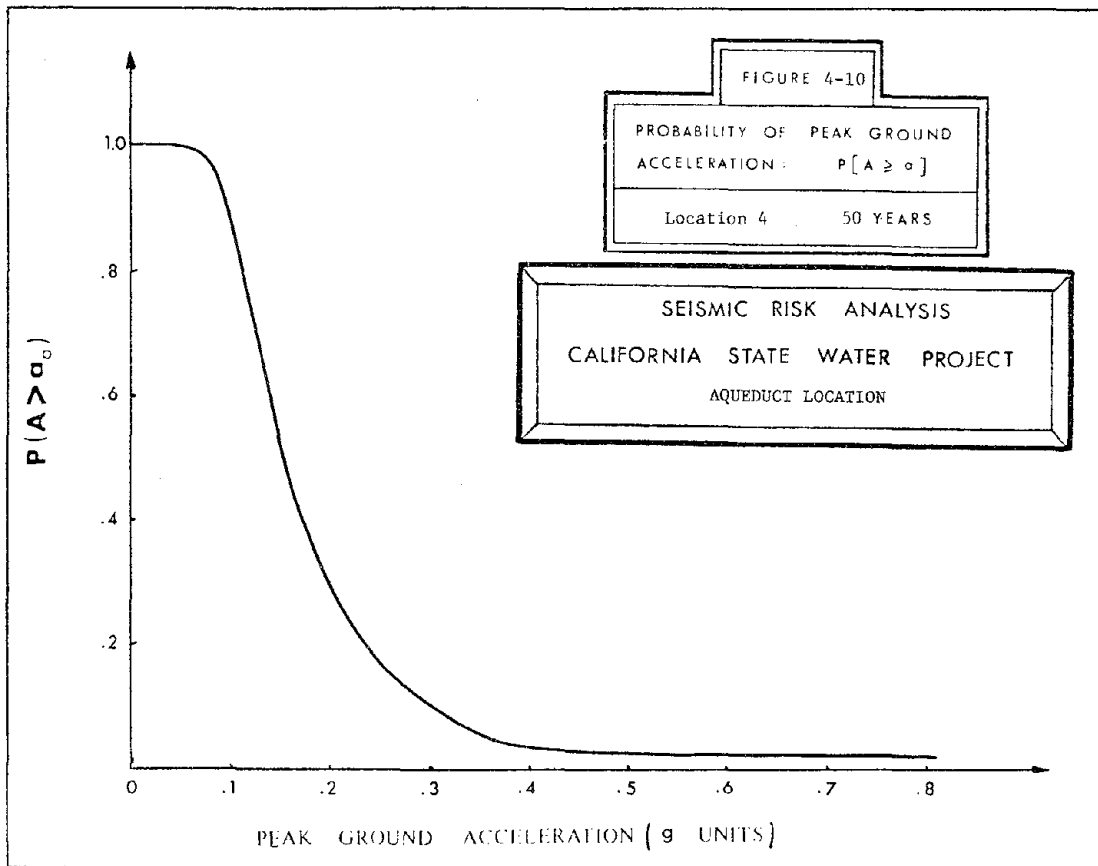
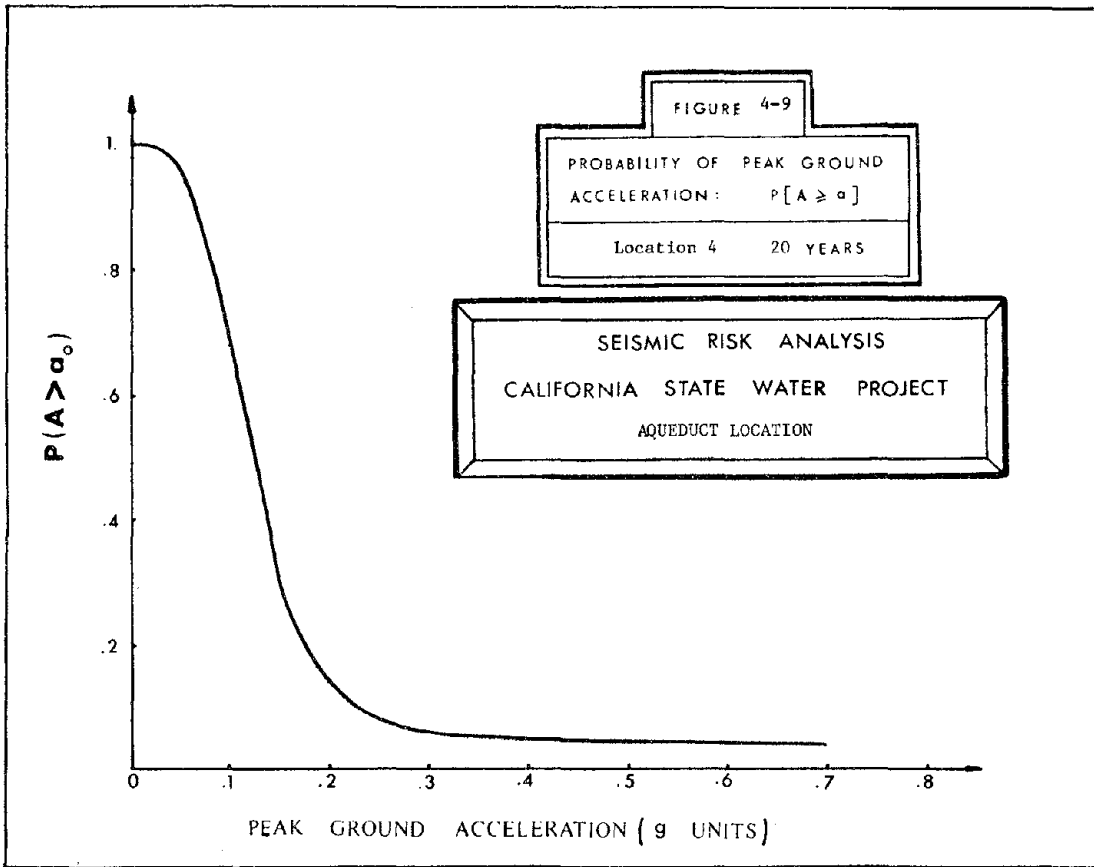
Table 4-2

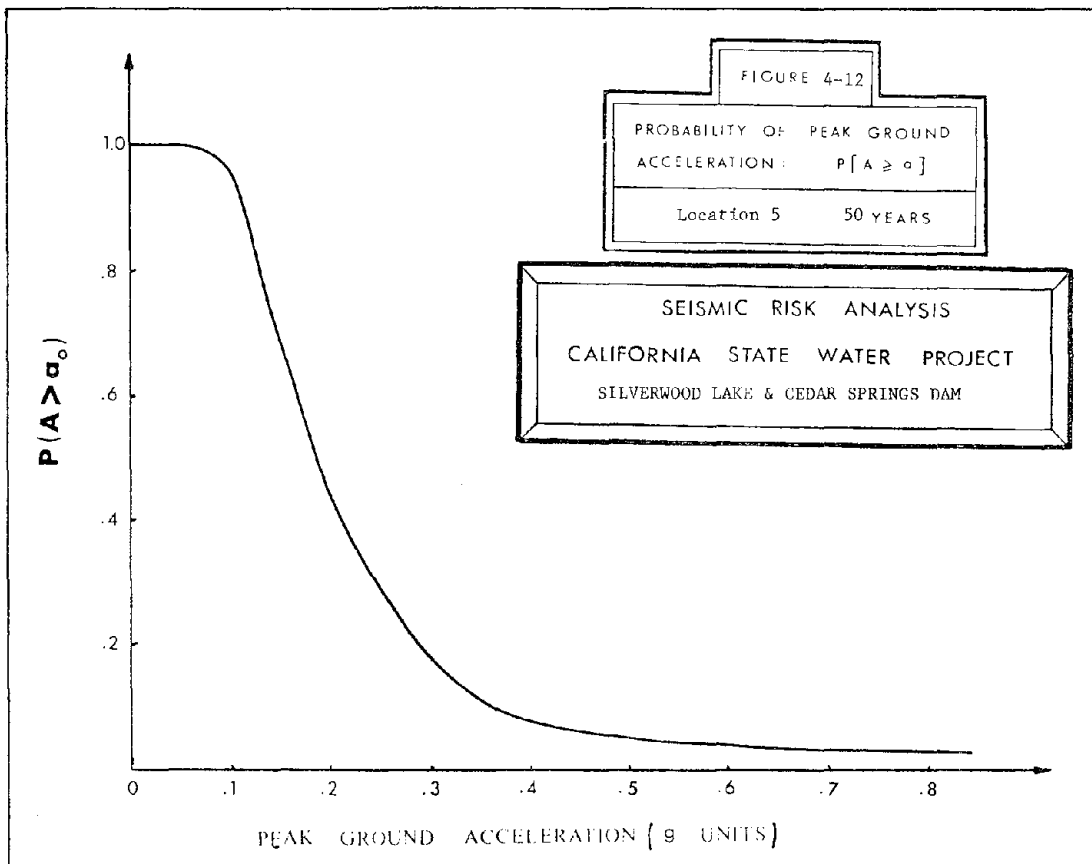
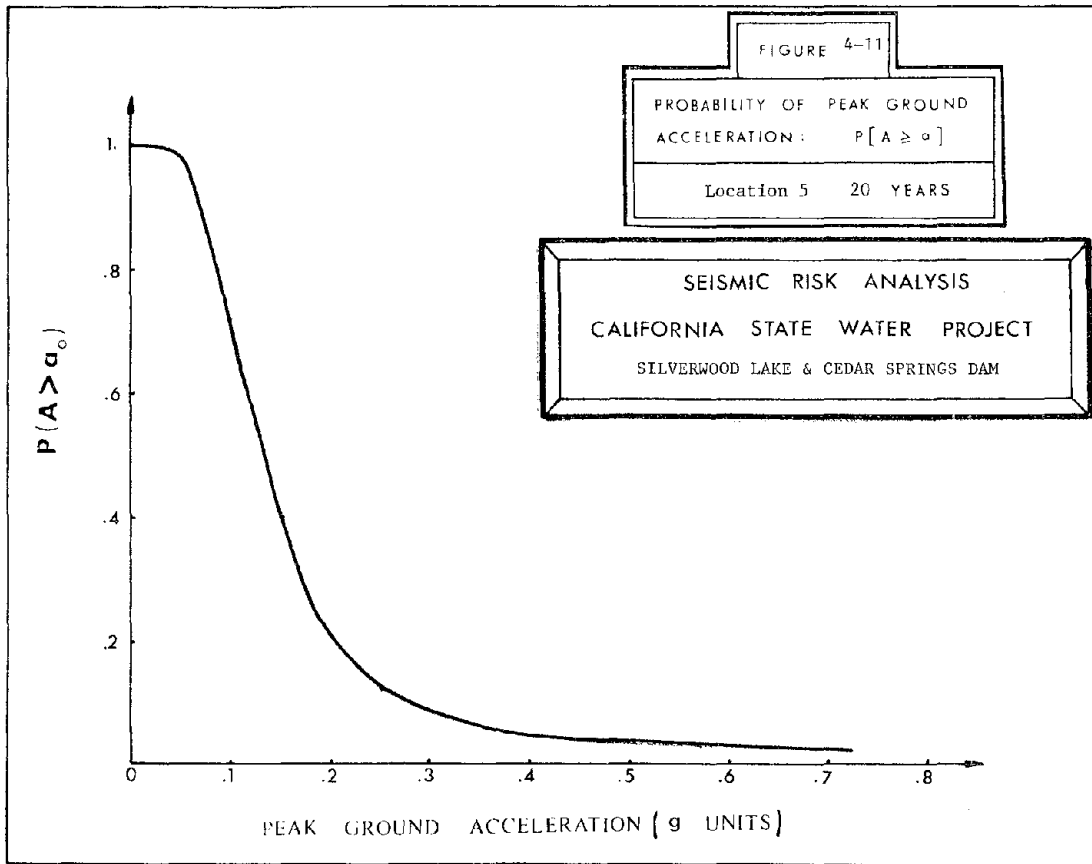
Site No.	Site Name	Longitude	Latitude
1	Tehachapi Afterbay	118.70°E	34.83°N
2	Pearblossom	117.94°E	34.54°N
3	Aqueduct	117.71°E	34.52°N
4	"	117.48°E	34.48°N
5	Cedar Springs Dam	117.34°E	34.34°N
6	San Bernardino Tunnel	117.36°E	34.26°N
7	" " "	117.36°E	34.22°N
8	Devil Canyon	117.36°E	34.23°N
9	Santa Ana Pipeline	117.33°E	34.04°N
10	" " "	117.28°E	33.97°N
11	Perris Dam	117.23°E	33.93°N

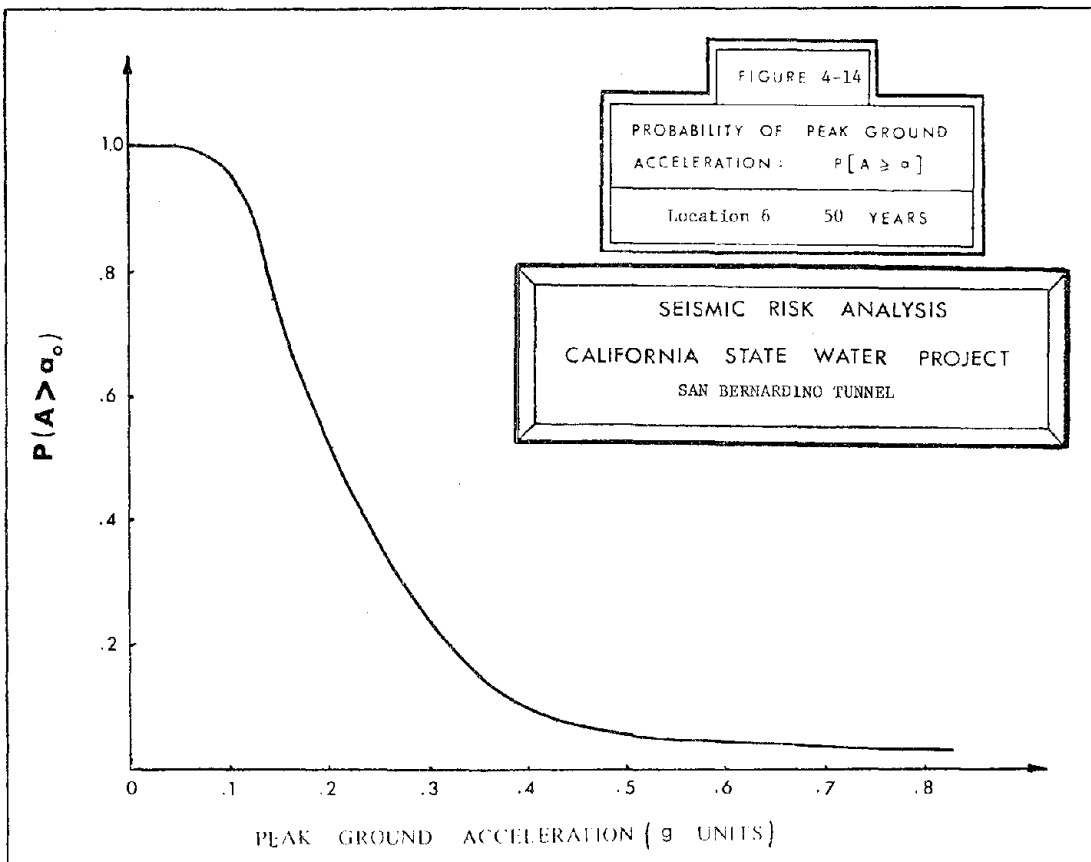
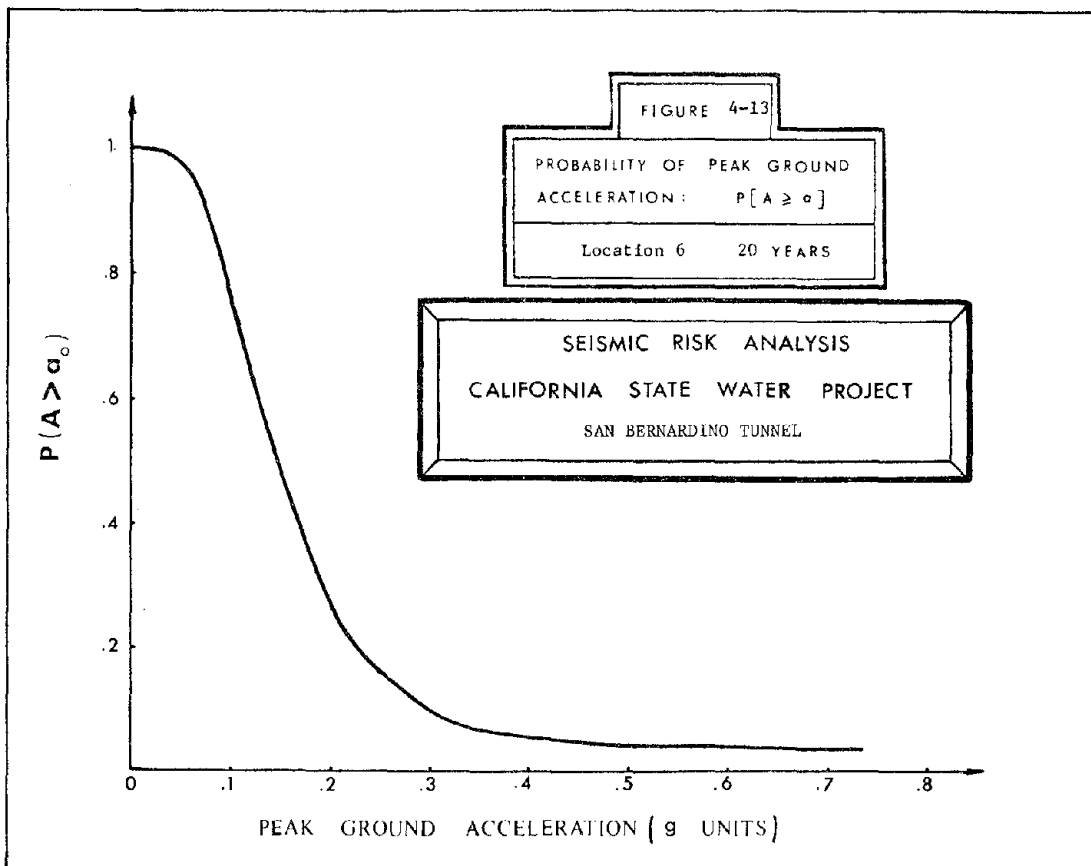


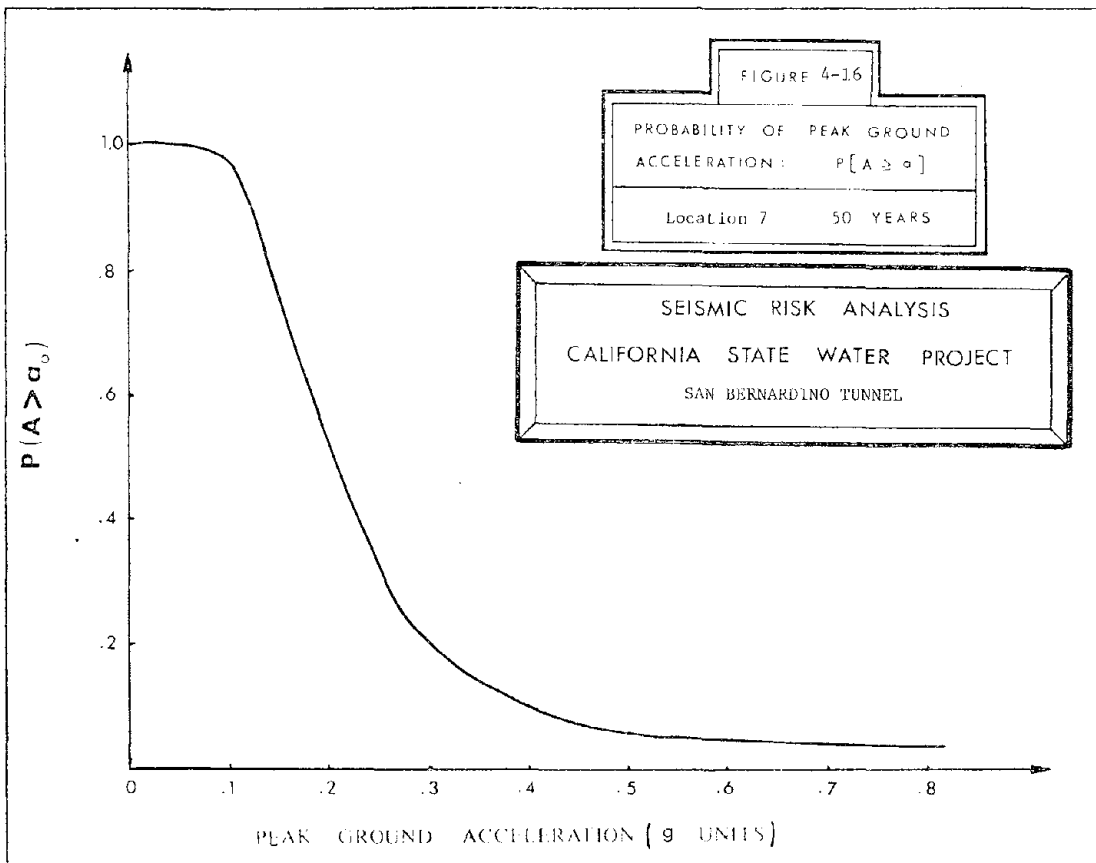
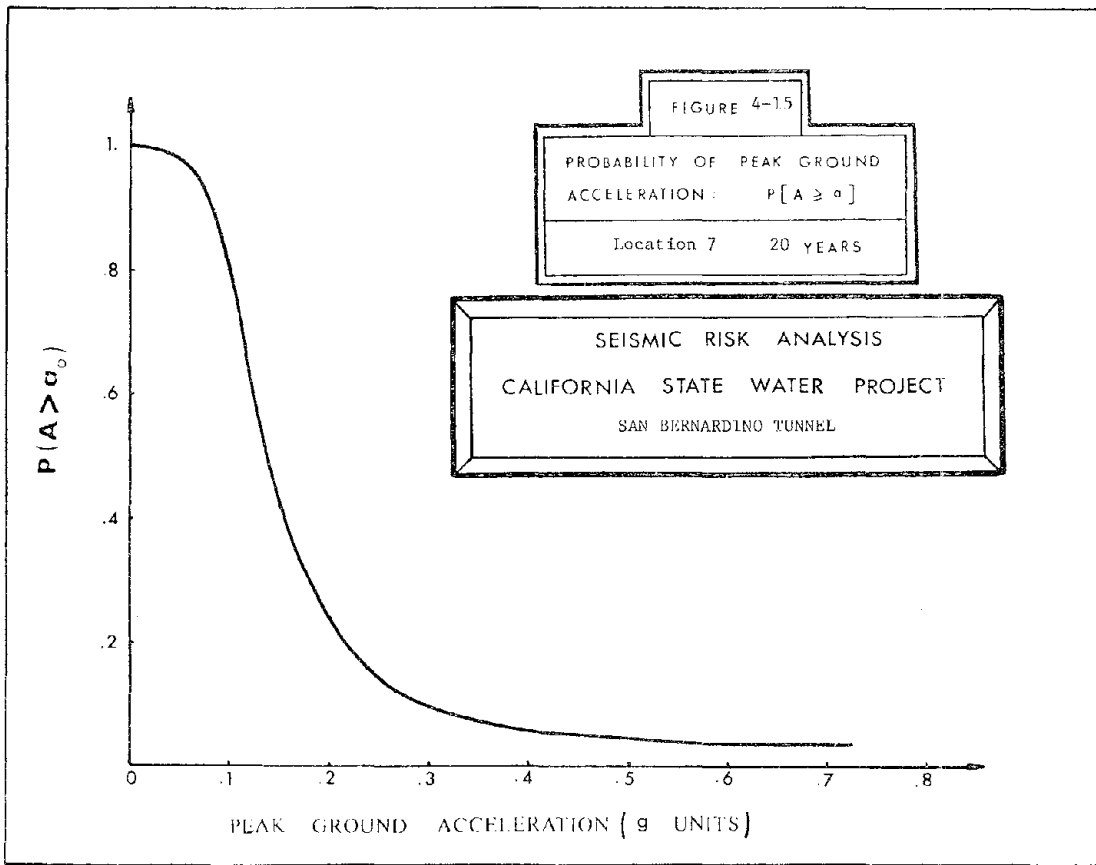


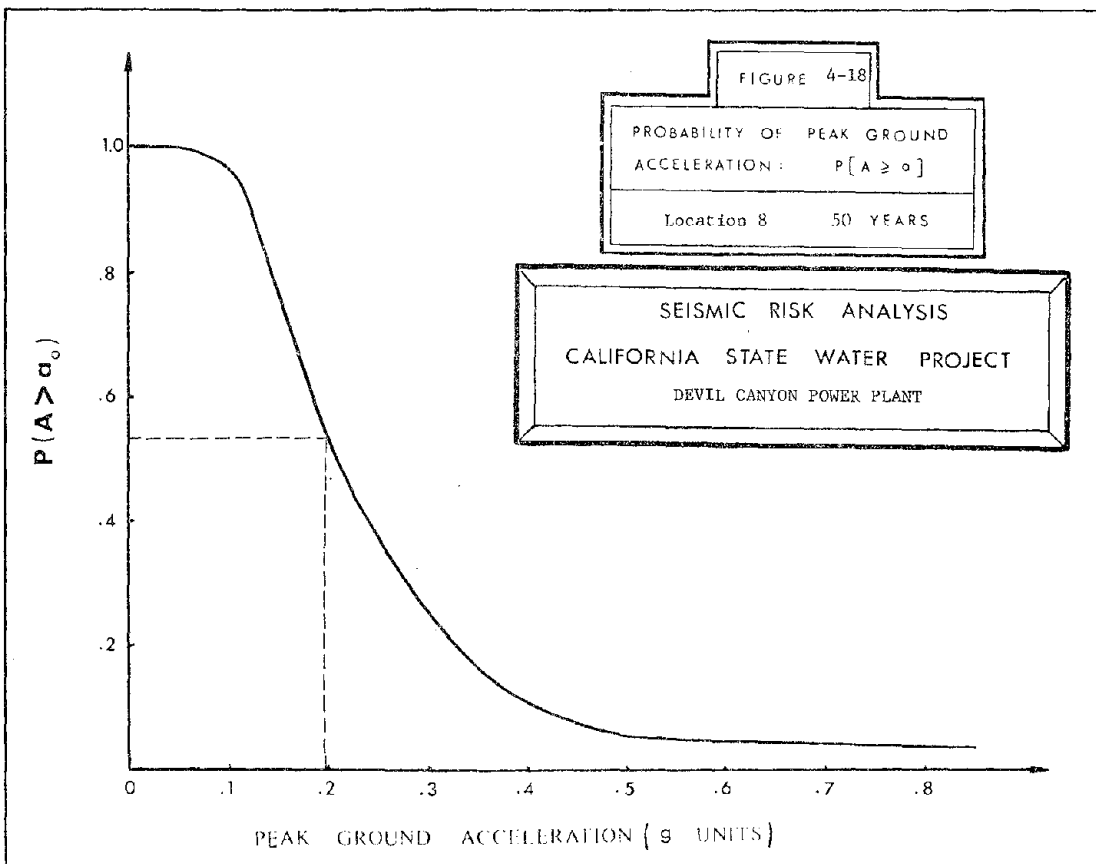
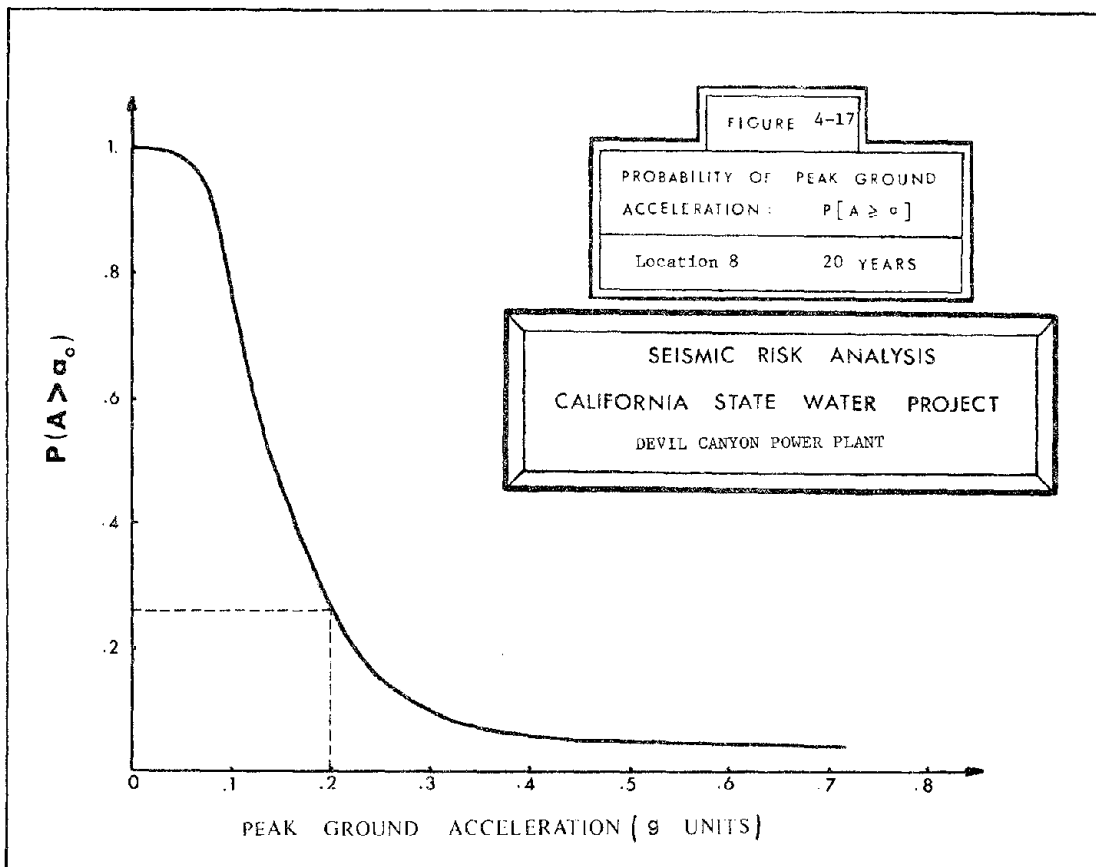


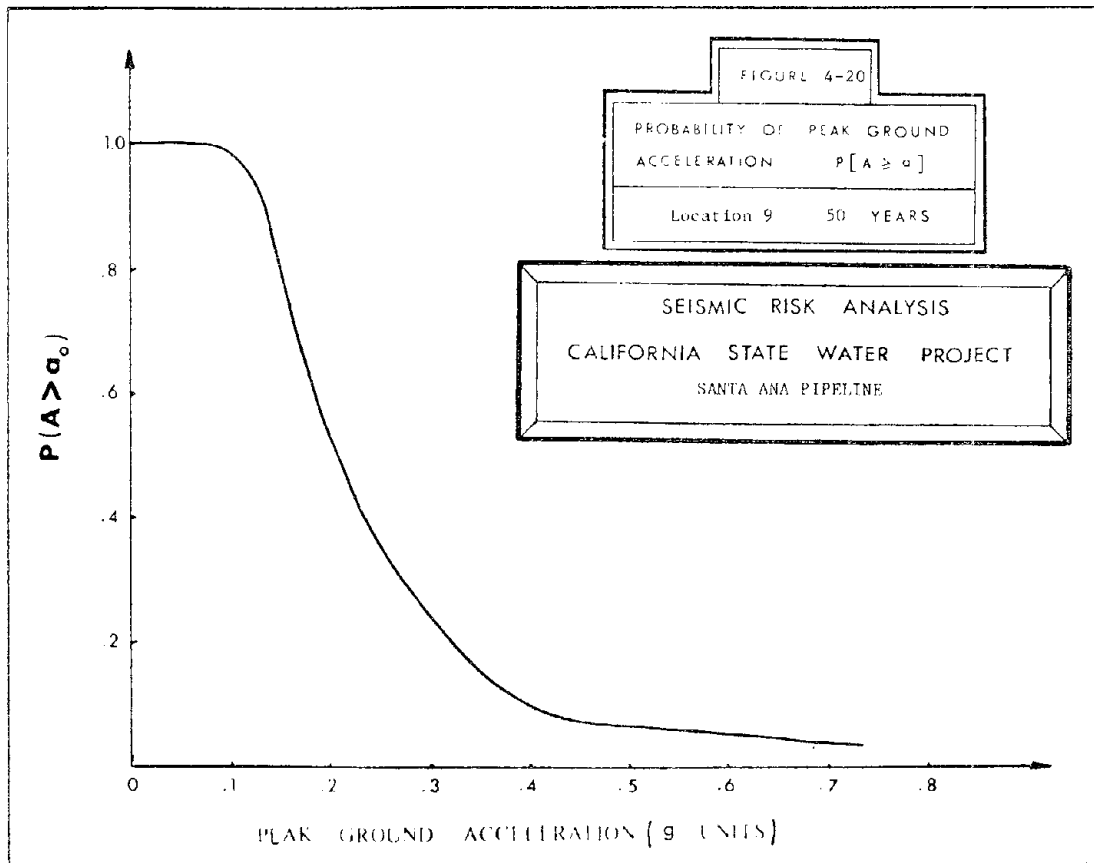
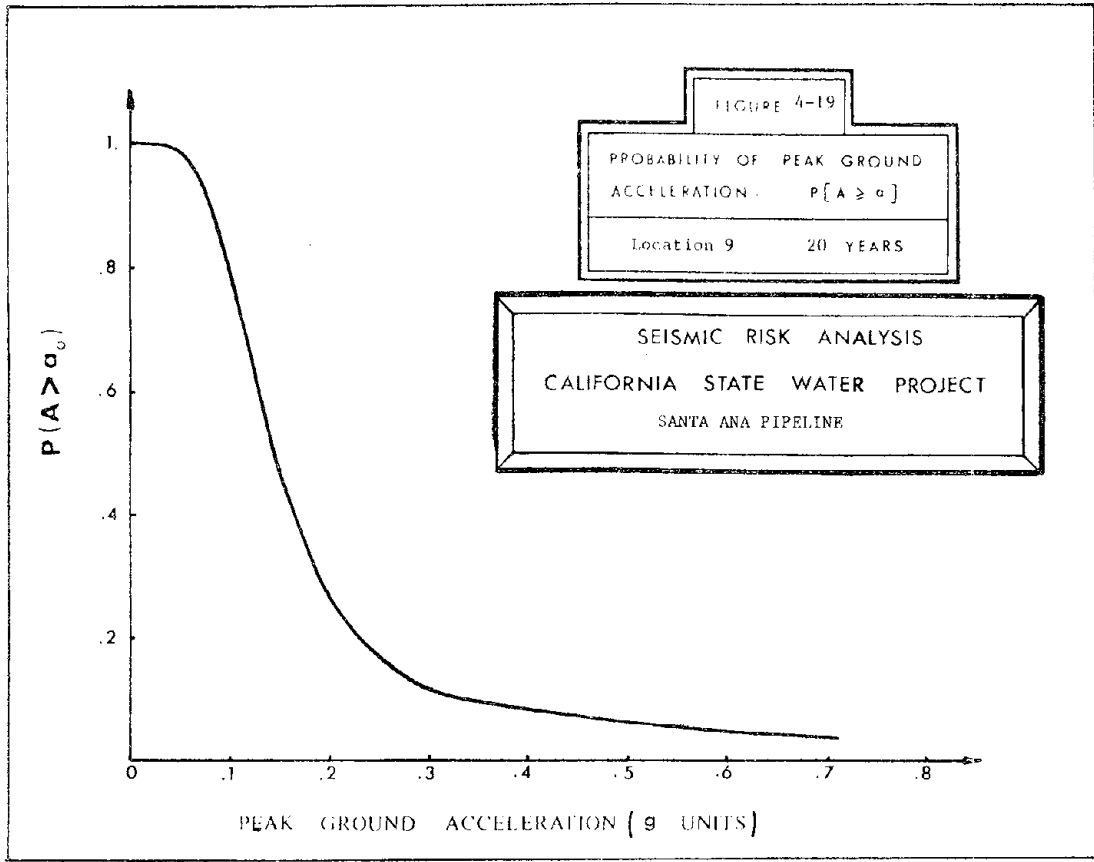


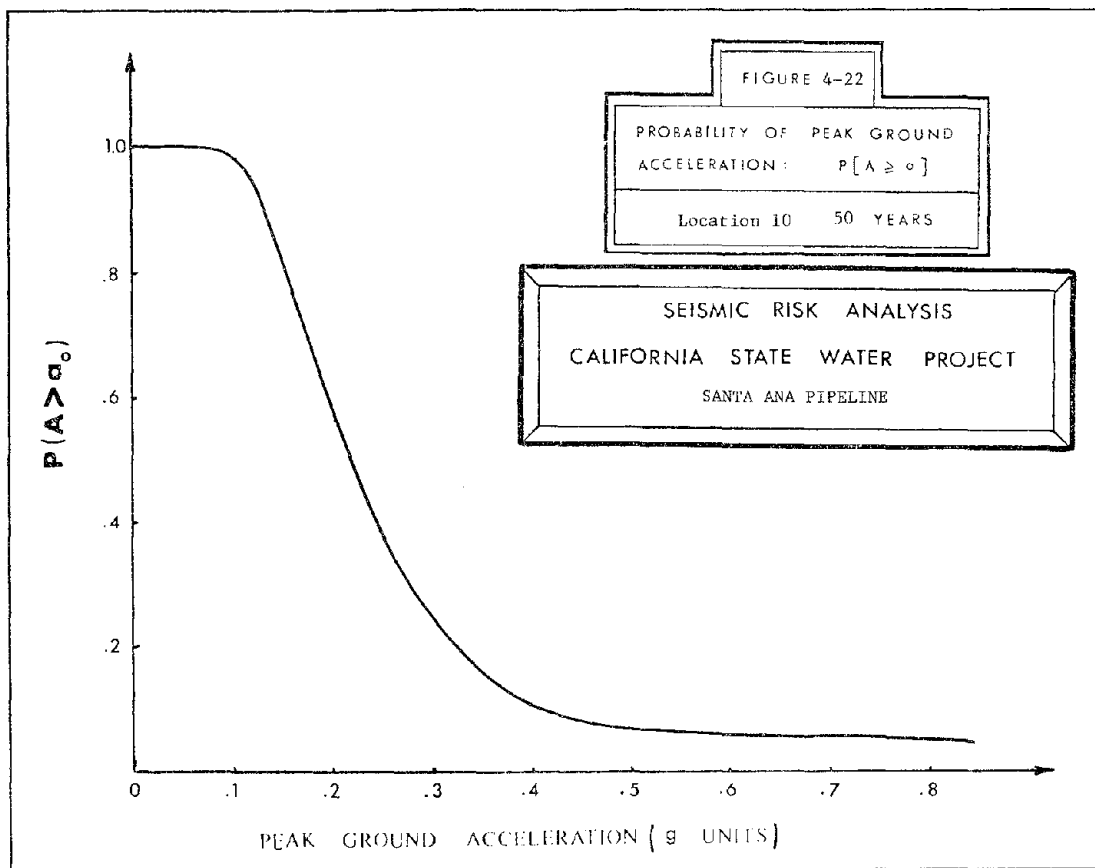
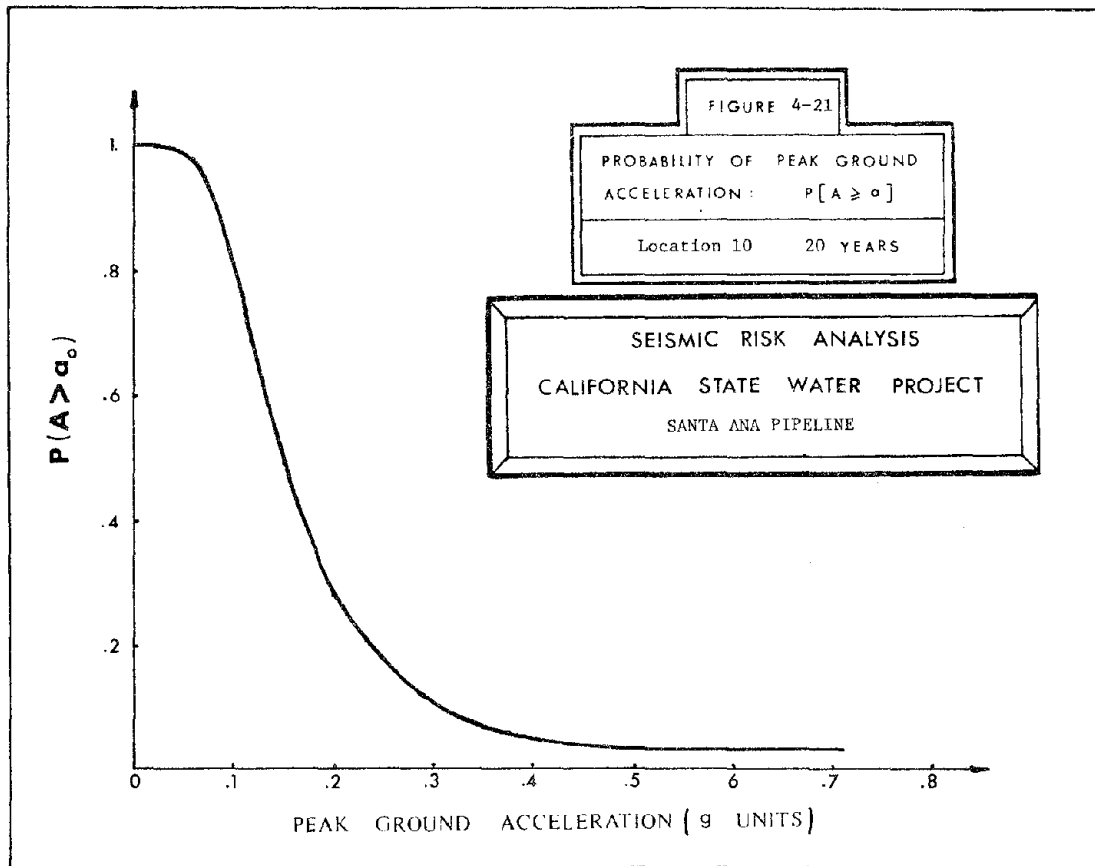


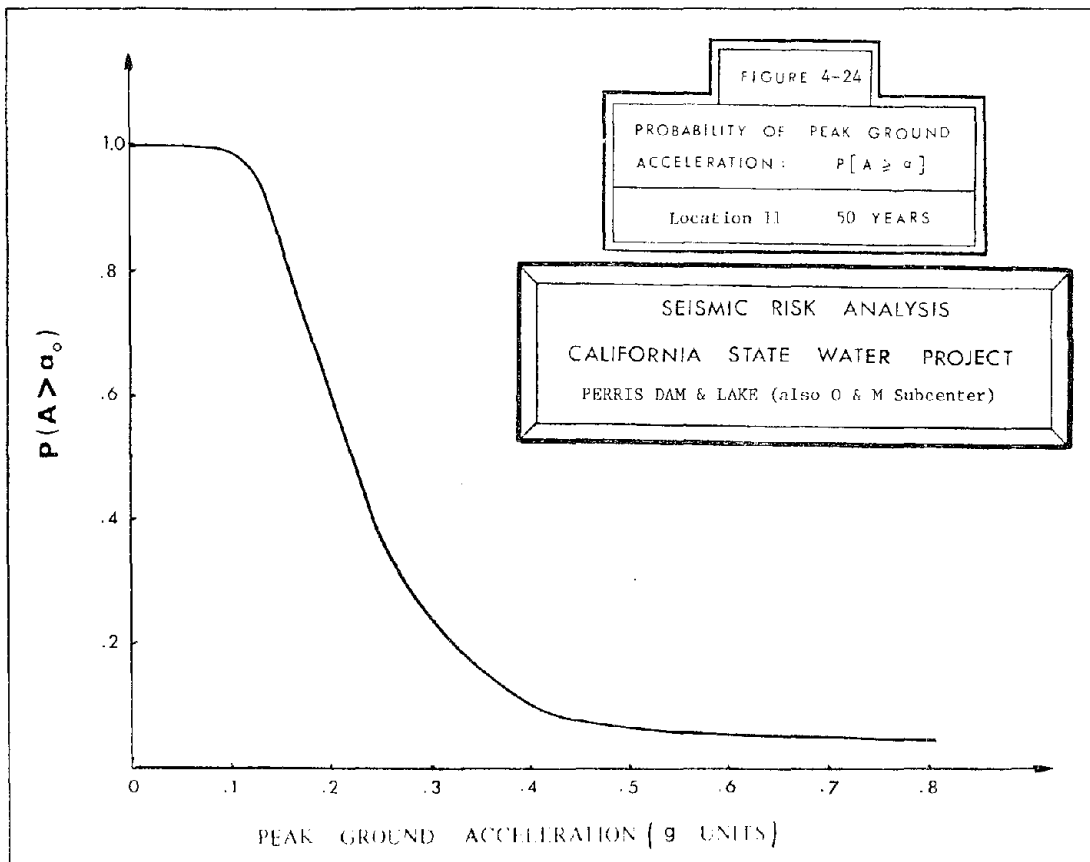
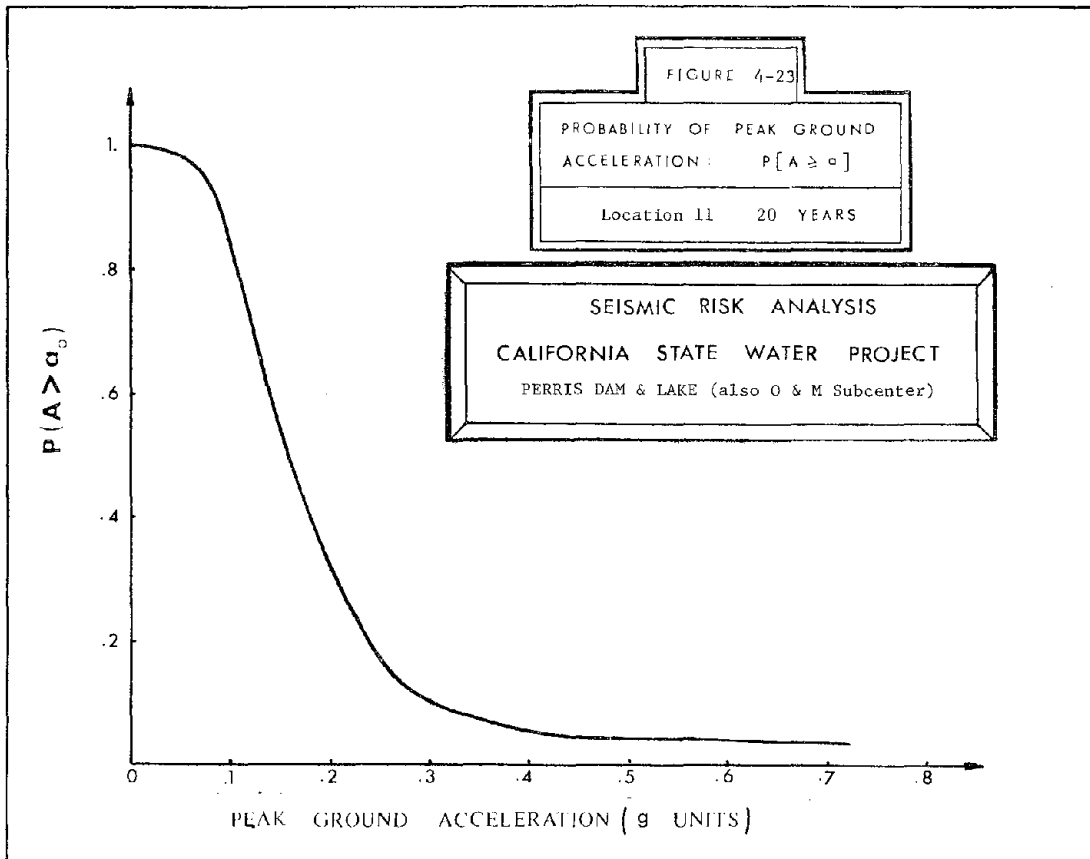












When one compares the cumulative distribution plots for different sites along the Reach C, one can get the idea about relative seismicity of each site. It can be said that the iso-acceleration maps presented in charts 3, 4 and 5 as well as the cumulative distribution plots presented in Figures 4-3 through 4-24 represent engineering information about seismic hazard for the region under consideration. For a given design of a facility, these hazard maps or hazard graphs can be used to evaluate the seismic risk for the SWP Reach C. This aspect will be discussed in Chapter 5.

Acceleration Zone Graphs (AZG)

In developing the probabilistic information about the peak ground acceleration as a function of time, it is assumed that the forecasting process is Poisson. This process implies that the events are independent in time and space. Using this assumption and the appropriate attenuation relationship, the iso-acceleration maps for the region were developed. For a given site, the cumulative distribution functions were also presented in the previous section.

Consider the cumulative distribution function of peak ground acceleration for the Devil Canyon Power Plant. (Figure 4-17). Then, the probability of exceeding 0.20g in 20 years is

$$P_{20}(A > 0.20g) = .254 \quad 4-2$$

Equation 4-2 implies that there is approximately 25 percent chance of exceeding 0.20g at least once in 20 years. Thus, there is 75 percent chance that 0.20g will not be exceeded in 20 years. From the Binomial

probability law, for independent trials, with probability p of success at each trial, the probability of r successes in n trials is given by

$$p_n(r) = \frac{n!}{r!(n-r)!} p^r (1-p)^{n-r} \quad 4-3$$

$$r = 0, 1, \dots, n;$$

$$n = r, r + 1, \dots$$

Let each trial be a one year duration for which one is observing the level of peak ground acceleration. Define success as that event when the peak ground acceleration for a year exceeds 0.20g. Thus, the probability of zero exceedance of level 0.20g in 20 years is the same as the probability of zero success in 20 trials. Hence, from equation 4-3

$$\begin{aligned} p_{20}(0) &= p^0 (1-p)^{20} \\ &= (1-p)^{20} \end{aligned}$$

From equation 4-2

$$p_{20}(0) = .746$$

$$(1-p)^{20} = .746$$

$$p = .01454$$

Thus, there is approximately 1.4 percent chance that in any given year, a peak ground acceleration of 0.20g will be exceeded. However, the return period is defined as

$$\text{Return period} = \text{RP} = \frac{1}{p} \quad 4.4$$

Thus, the return period RP for a peak ground acceleration of 0.2g at the Devil Canyon Power Plant is $\frac{1}{.014} = 69$ years.

It should be pointed out that this return period of 69 years, corresponding to 0.2g, obtained by using the cumulative distribution function for twenty years exposure time, does not change if one uses the cumulative distribution function corresponding to 50 year exposure time for the same site. For example, for a 50 year exposure time, the probability of exceeding 0.2g is fifty two percent. Thus,

$$P_{50}(A \geq 0.20g) = .52 \quad 4-5$$

Hence $P_{50}(A < 0.20g) = .48$

or $P_{50}(0) = (1-p)^{50} = .48$

which gives $p = .01454$

and hence $\text{Return Period RP} = 69 \text{ years}$

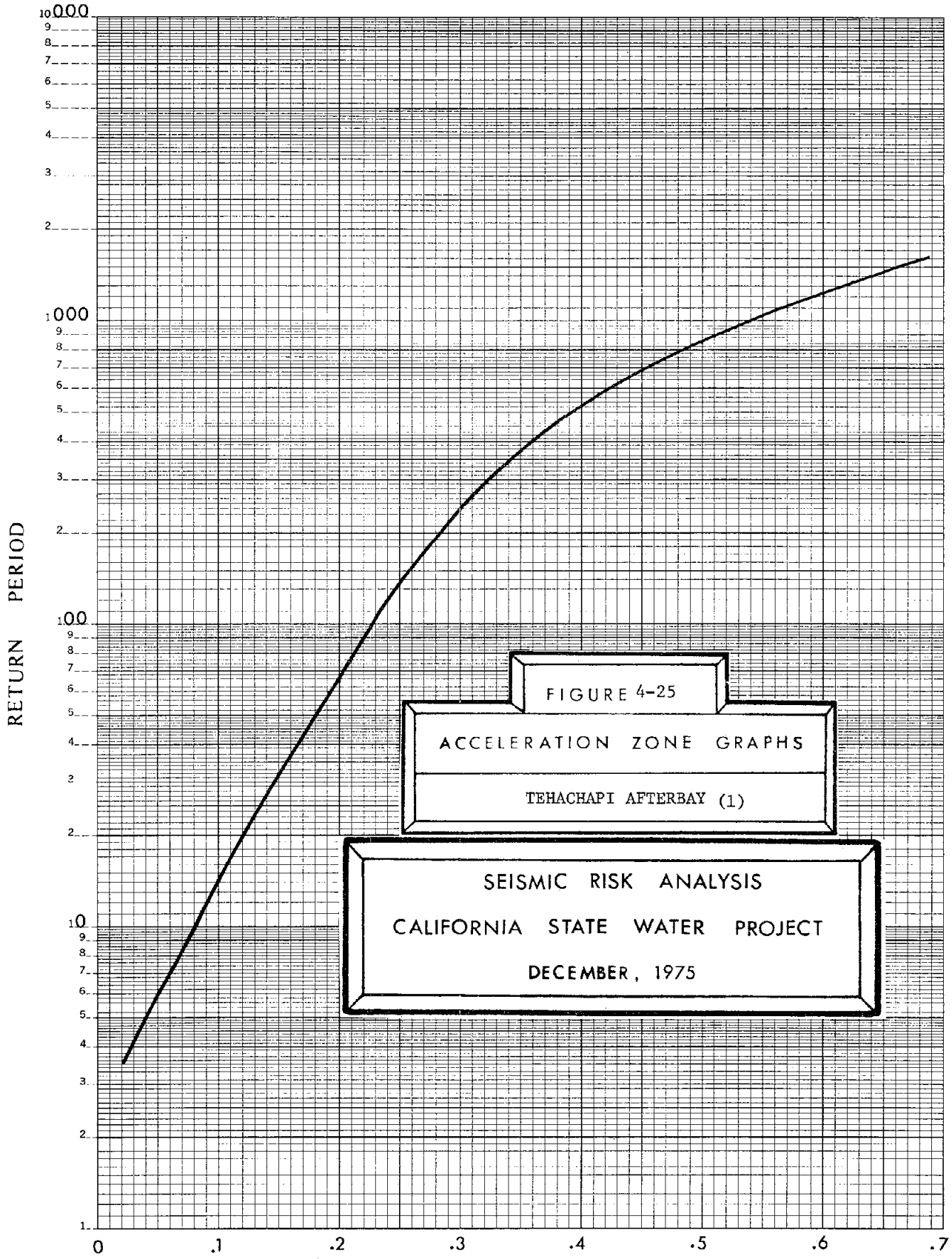
Table 4-3 shows return periods for all the eleven sites considered for various levels of peak ground accelerations. It should be emphasized that the reciprocal of the return period represents the "risk" or probability of exceeding a given level of the peak ground acceleration per year. The following statements should be understood in using the concept of return period:

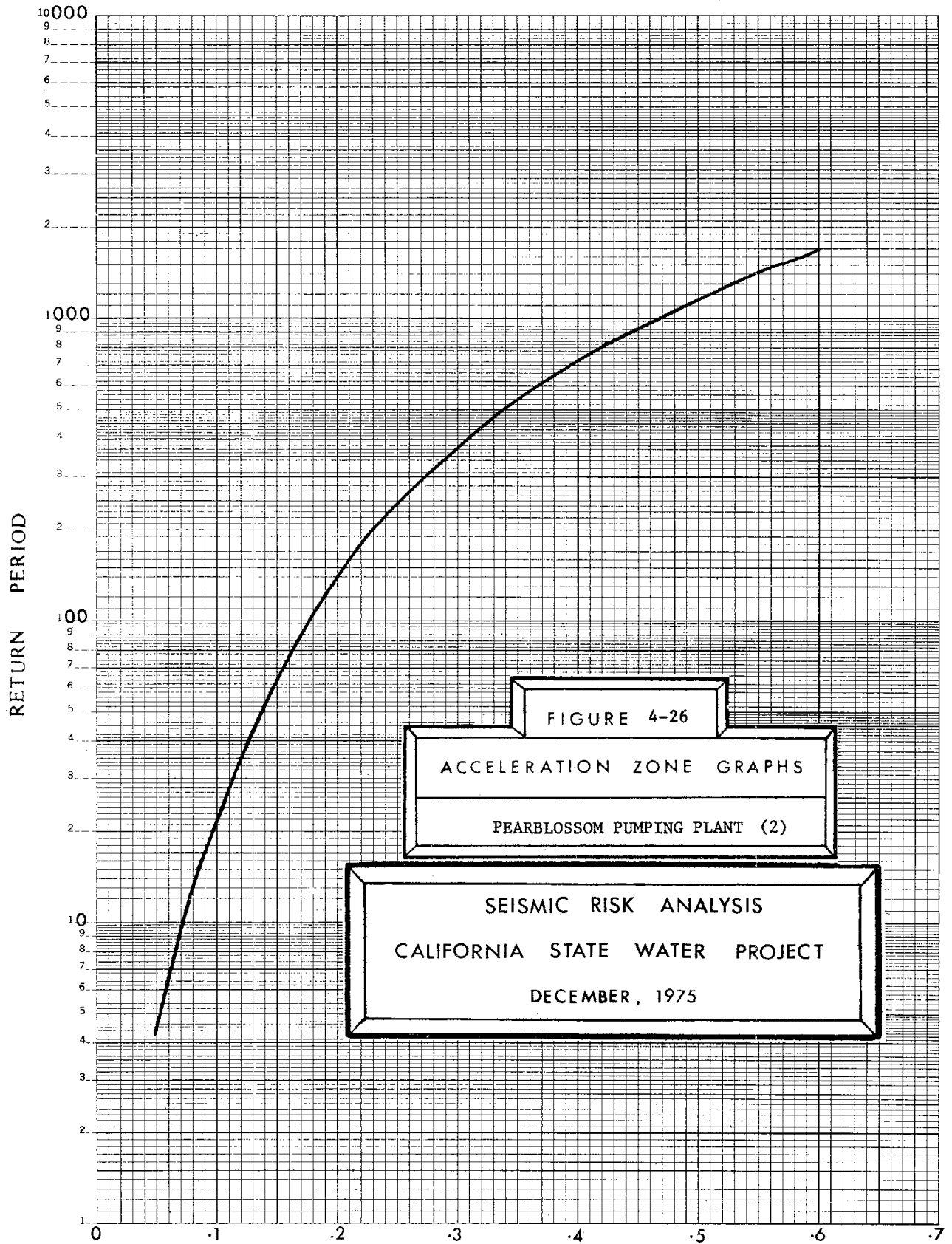
- (1) A return period is the mean (or average) waiting time for an event of interest. Thus, the average waiting time between two events producing peak ground accelerations above 0.2g at the Devil Canyon Power Plant is approximately 69 years.

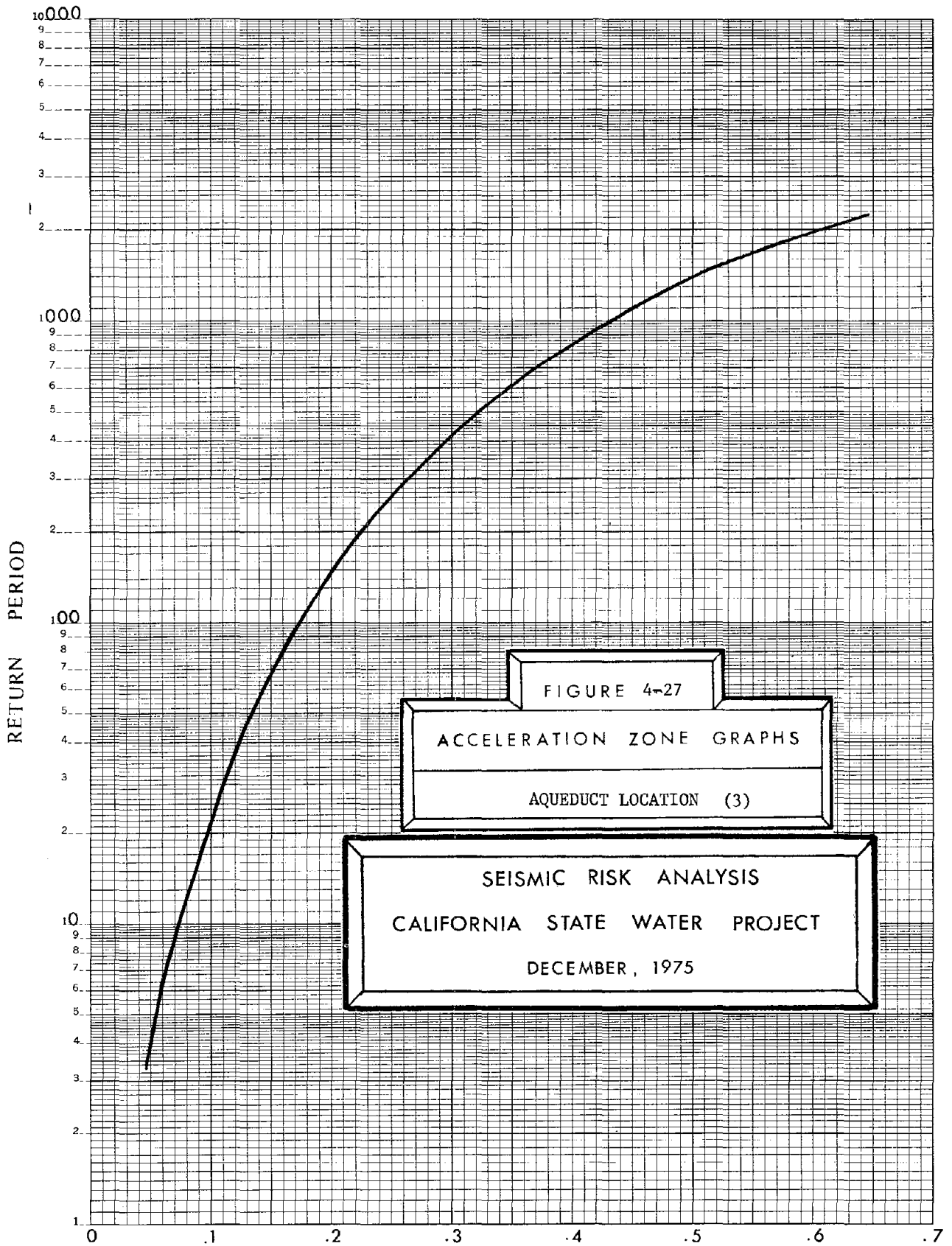
- (2) The probability that an event corresponding to a return period RP will occur in any given year is given by $p = 1/RP$. Thus, the probability of exceeding 0.20g for the Devil Canyon Power Plant is $1/69 = .014$.
- (3) The probability that not a single event of the RP type will occur in RP years is approximately given by .368. Thus, in 69 years, there will not be a single event producing the peak ground acceleration above 0.20g is approximately 0.368.

A graph, relating the peak ground acceleration and the return period, is called an Acceleration Zone Graph (AZG). A separate AZG can be obtained for each of the eleven sites considered here. Figures 4-25 through 4-35 give AZG's for these eleven sites. It can be seen from these graphs that a return period corresponding to any level of peak ground acceleration can be obtained. The reciprocal of that return period gives the "risk" or probability of exceeding the corresponding PGA per year.

As mentioned above, the return period and hence "risk" per year of exceeding any specific level of PGA for a given site can be obtained from an AZG corresponding to that site. However, to obtain the probability of exceeding a specific level of PGA at a site during a given economic life, one needs to relate the economic life, return period and the overall risk. In reference 1, these relationships were developed. Table 4-4 and Figure 4-36 gives a relationship between the economic life, the return period and the probability of exceedance during the economic







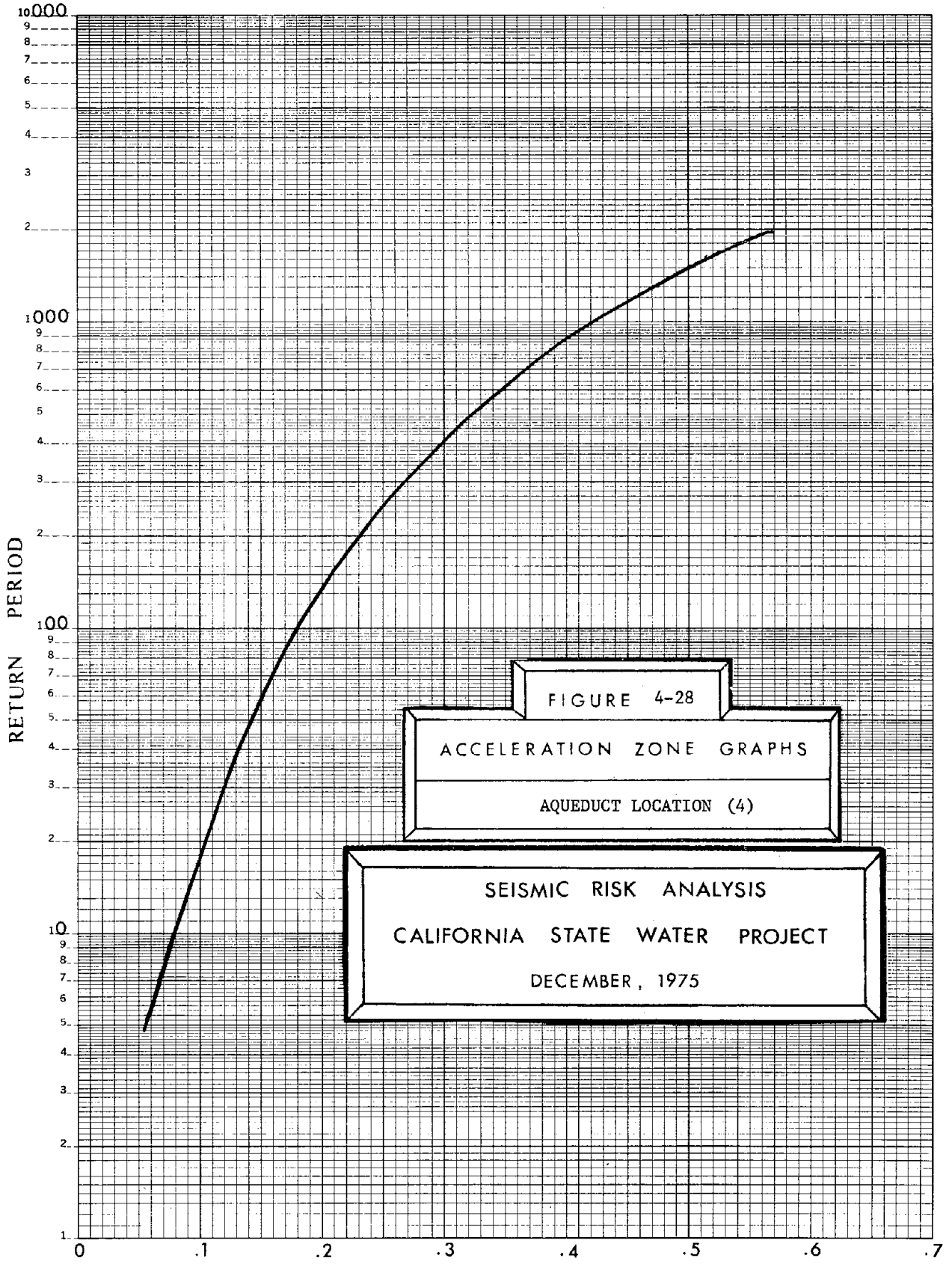


FIGURE 4-28

ACCELERATION ZONE GRAPHS
 AQUEDUCT LOCATION (4)

SEISMIC RISK ANALYSIS
 CALIFORNIA STATE WATER PROJECT
 DECEMBER, 1975

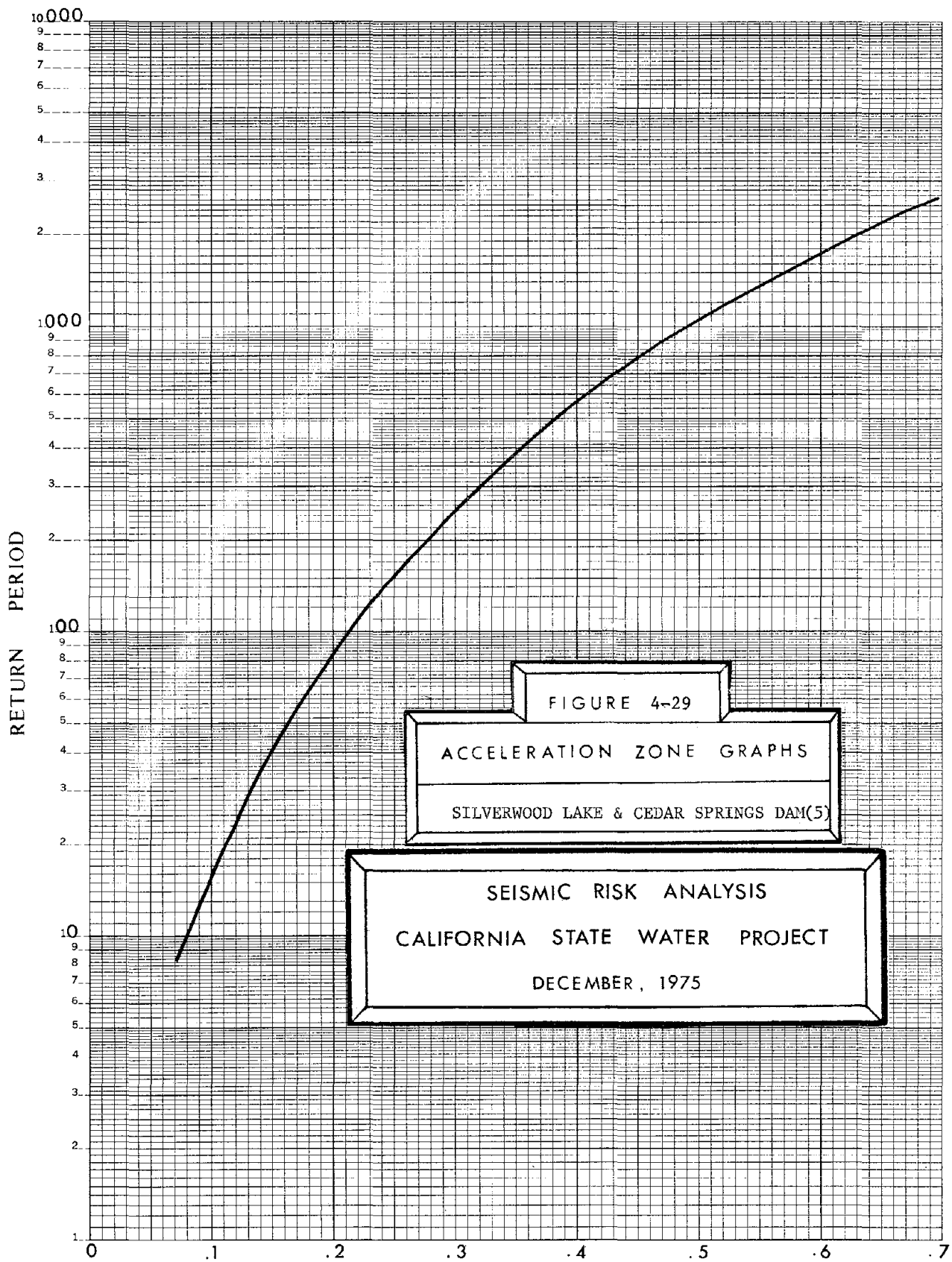


FIGURE 4-29

ACCELERATION ZONE GRAPHS

SILVERWOOD LAKE & CEDAR SPRINGS DAM(5)

SEISMIC RISK ANALYSIS
 CALIFORNIA STATE WATER PROJECT
 DECEMBER, 1975

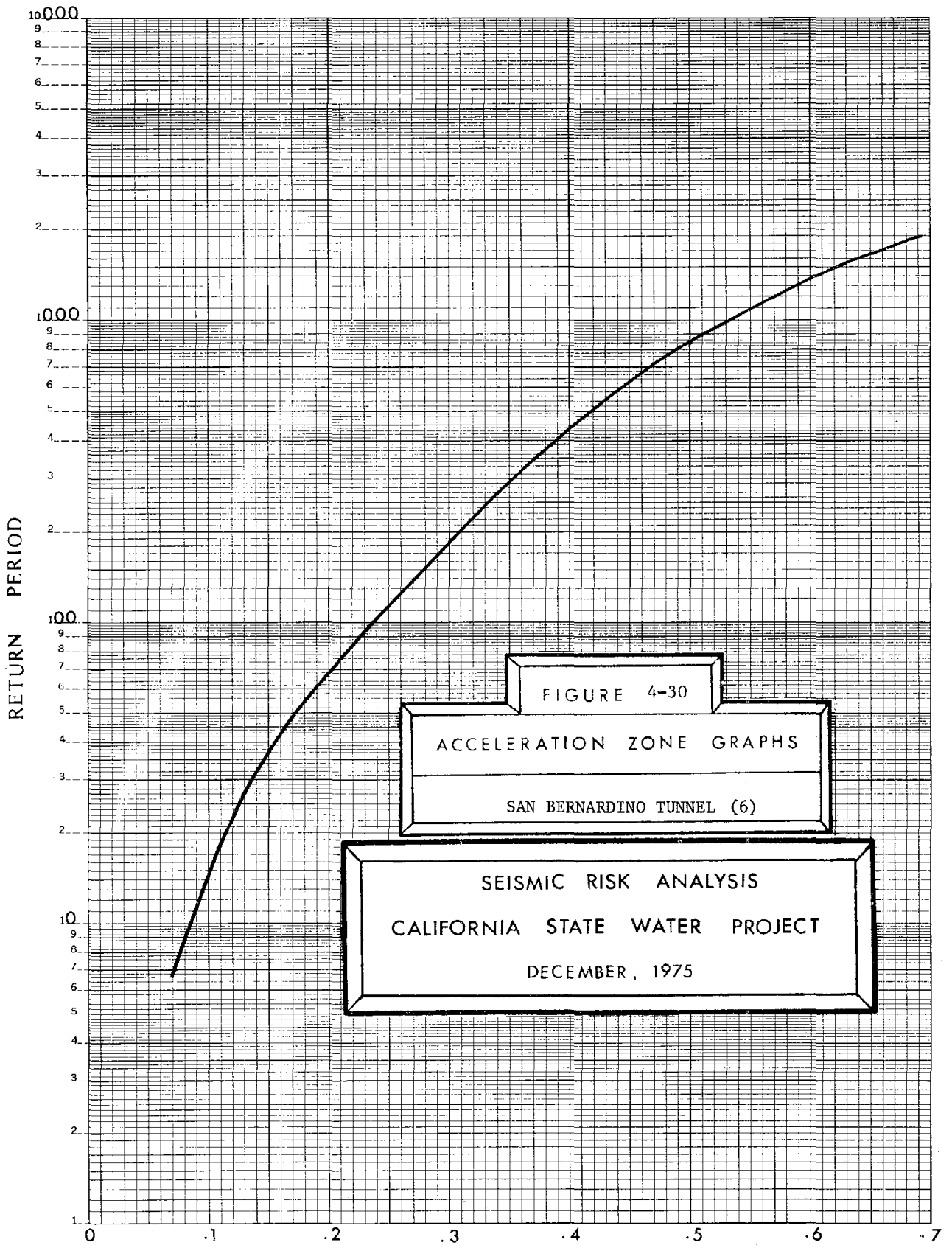
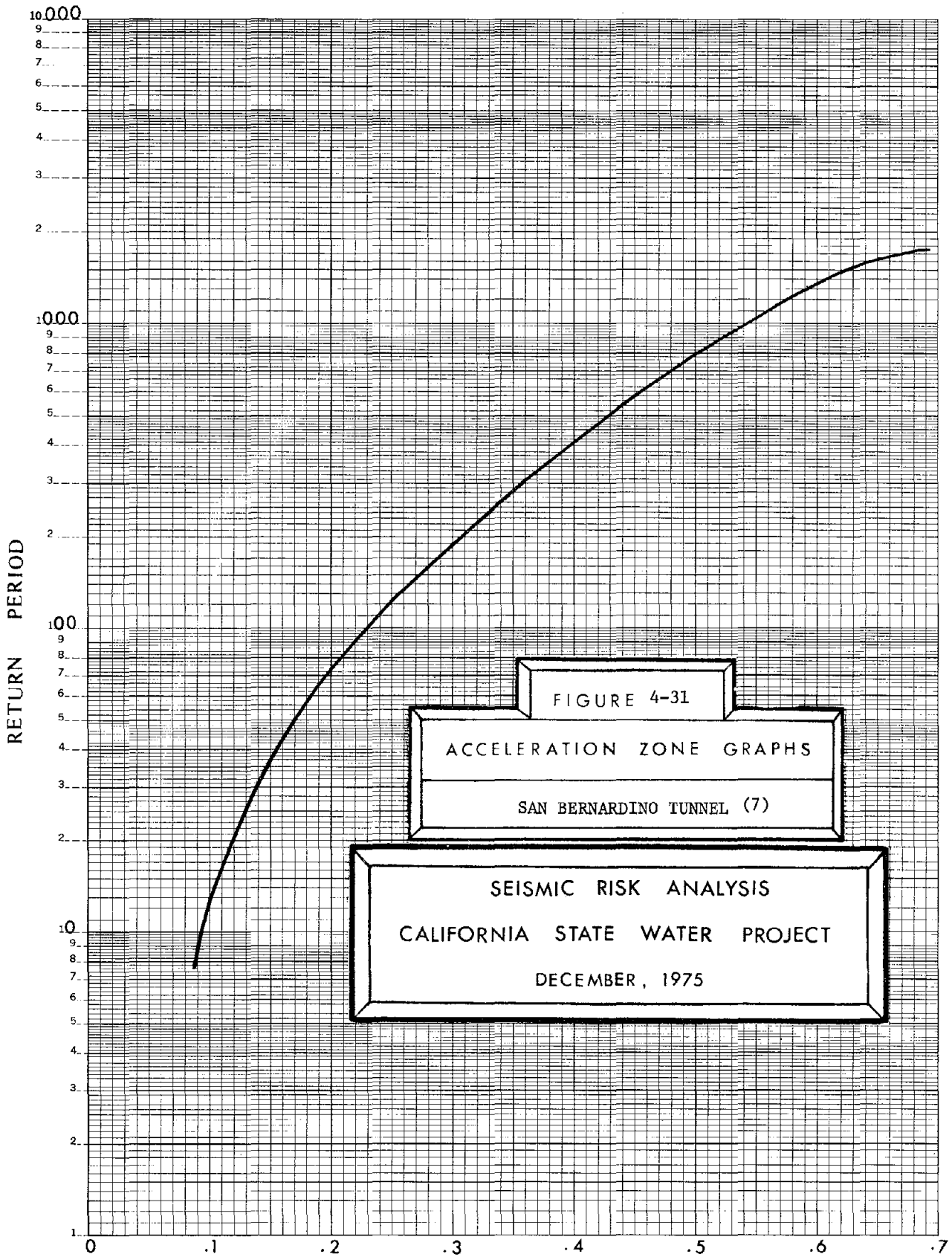
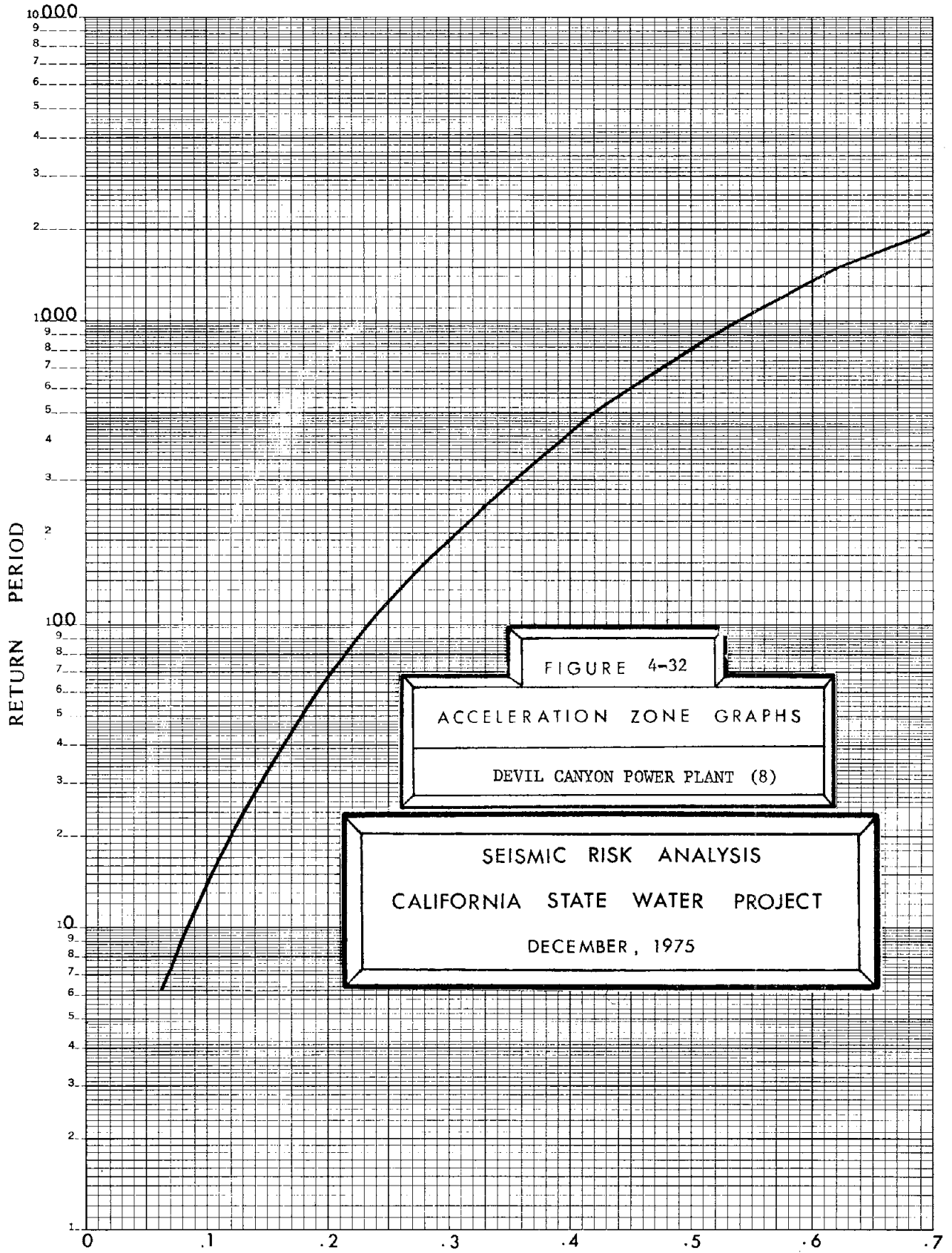


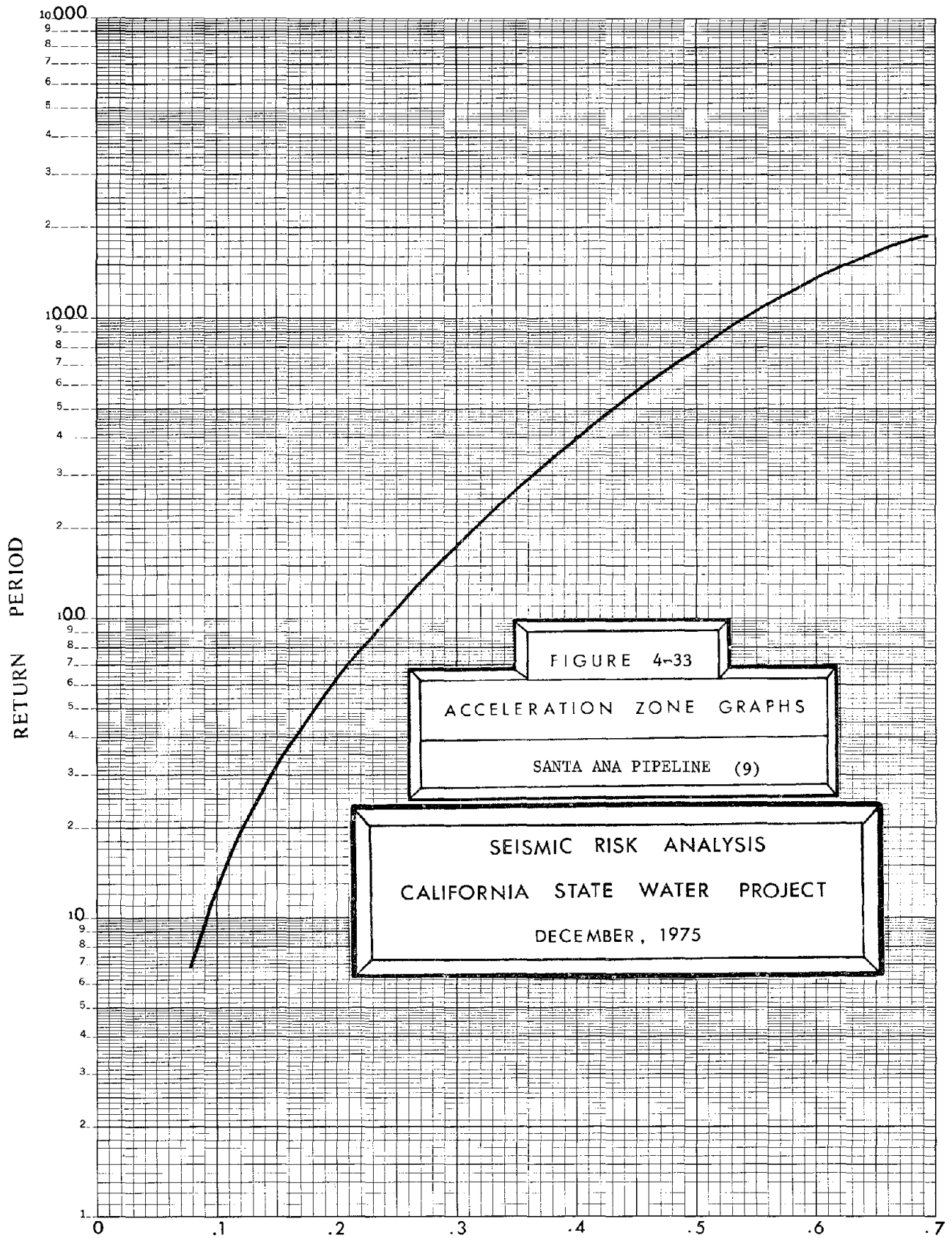
FIGURE 4-30

ACCELERATION ZONE GRAPHS
 SAN BERNARDINO TUNNEL (6)

SEISMIC RISK ANALYSIS
 CALIFORNIA STATE WATER PROJECT
 DECEMBER, 1975







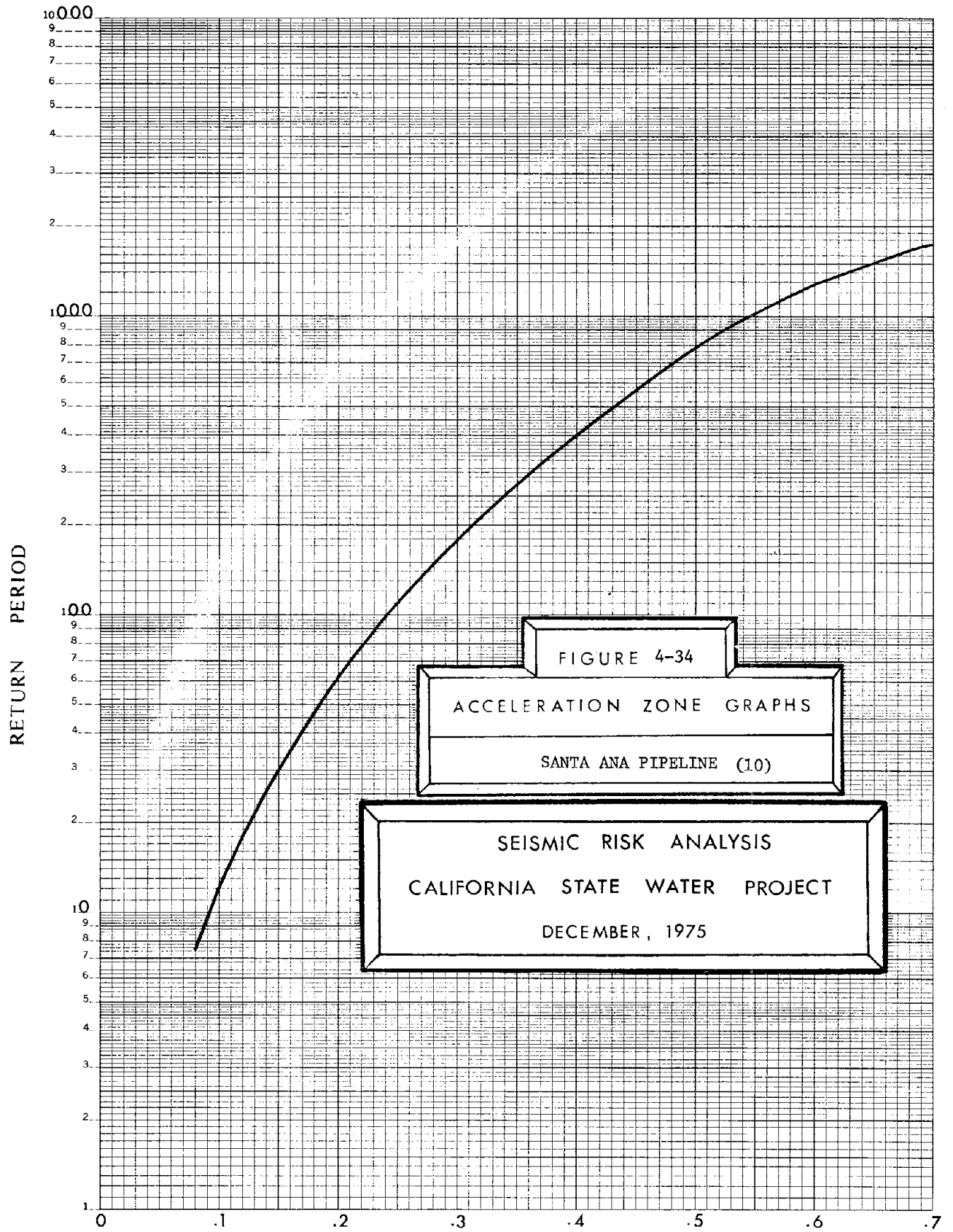


FIGURE 4-34

ACCELERATION ZONE GRAPHS

SANTA ANA PIPELINE (10)

SEISMIC RISK ANALYSIS
 CALIFORNIA STATE WATER PROJECT
 DECEMBER, 1975

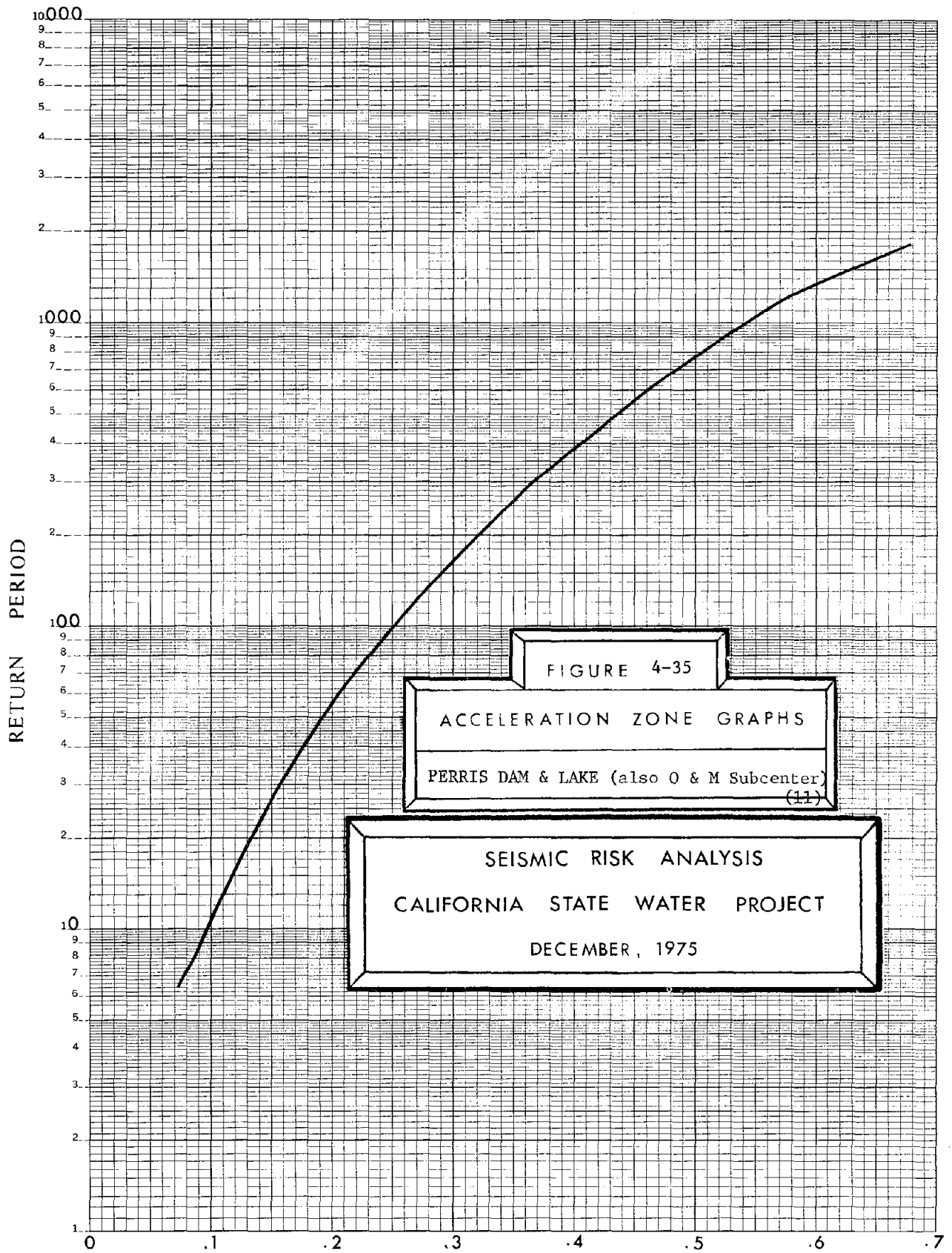


Table 4-3

PGA g units	Tehachapi Afterbay #1	Pearblossom Pumping Plant #2	Aqueduct Loc. 3	Aqueduct Loc. 4	Silverwood Lake #5	San Bernardino Tunnel #6	San Bernardino Tunnel #7	Devil Canyon #8	Santa Ana Pipeline #9	Santa Ana Pipeline #10	Perris Dam #11
.05	6	5	4	4	5	3	3	5	3	3	4
.10	14	22	22	18	16	15	13	14	13	12	11
.15	32	64	69	58	40	37	37	33	32	30	22
.20	66	140	146	135	84	70	74	69	64	62	56
.25	114	245	260	250	155	115	120	120	110	110	100
.30	240	375	420	400	250	185	190	190	175	180	165
.35	370	540	610	610	380	290	280	290	270	275	260
.40	530	730	830	870	570	440	420	430	400	400	380
.45	690	920	1100	1160	790	630	580	600	570	570	560
.50	860	1150			1080	840	790	800	780	780	770
.55	1060					1100	1050	1060	1070	1030	1030
.60											

Return Period in Years for Various Sites

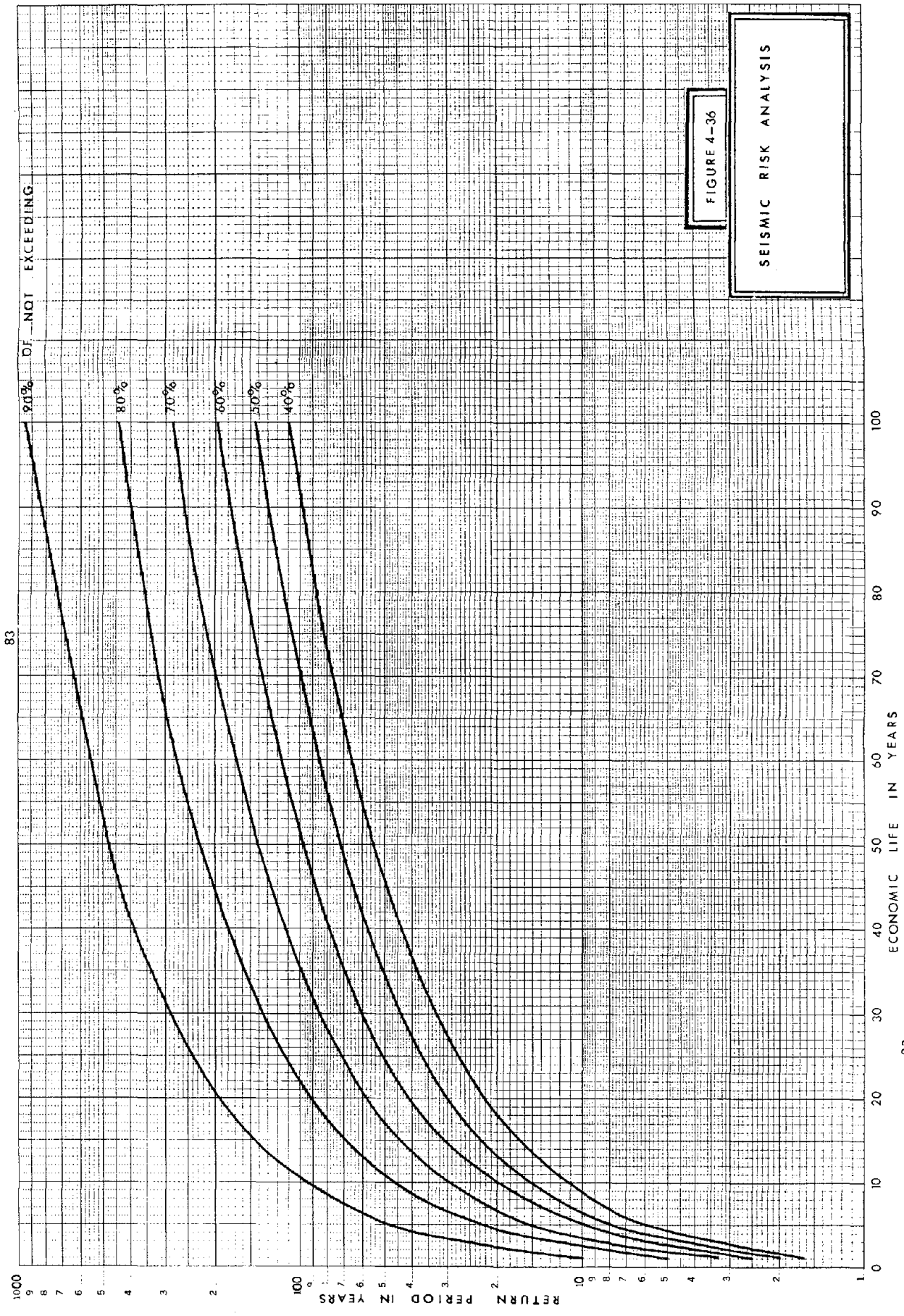
life. As an example, consider the Devil Canyon Power Plant site. From Table 4-3, the return period corresponding to 0.5g peak ground acceleration is 800 years. Thus, the probability of exceeding 0.5g per year is 0.125 percent. (1/800). If the economic life of the power plant is 100 years, what is the probability of exceeding 0.5g during this 100 year economic life? From Table 4-4 or Figure 4.36 and by interpolation, this probability would be 11.75 percent. As another example, assume that one wishes to determine the peak ground acceleration which has 10% chance of exceedance in a 50 year economic life of a facility. From Table 4-4, this probability corresponds to a return period of 475 years. Thus, for the Devil Canyon Power Plant site, the corresponding PGA is approximately .41g. Thus, by appropriately using Tables 4-3 and 4-4 and the AZG's for a given site, one could determine the "loading" in terms of PGA and the associated "risks" or probabilities of exceedances for various economic time periods. Table 4-5 and Table 4-6 shows probabilities of exceeding 0.2g and 0.5g for various time periods and for the eleven sites under consideration. It can be seen that for all the sites, the probability of exceeding 0.2g is very high. In seven out of eleven sites, there is more than 10% chance that 0.5g PGA will be exceeded in the next 100 years. The significance of these results will be discussed in the next chapter.

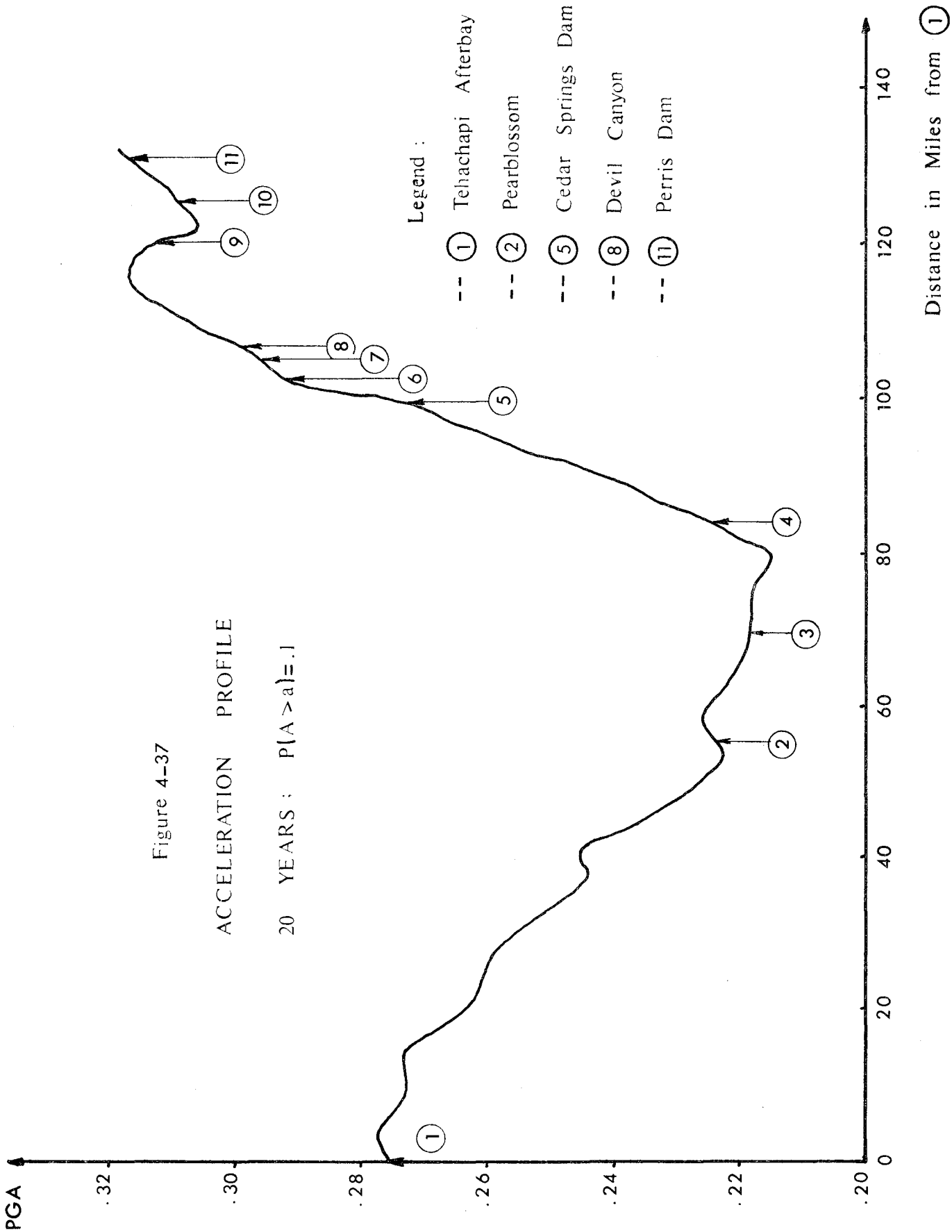
Figures 4-37, 4-38 and 4-39 show the acceleration profile of the Reach C for 20, 30 and 50 years respectively. It can be seen from these three figures that the highest ground shaking hazard lies between the Devil Canyon Power Plant and the Paris Dam. Again, the significance of this observation will be discussed in Chapter 5.

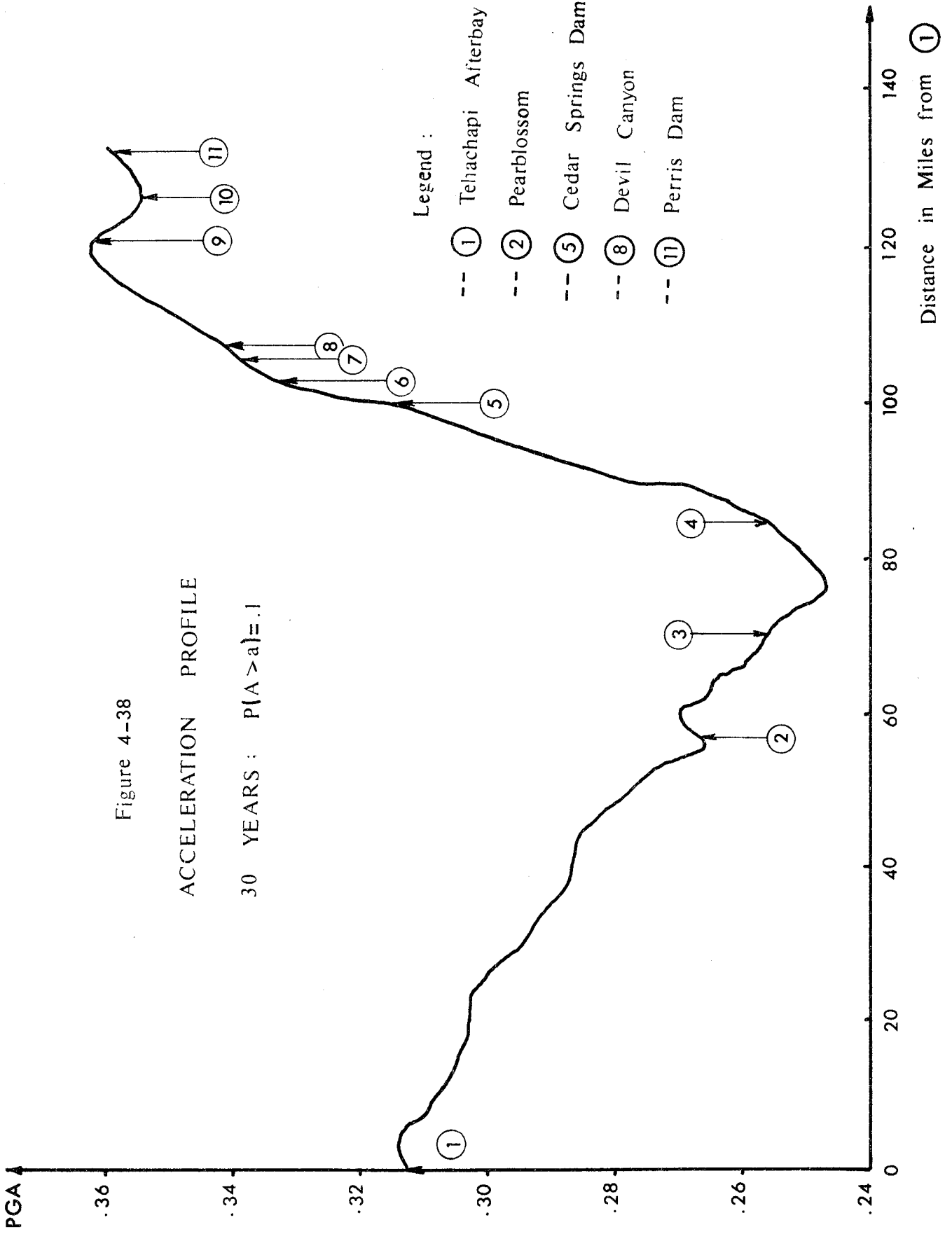
Table 4-4

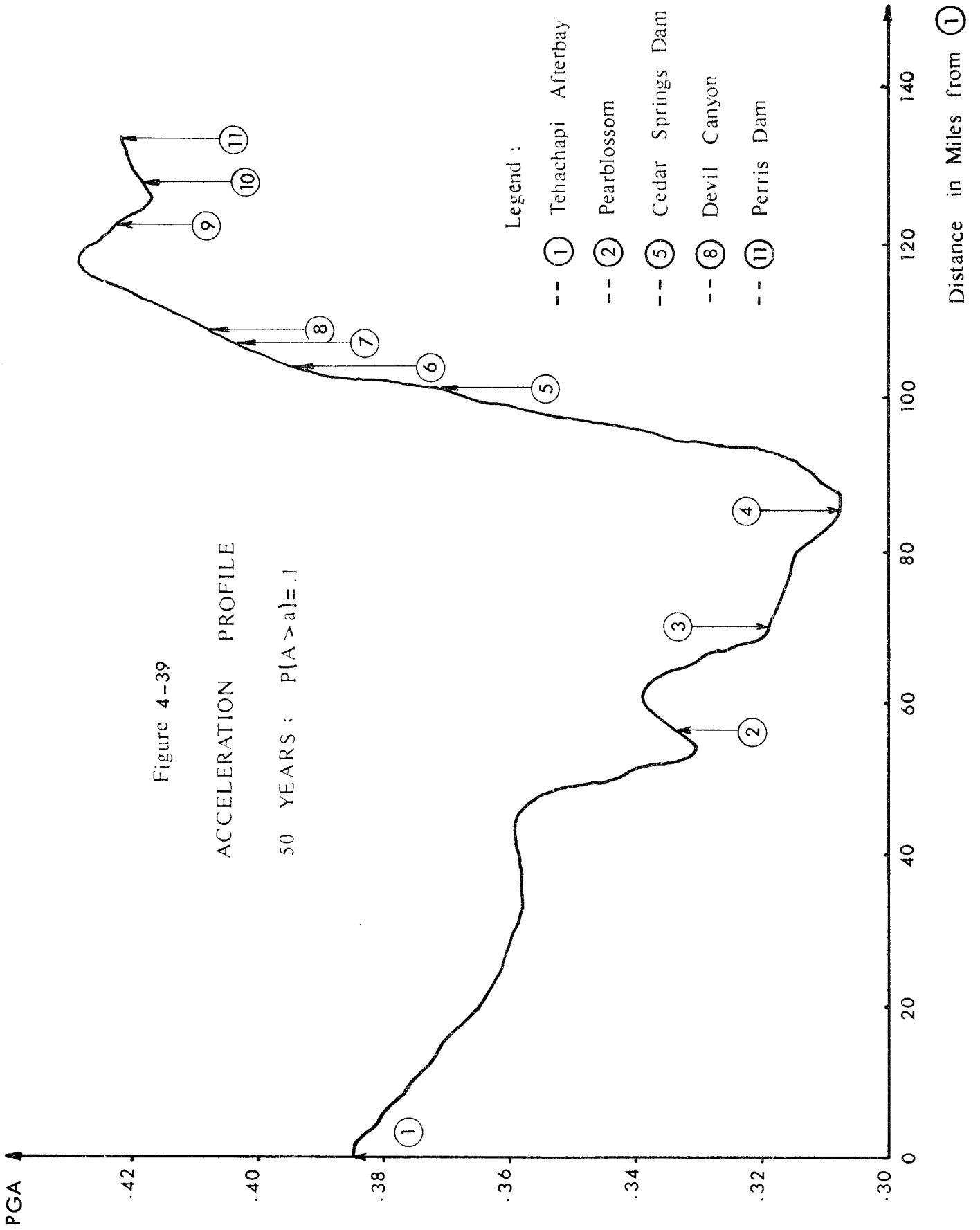
Return Period as a Function of Economic Life and Probability of Non-Exceedance

Economic Life Years	"Risk" or Probability of exceeding %					
	10	20	30	40	50	100
10	95	190	285	390	475	950
20	45	90	135	180	225	449
30	29	57	84	113	140	281
40	20	40	59	79	98	196
50	15	29	44	58	72	145
60	11	22	33	44	55	110
70	9	17	25	34	42	84
80	7	13	19	25	31	63
90	5	9	14	18	22	44
95	4	7	11	14	18	34
99	3	5	7	9	11	22
99.5	2	4	6	8	10	19









Finally, Figures 4-40 and 4-41 show for various sites the relative seismic hazard as a function of time. For example, from Figure 4-40 or Table 4-5 there is 30 percent chance of exceeding 0.2g at the Pearblossom (site 2) pumping plant in 50 years. Again, it can be seen that for any given time period, Figures 4-40 and 4-41 or Tables 4-5 and 4-6 give an indication of relative ground shaking hazards and hence "risk potential" at various sites considered.

Table 4-5

Probability of Exceeding 0.2g in Percentage

Site	Time Period in Years			
	20	30	50	100
1	26	36.7	53.4	78.3
2	13.3	19.3	30	51
3	12.8	18.6	29	49.7
4	13.8	20	31	52.4
5	21.3	30	45	69.8
6	25	35	51.3	76.3
7	23.8	33.5	49.3	74.3
8	25.6	35.9	52.3	77.3
9	27.7	38.6	55.6	80.3
10	27.8	38.6	55.6	80.3
11	30.2	41.7	59.4	83.5

Table 4-6

Probability of Exceeding 0.5g in Percentage

Site	Time Period in Years			
	20	30	50	100
1	2.3	3.4	5.6	11
2	1.7	2.6	4.3	8.3
3	1.4	2.1	3.5	6.9
4	1.3	2.0	3.3	6.4
5	1.8	2.7	4.5	8.8
6	2.3	3.5	5.8	11.2
7	2.5	3.7	6.1	11.9
8	2.5	3.7	6.1	11.6
9	2.5	3.8	6.2	12.0
10	2.5	3.8	6.2	12.0
11	2.6	3.8	6.3	12.2

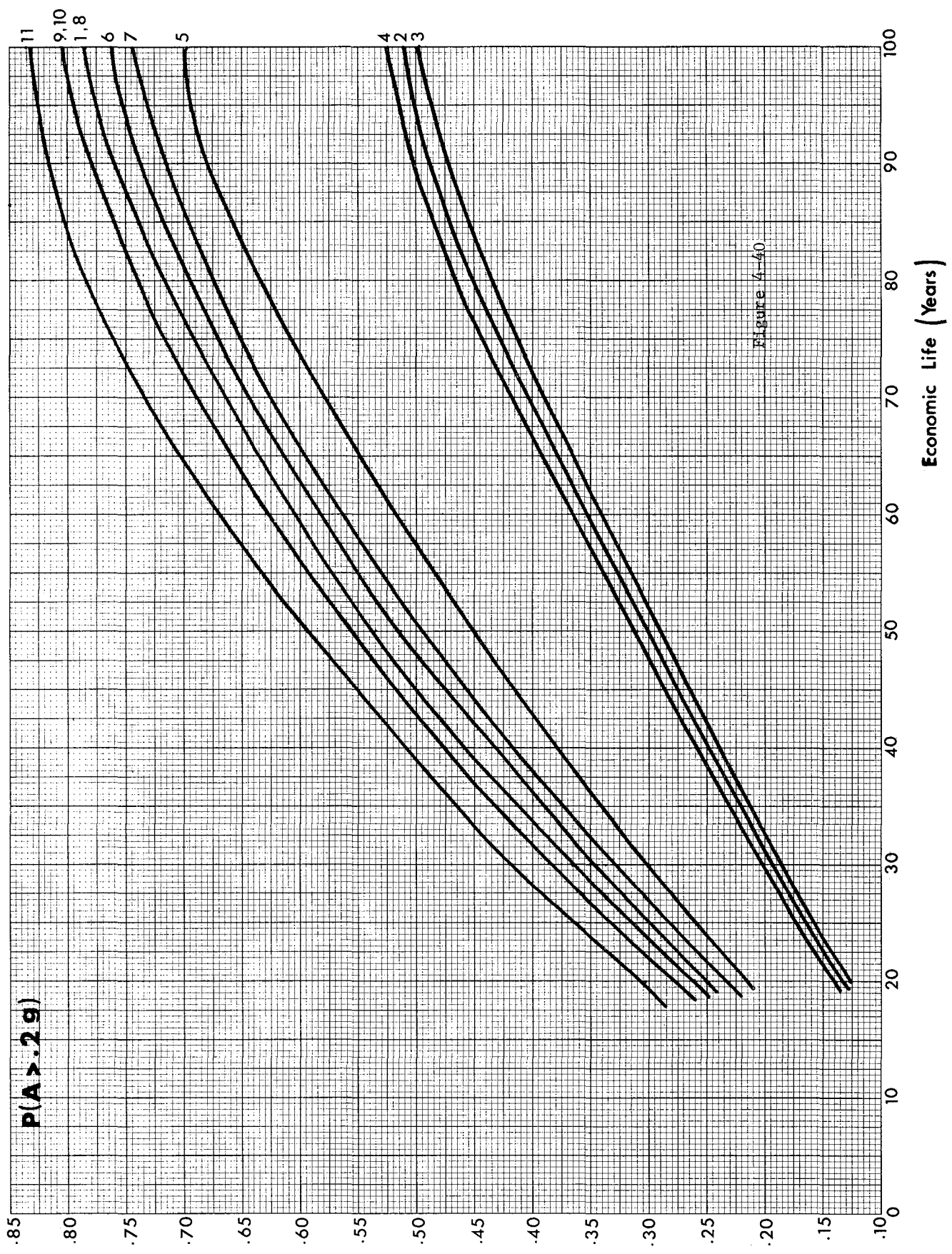


Figure 4-40

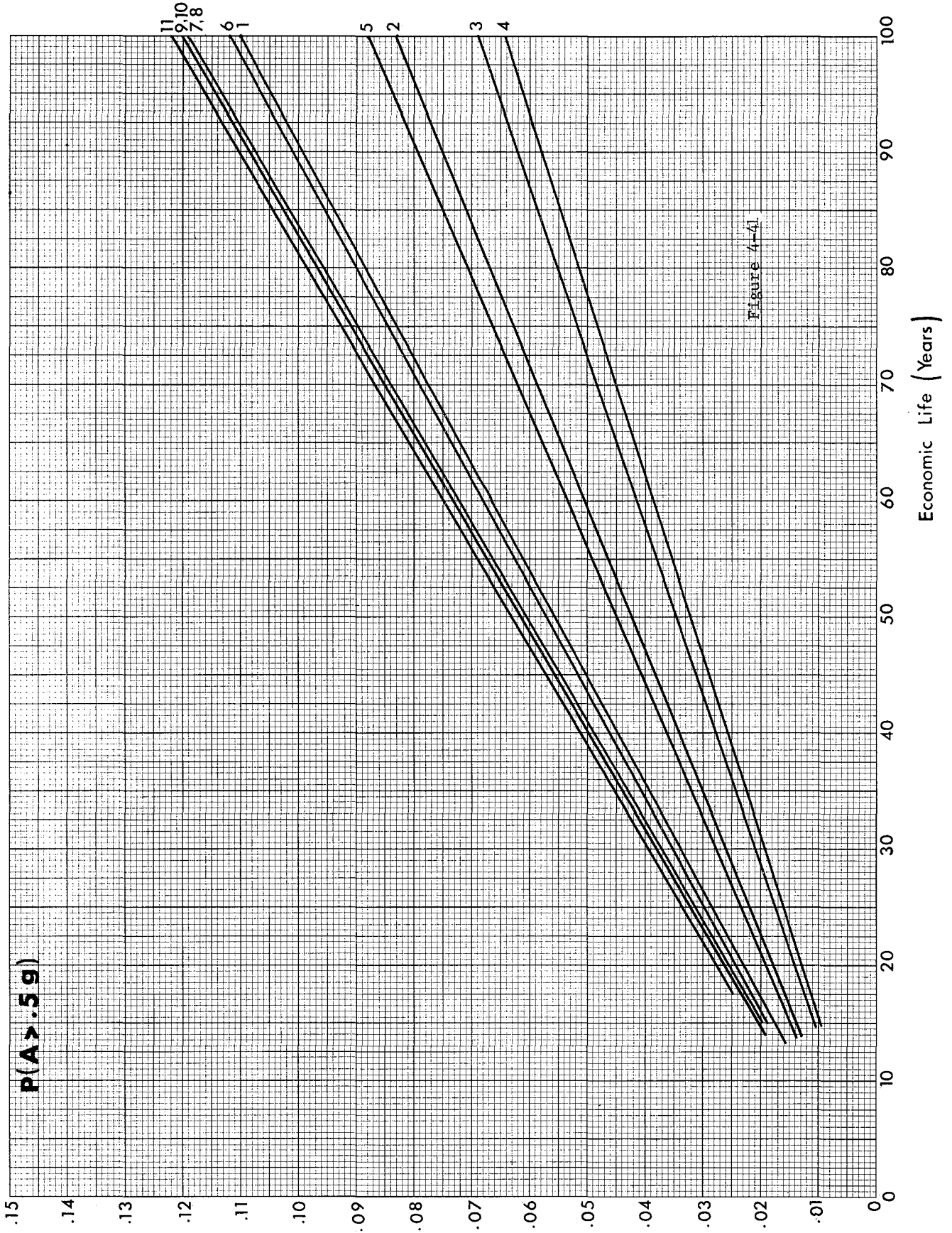


Figure 4-41

Chapter 5

DISCUSSION OF SEISMIC RISK FOR REACH C

In Chapter 4, a probabilistic description of the ground shaking hazard for the State Water Project, Reach C was presented in various formats. These formats were:

- 1) Iso-acceleration maps for the Reach C.
- 2) Cumulative Distribution Functions for the eleven sites within Reach C.
- 3) Acceleration Zone Graphs.
- 4) Peak Ground Acceleration profiles.

Using one of the above formats, one could ascertain the seismic ground shaking hazard. To estimate the probable risk due to the probable hazards described in Chapter 4, one has to determine the types of facilities, their construction and design characteristics and the consequences of failures of those facilities. Thus, the first step would be to look at the seismic design criteria used for facilities such as pumping and power plants, operations and maintenance centers, switching yards, etc. No detailed study of the dam design, pipeline design or the aquaduct design is made for the current report. The description of the type of structures and the earthquake design criteria used for the SWP facilities is taken from reference .

Recommendations for the design of major power and pumping plants were as follows:

1. The San Andreas and San Jacinto faults were recognized as the most probable sources of damaging earthquakes.
2. It was assumed that large earthquakes would cause ground shaking that would in the vicinity of the fault, have a maximum horizontal acceleration of 0.50g and a maximum vertical acceleration of 0.33g, with a duration of strong shaking of 60 seconds.
3. Rigid structures with a natural period of vibration approaching zero would be subjected, independent of damping, to an acceleration equal to maximum ground acceleration. Power and pumping plant substructures having a damping of more than 3% of critical and a natural period of less than 0.15 seconds fall in this category and therefore would be subjected to a maximum uniform horizontal acceleration of 0.5g and a maximum uniform vertical acceleration of 0.33g, within the distance of approximately 12 miles from the two faults mentioned above.
4. Structures with a natural period of vibration exceeding 0.15 seconds may be subjected to acceleration exceeding maximum ground acceleration. Acceleration and velocity response spectra for the 1933 El Centro Earthquake were used to obtain spectral acceleration response for structures with natural period above 0.15 secs. (See Figure 5-1).

(Taken from Ref. 39)

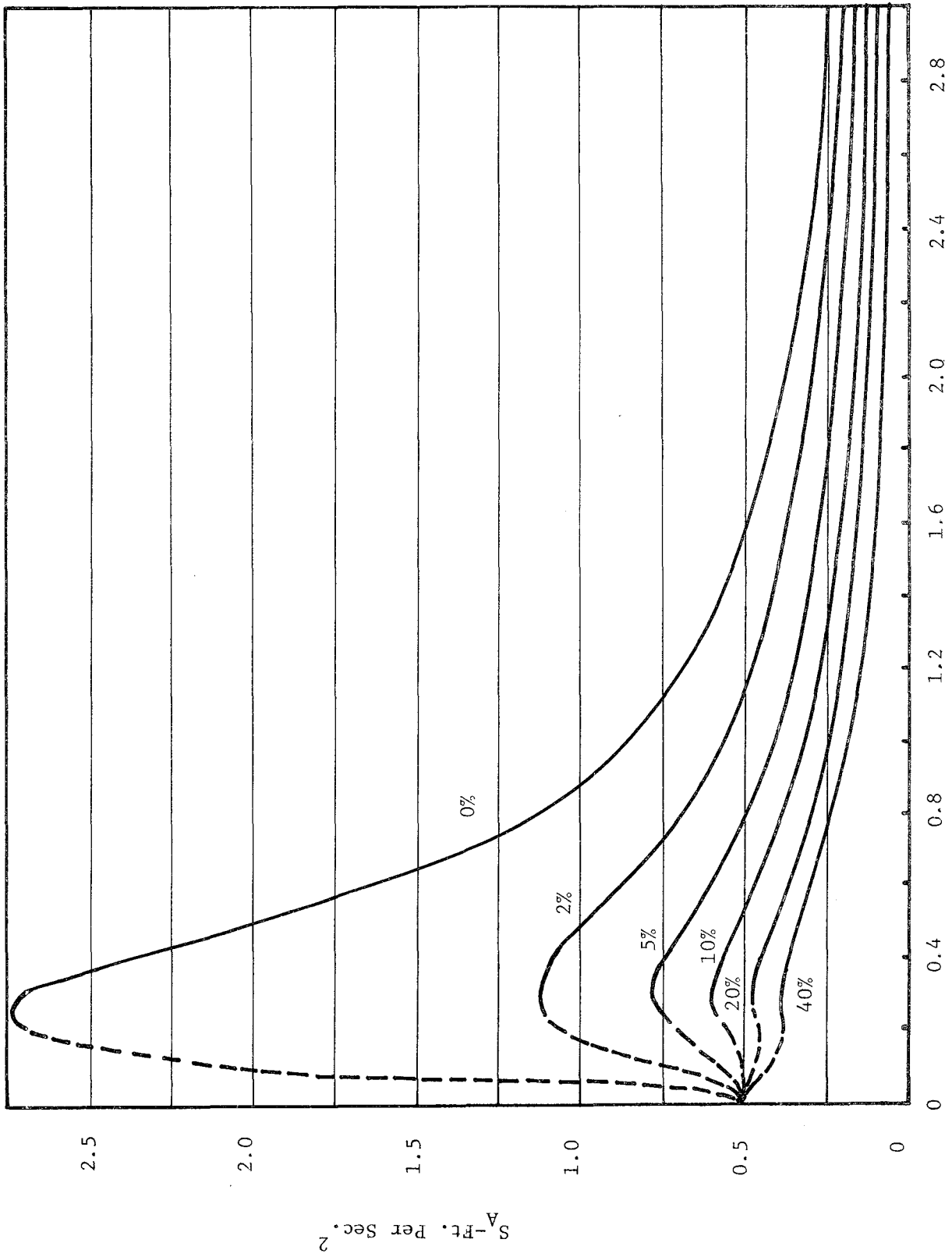


Fig. 5-1. Average acceleration spectra drawn to a normalized scale.

5. It was assumed that ground motion would be of uniform intensity (0.5g) over a distance of approximately 12 miles on each side of the fault. For points further than 12 miles from the fault, ground motion for a period less than 4 seconds were assumed to alternate according to Figure 5-2. For periods greater than 4 seconds the intensity of ground shaking was considered to be uniform.
6. For sites founded on sound rock, the intensity of ground shaking could be reduced, but each site should be considered a special case and each reduction made with caution.
7. For the design earthquake, ground motion would govern the short period design at sites within 12 miles of the San Andreas and San Jacinto faults. However at greater distances from these faults, ground shaking from a close small earthquake might be potentially more damaging than a distant large earthquake.

From the above seven recommendations, it can be seen that all the power plant and pumping plant substructures and superstructures were designed for a peak ground acceleration of 0.50g. It is also known that the switchyard equipment was designed for a peak ground acceleration of 0.20g.

What can be inferred from this knowledge? There are two pieces of information available. The first being the probability of exceeding 0.5g peak ground acceleration in various time spans along the Reach C. The second is that the designs of most of the facilities is based on

ATTENUATION FACTOR
for
GROUND ACCELERATION

$$n = \left(1 + \frac{1}{2.5T}\right)$$

$$\left(\frac{1.25}{1 + \frac{y}{y_0}}\right)^n$$

$$n = \left(T + \frac{1}{2.5T}\right)$$

T = Period of component
in seconds.

12 < y = distance from fault.

y₀ = 48 miles

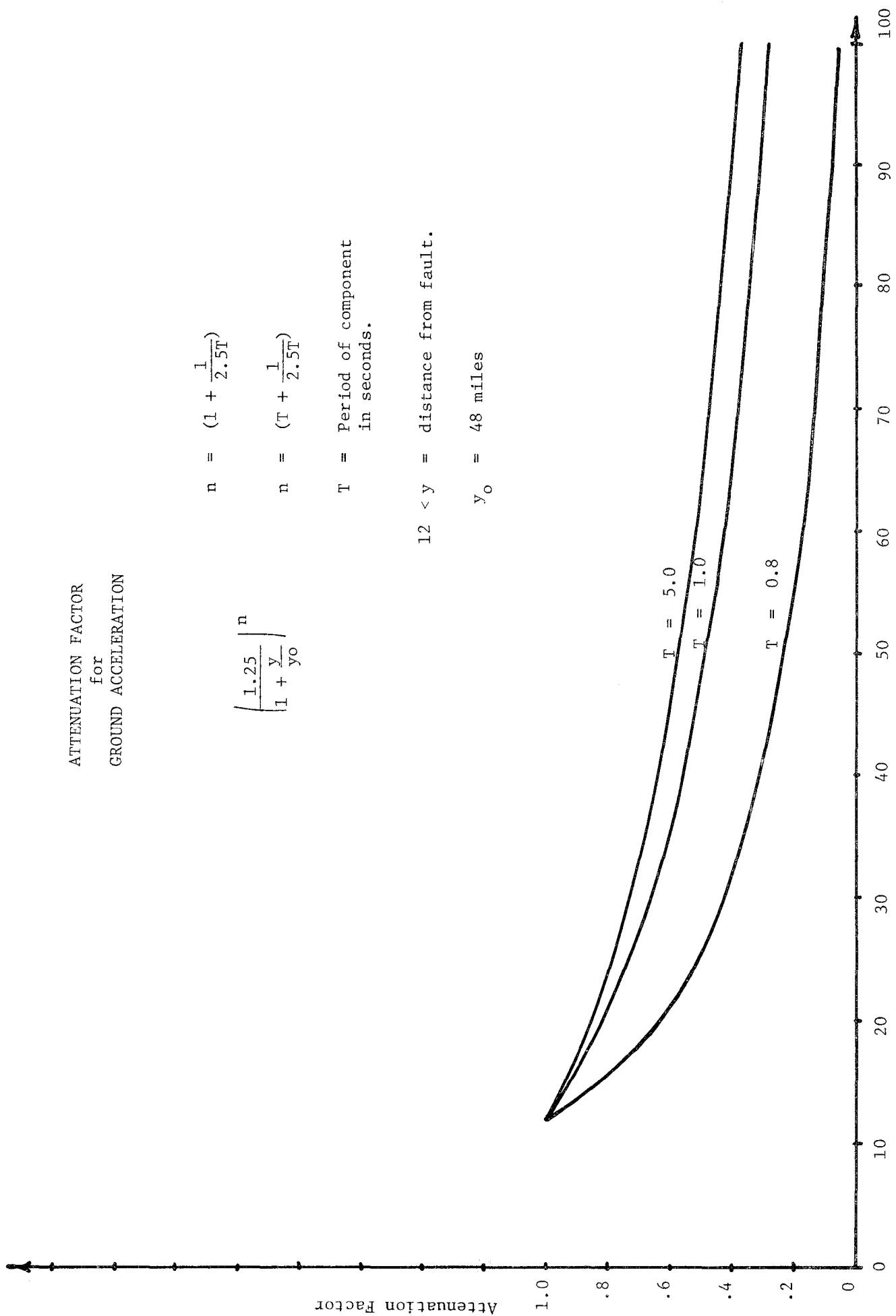


Figure 5-2
y = Perpendicular Distance from Fault, in Miles

(Taken from Ref. 39)

0.5g peak ground acceleration.

Assuming that the design details and workmanship were of good quality and that the probability of the resistance falling below the design level is small, one can assume that the damage potential to the structures below 0.5g peak ground acceleration would be negligible. The damage potential can be hypothesized as shown in Figure 5-3. Thus, it can be seen that conservatively, the risk of damage or condemnation to any power plant or pumping plant can be evaluated in terms of the probability of the peak ground acceleration exceeding 0.5g. Since this level of acceleration has a minimum return period of approximately 800 years, it can be seen that the risk of damage to power or pumping plants and hence water delivery interruption during the next fifty years is very small. In fact, this probability is only about six percent in 50 years and about 12 percent in 100 years. This is a very small risk and hence should not be of great concern.

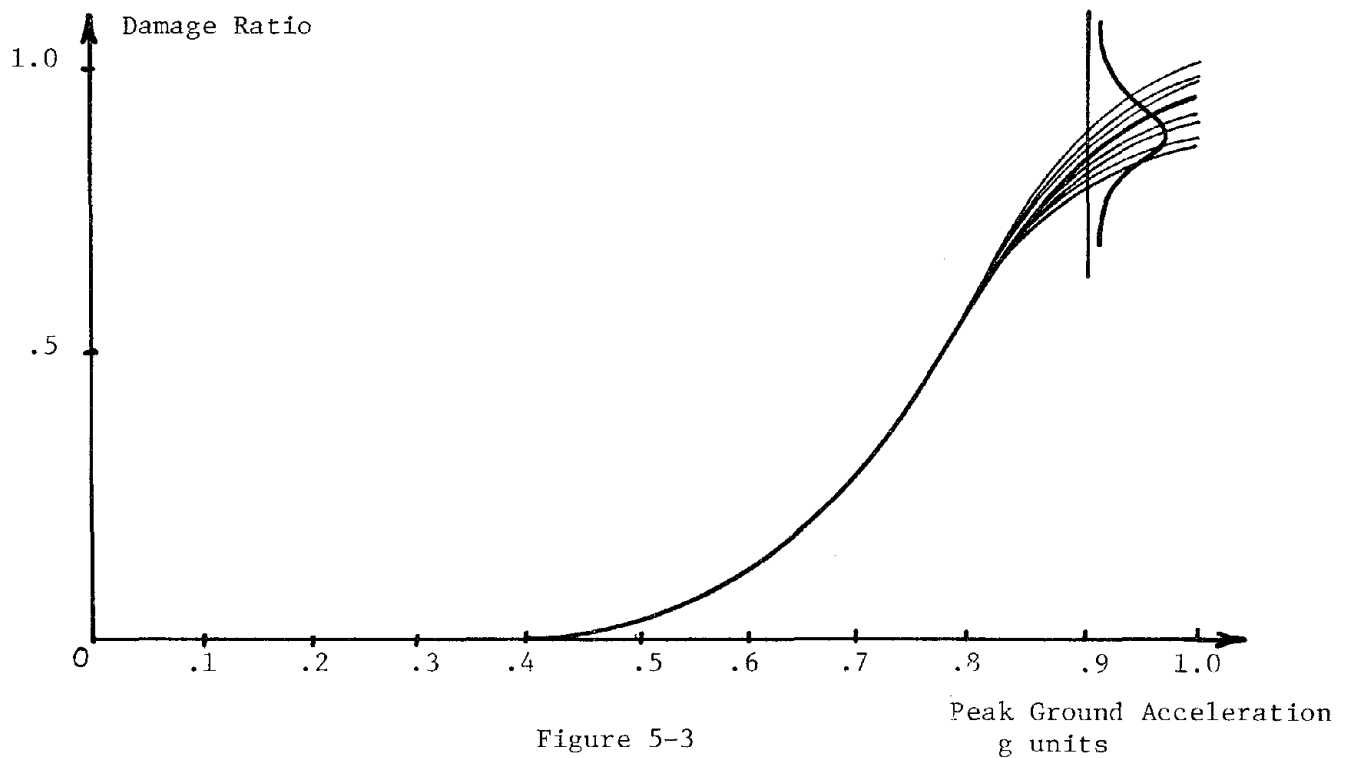


Figure 5-3

If one considers the design level of the switchyards, which are very essential for functioning of the pumping and power plants, the conclusion is quite different. From Table 4-5 or Figure 4-41, one can see that the probability of exceeding 0.2g peak ground acceleration during 20, 30, 50 or 100 years is very substantial. In fact for 50 and 100 years it can be said that for all the sites, we can be reasonably sure that 0.2g peak ground acceleration will be exceeded. This implies that for the switchyard equipment, the risk of damage is high.

Figure 5-4 shows the design levels of the pumping and power plant structures as well as the switching yard equipment structures.

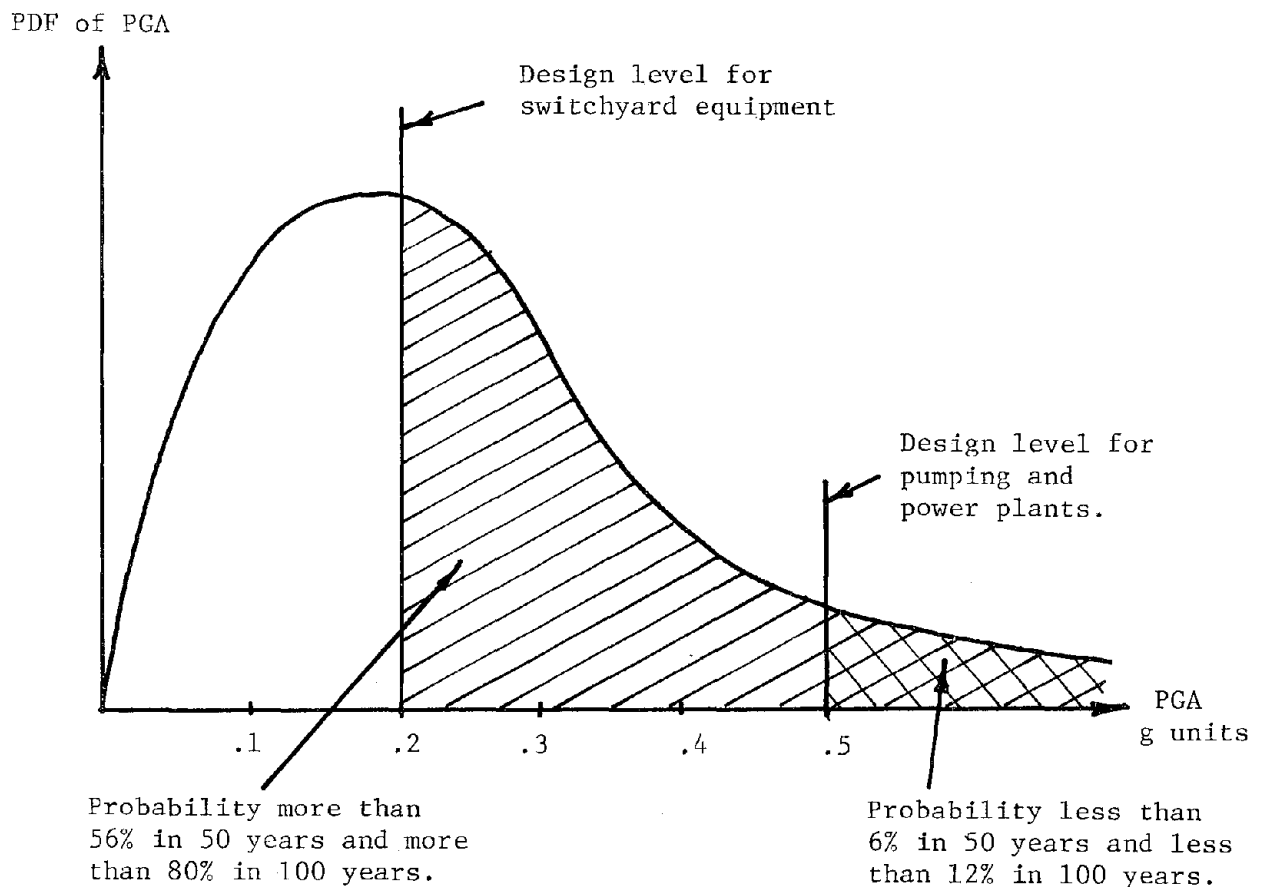


Figure 5-4

It can be seen that the probability of exceeding the design levels (and hence risk) is high for switchyard equipment and low for power and pumping plant structures.

In decreasing order of damage risk, the various sites for 50 years and 100 years economic life are as follows:

Table 5-1

Site Name	"Risk" in percentage	
	50 Years	100 Years
Perris Dam (site 11)	59	83
Santa Ana Pipeline (sites 9 and 10)	56	80
Tehachapi Afterbay (site 1)	53	78
Devil Canyon (site 8)	52	77
San Bernardino Tunnel (site 6)	51	76
San Bernardino Tunnel (site 7)	49	74
Cedar Springs Dam (site 5)	45	70
Aqueduct (site 4)	31	52
Pearblossom (site 2)	30	51
Aqueduct (site 3)	29	50

As can be seen from the above table, the damage risk to switchyard equipment south of the Devil Canyon Power Plant is larger than the damage risk north of the plant. One decision alternative would be to provide

a maintenance center in the region where the risk of damage is the greatest. In any case, some modifications should be initiated to increase the seismic resistance of these equipment beyond the current 0.20g level.

Another method of determining the risk to various facilities and the aqueduct is to develop the appropriate design spectra, based on the available knowledge on peak ground accelerations, acceptable risk and the type facilities at various sites. Based on the dynamic characteristics of the structures under consideration and the design spectra developed, one could obtain the performance characteristics of various facilities. This approach of determining the damage risk level is not followed in this report. However, the above methodology is presented in a recent report published by the John A. Blume Earthquake Engineering Center. See Reference 39. It is felt that for the current study, evaluation of risk, based on the information of facility design level and the seismic hazard is rational, realistic and sufficient.



Chapter 6

SUMMARY, CONCLUSIONS AND RECOMMENDATIONS

Seismic ground shaking hazard information is presented in this report for the State Water Project, Reach C. In particular the hazard information is presented in the following format:

- Iso-acceleration maps for time periods of 20, 30 and 50 years having a 10 percent chance of exceedance. This corresponds to return periods of 190 years, 285 years and 475 years respectively.
- The cumulative distribution function corresponding to each of the eleven sites. The time periods considered are 20 years and 50 years. For a given site, these graphs permit the evacuation of the probability of exceeding any level of PGA for a 20 or 50 year time period.
- Acceleration zone graphs for the eleven sites shown on Chart 1. These graphs can be used to obtain the level of PGA corresponding to any selected value of a return period for a given site.
- The peak ground acceleration profile along the SWP Reach C. This form of hazard information can be used to determine the locations corresponding to the highest or the lowest seismic hazard.

- Tables are given which provide the probability of exceeding 0.2g and 0.5g during the next 20 years and 50 years for various key locations along the aquaduct.

With the use of the hazard information developed in this study, an evaluation of seismic risk for the pumping and power plants and the switchyard facilities was made.

With respect to the pumping and power plants, the design load level employed for the substructures and superstructures corresponded to a horizontal peak ground acceleration of 0.5g. The hazard or probability of exceeding this design level during the next 50 years is very small (of the order of 5 percent).

However, for the switchyard, the design load level was 0.2g and the probability of exceeding this value during the next 50 years is large (of the orders of 30 to 60 percent). For a 100 year period it is almost certain that this design level would be exceeded.

The highest ground shaking hazard exists in the region of the Reach C which is south of the Devil Canyon Power Plant; and within this region the area around Ferris Dam has the greatest seismic hazard.

From the above findings, observations, and conclusions, the following recommendations can be made:

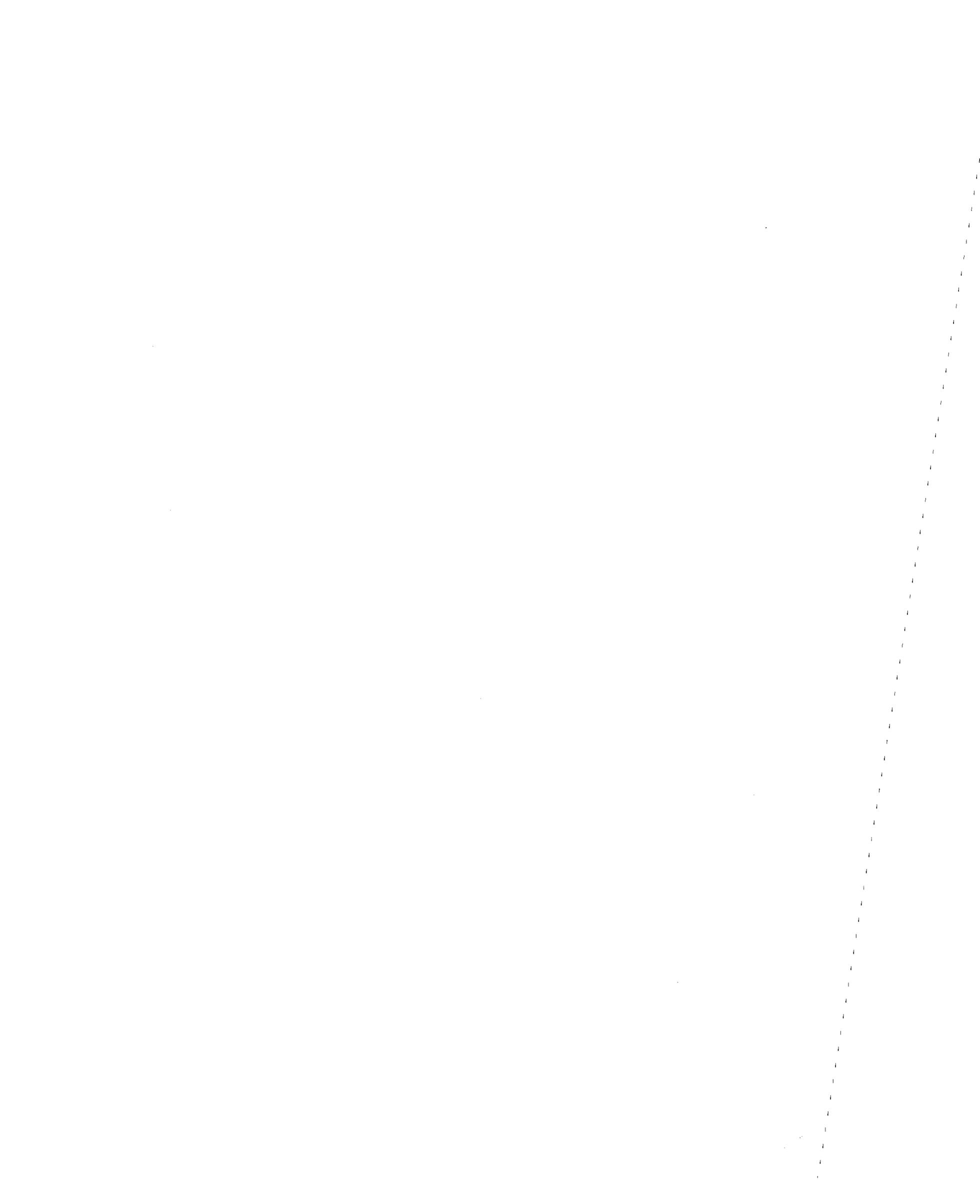
- The risk of damage or destruction to the pumping and power plant substructures and superstructures is minimal during the next 50 to 100 years, and therefore

no action is required. However, for the mechanical and electrical equipment within these plants it is recommended that a thorough survey be made to evaluate their ability to resist seismic loads.

- All switchyard equipment should be modified so as to resist a minimum peak ground acceleration of 0.3g. This load level corresponds to a return period of approximately 200 years or more along the Reach C.
- Since the ground shaking hazard along the Santa Ana Valley pipeline is relatively high (in excess of 0.5g for a 1000 year return period), an investigation should be made to determine the advisability of providing a cut-off facility for this portion of the Reach C.
- Because of the large risk potential, a central operations and maintenance center with facilities and capabilities for dealing with earthquake induced damage should be set up for the region south of the Devil Canyon Power Plant.

This is the first of three reports on seismic hazard mapping for the State Water Project. The second report will deal with Reach B and will include the region from the South Portal of the Carley V. Porter Tunnel to the Castaic Dam Lagoon.

It is hoped that the work for Reach A, which includes all the facilities between the Oroville Dam to the South Portal of the Carley V. Porter Tunnel, will be approved in the near future. In order to assess the complete reliability of the State Water Project it is essential that all three of these reports be completed.

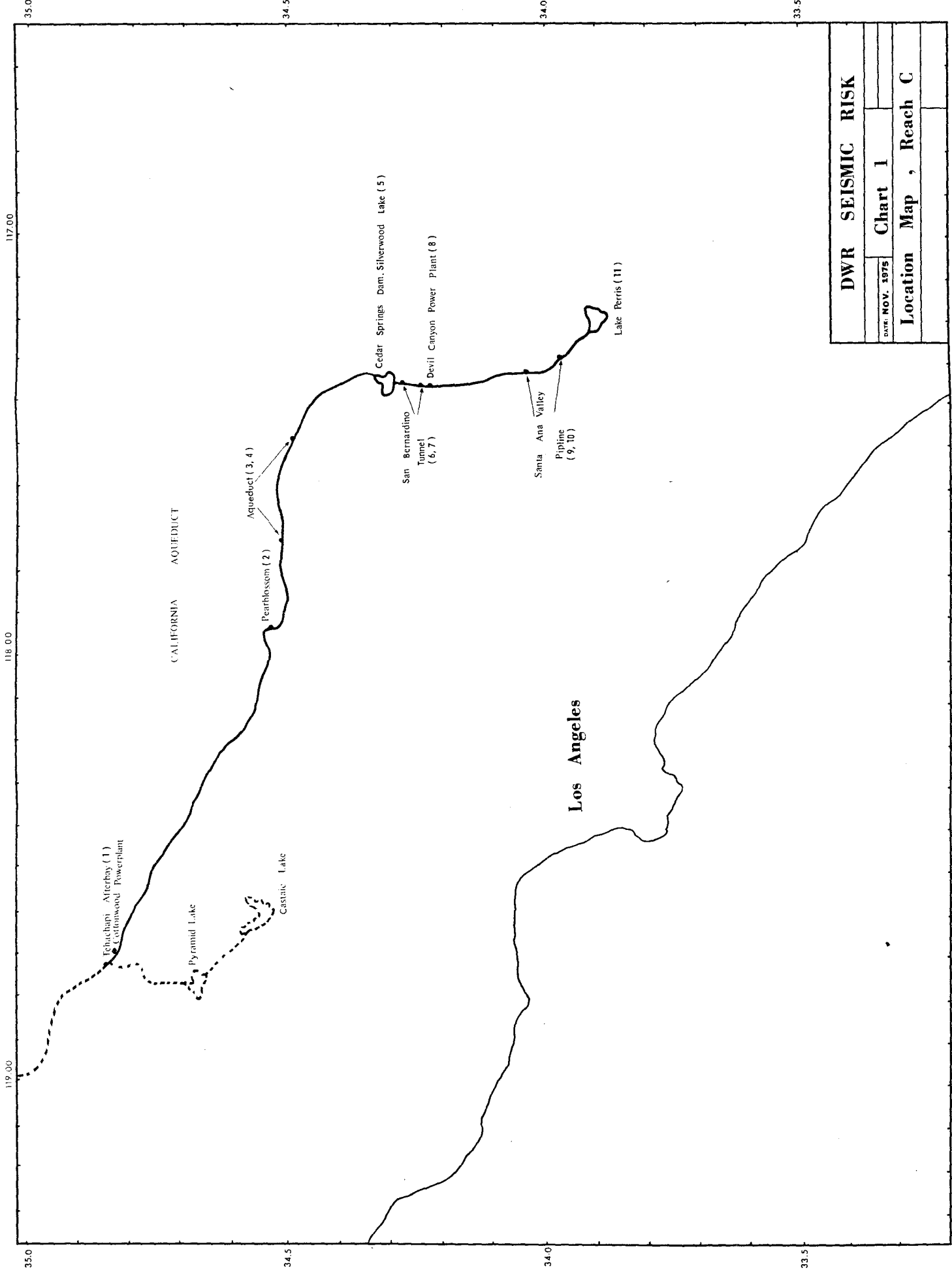


REFERENCES

1. Shah, H. C. et al, "A Study of Seismic Risk for Nicaragua, Part I" Technical Report No. 11, John A. Blume Earthquake Engineering Center, Stanford University, January, 1975.
2. Kiremidjian, A. S., Shah, H. C., "Seismic Hazard Mapping of California" Technical Report No. 21, John A. Blume Earthquake Engineering Center, Stanford University, November 1975.
3. Barosh, P. J., 1969, "Use of seismic intensity data to predict the effects of earthquakes and underground nuclear explosions in various geologic settings," USGS Bull 1279, 93 pp.
4. Boore, D. M., and Hill, D. P., 1973, "Wave Propagation Characteristics in the Vicinity of the San Andreas Fault"; Proceedings of the Conference on Tectonic Problems of the San Andreas Fault System, edited by Robert L. Kovach and Amos Nur, Geological Sciences, Vol XIII, School of Earth Sciences, Stanford University.
5. Borchardt, R. D., et al, 1972, "Ground Motion Predictions", in Microzonation Conference: International Conference on Microzonation for Safer Construction Research and Applications, Seattle, Washington, October 30-November 3, 1972, Proc, vol II, pg. 862. (not consulted).
6. "Earthquake Epicenter and Fault Map of California, south area", in "Crustal Strain and Fault Movement Investigation; Faults and Earthquake Epicenters in California", The Resources Agency of California, Department of Water Resources, Bull 116-2, January, 1964.
7. "Engineering Geology of Cedar Springs Dam and Reservoir", Office Report, DWR, July, 1968.
8. "Engineering Geology of Pearblossom Pumping Plant Discharge Line", Office Report, DWR, August, 1969.
9. "Engineering Geology, Perris Dam and Lake", Office Report, DWR, August, 1970.
10. "Final Geologic Report of Pearblossom Pumping Plant", Project Geology Report C-48, DWR, April, 1969.
11. "Final Geologic Report of Pearblossom Pumping Plant Site Development", Project Geology Report C-30, DWR, November, 1967.
12. "Geology and Construction Materials Data, Pearblossom Pumping Plant Site Development", Project Geology Report D-58, DWR, February, 1967.

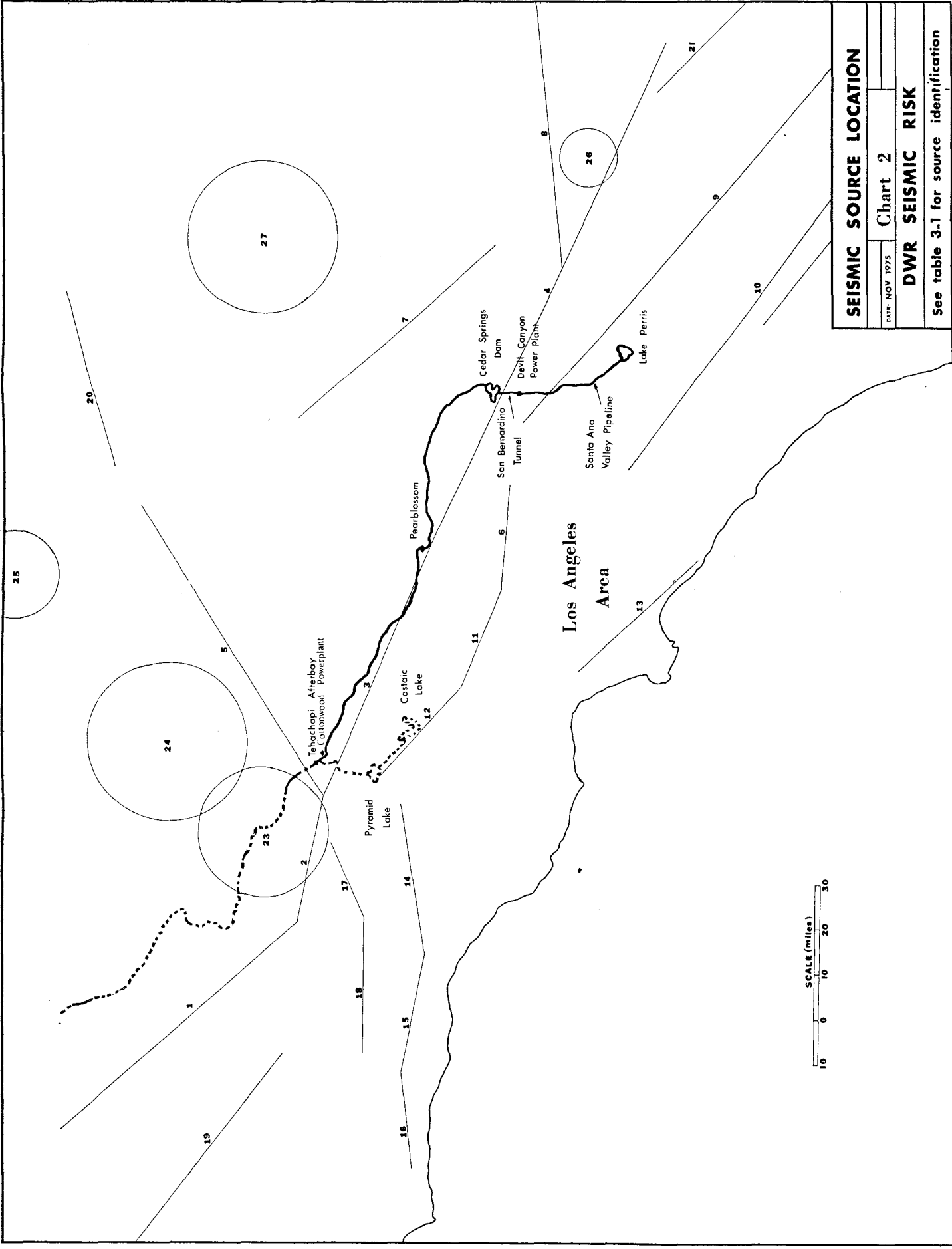
13. "Geology and Construction Materials Data, Perris Dam Inlet Works and Outlet Works", Project Geology Report D-127, DWR, February, 1971.
14. "Geologic Data, Devil Canyon Power Plant Penstock", Project Geology Report D-118, DWR, January, 1970.
15. "Geologic Data, Devil Canyon Power Plant", Project Geology Report D-108, DWR, April, 1969.
16. Newmark, N. M., et al, 1972, "Methods for determining site characteristics" in Microzonation Conference, vol I, pp 113-129. (not consulted).
17. Nichols, D. R., et al, 1972, "Geologic parameters for ground response maps", in Microzonation Conference, vol II, pp 860-861. (not consulted).
18. Page, R. A., et al, 1972, "Ground motion values for use in seismic design of the Trans-Alaska pipeline system", USGS Circular 672.
19. Rogers, T. H., 1967, "Geologic Map of California, San Bernardino Sheet", California Division of Mines and Geology, Scale 1:250,000.
20. Rogers, T. H., 1965, "Geologic Map of California, Santa Ana Sheet", Calif. Div. of Mines and Geology, Scale 1:250,000.
21. Schnabel, P. B., and Seed, H. B., 1973, "Accelerations in rock for earthquakes in the western United States", Bull. Seis. Soc. of Amer., vol 63, no. 2, pp 501-516, April, 1973.
22. Seed, H. B., and Schnabel, P. B., 1972, "Soil and geologic effects on site response during earthquakes", in Microzonation Conference, vol. I, pp 61-85, (not consulted).
23. "The California State Water Project in 1969", DWR Bull. 132-69, Appendix C, pp 28-29.
24. "The California State Water Project Summary: 1971", DWR Bull. 132-72, Appendix C, pp 14-15.
25. "The California State Water Project Summary: 1972", DWR Bull. 132-73, Appendix C, pp 26-27.
26. Webb, R. W., and Norris, R. M., 1969, Geology of California, "unpublished" textbook for University Extension Course, University of California, Berkeley.

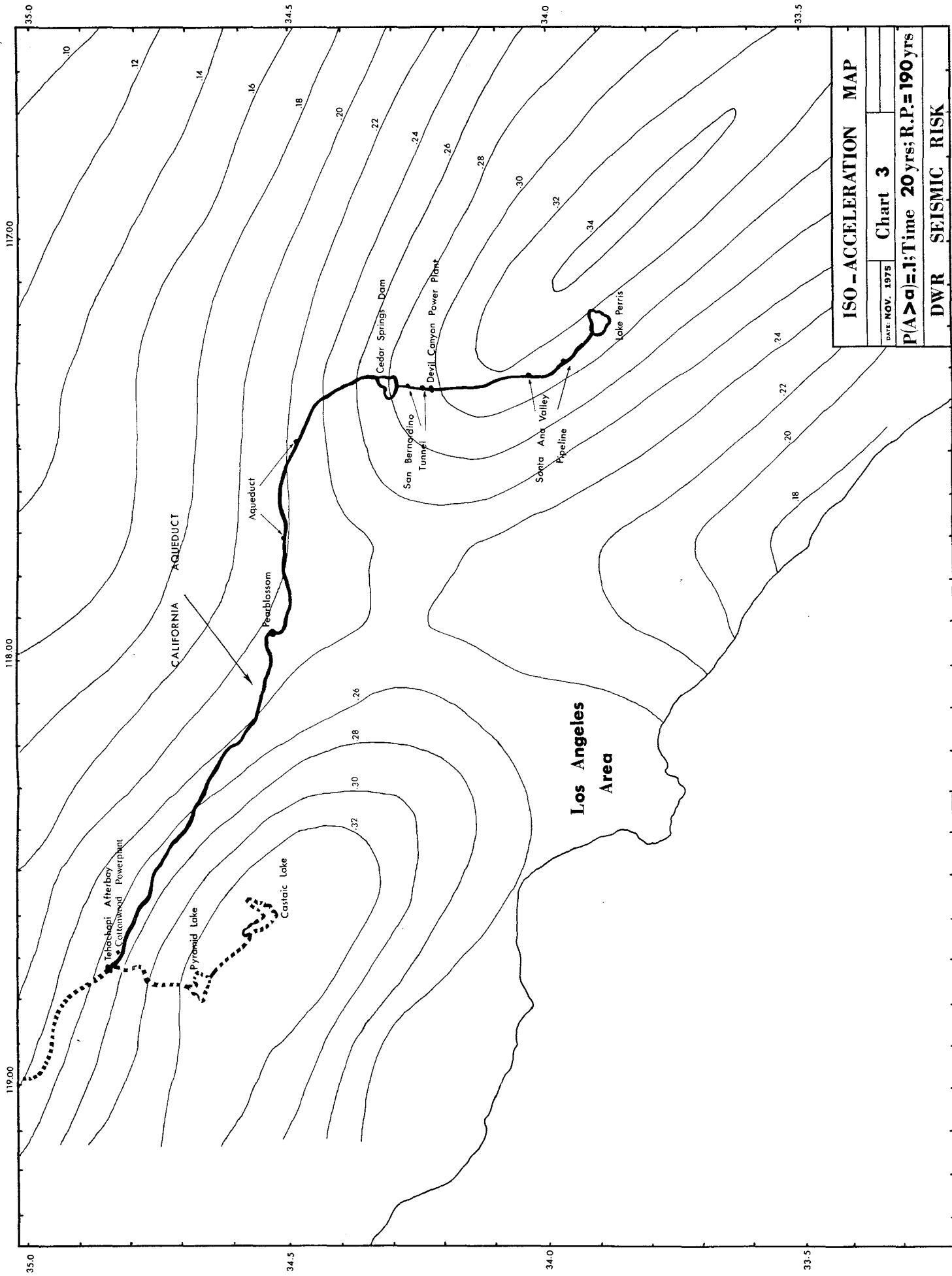
27. General Plan and Profile, Santa Ana Pipeline, 1969, DWR, # GP-S10-2, GP-S14-2, scale, approximately, 1:9600 (1 inch = 800 feet).
28. Jennings, Charles W., 1973, "State of California, Preliminary Fault and Geologic Map", California Division of Mines and Geology, Preliminary Report 13, scale, 1:750,000.
29. Office Report, "Engineering Geology of Devil Canyon Power Plant", April, 1969, DWR.
30. "Report of the Consulting Board for Earthquake Analysis," Hugo Benioff, Chairman, November 19, 1962, report to DWR.
31. "Santa Ana Pipeline, Hydraulic Profile", 1972, DWR, Horizontal scale: 1:24,000, vertical scale, 1:2400.
32. Wolfe, John E., 1968, "Earthquake Hazard Report, No. 21, Cedar Springs Dam Site", DWR report, unpublished.
33. Wolfe, John E., 1968, "Earthquake Hazard Report, No. 32, Devil Canyon Power Plant Area", DWR report, unpublished.
34. N. B. "Earthquake Epicenter and Fault Map of California, south area", referenced in December, 1974 report, is by Hill.
35. Greensfelder, R. W., "A Map of Maximum Expected Bedrock Acceleration from Earthquakes in California". California Division of Mines and Geology. 1973.
36. Donovan, N., "Earthquake Hazard for Buildings", Dames & Moore Engineering Bulletin 46, Dames & Moore, Los Angeles. 1974.
37. Richter, C., "Elementary Seismology", W. H. Freeman Press, San Francisco, 1958.
38. Shah, H. C., et al; "A Study of Seismic Risk for Nicaragua, Part II, Commentary." Technical Report No. 12A, John A. Blume Earthquake Engineering Center, Stanford University, April, 1976.
39. Bulletin No. 200. Nov. 1974. Vol. IV. "Power and Pumping Facilities" California State Water Project.



DWR SEISMIC RISK	
DATE: NOV. 1975	Chart 1
Location Map , Reach C	





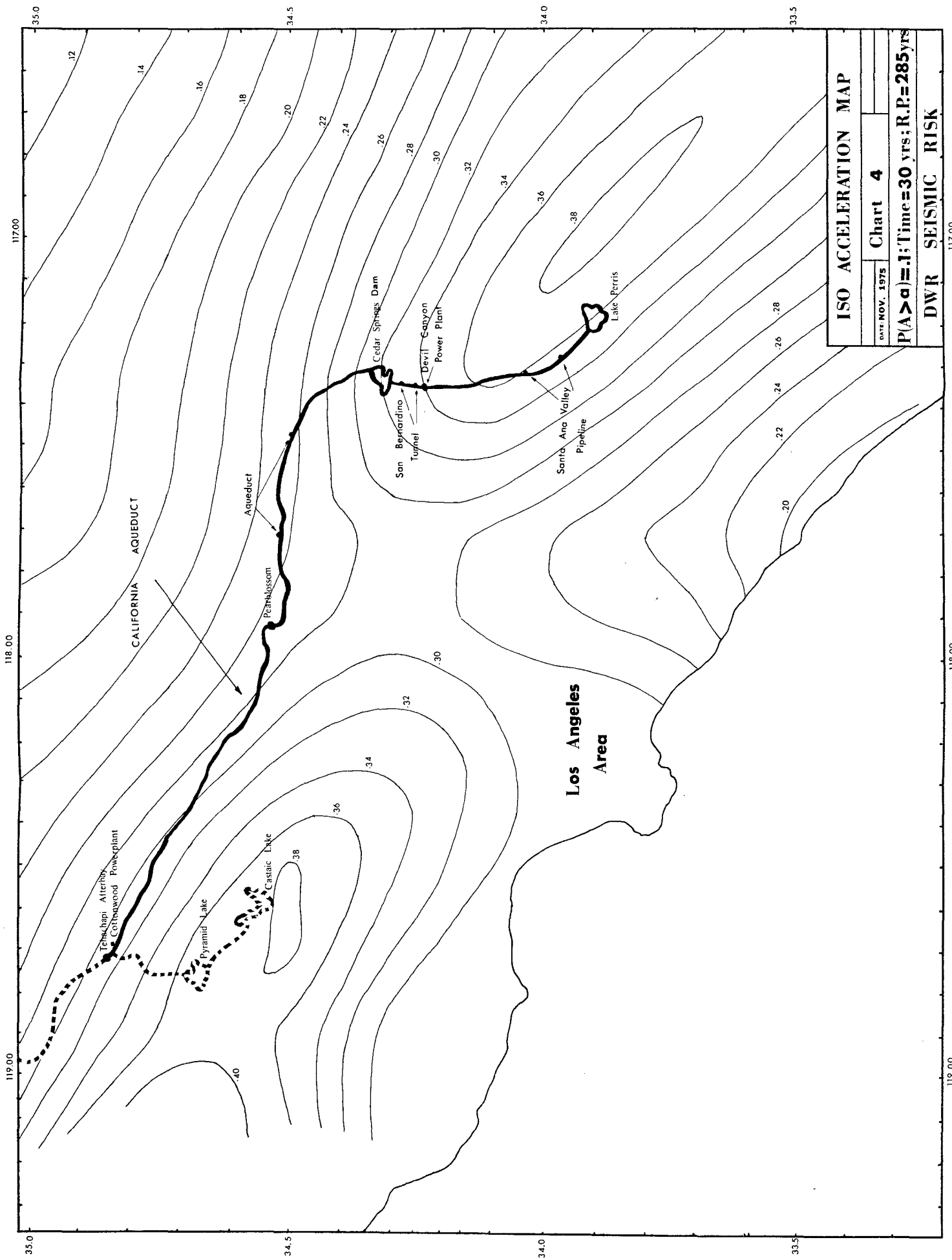


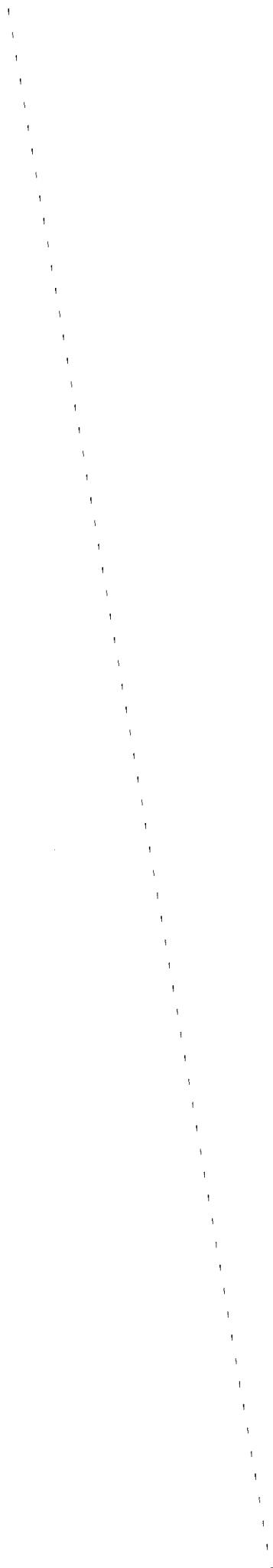
ISO - ACCELERATION MAP

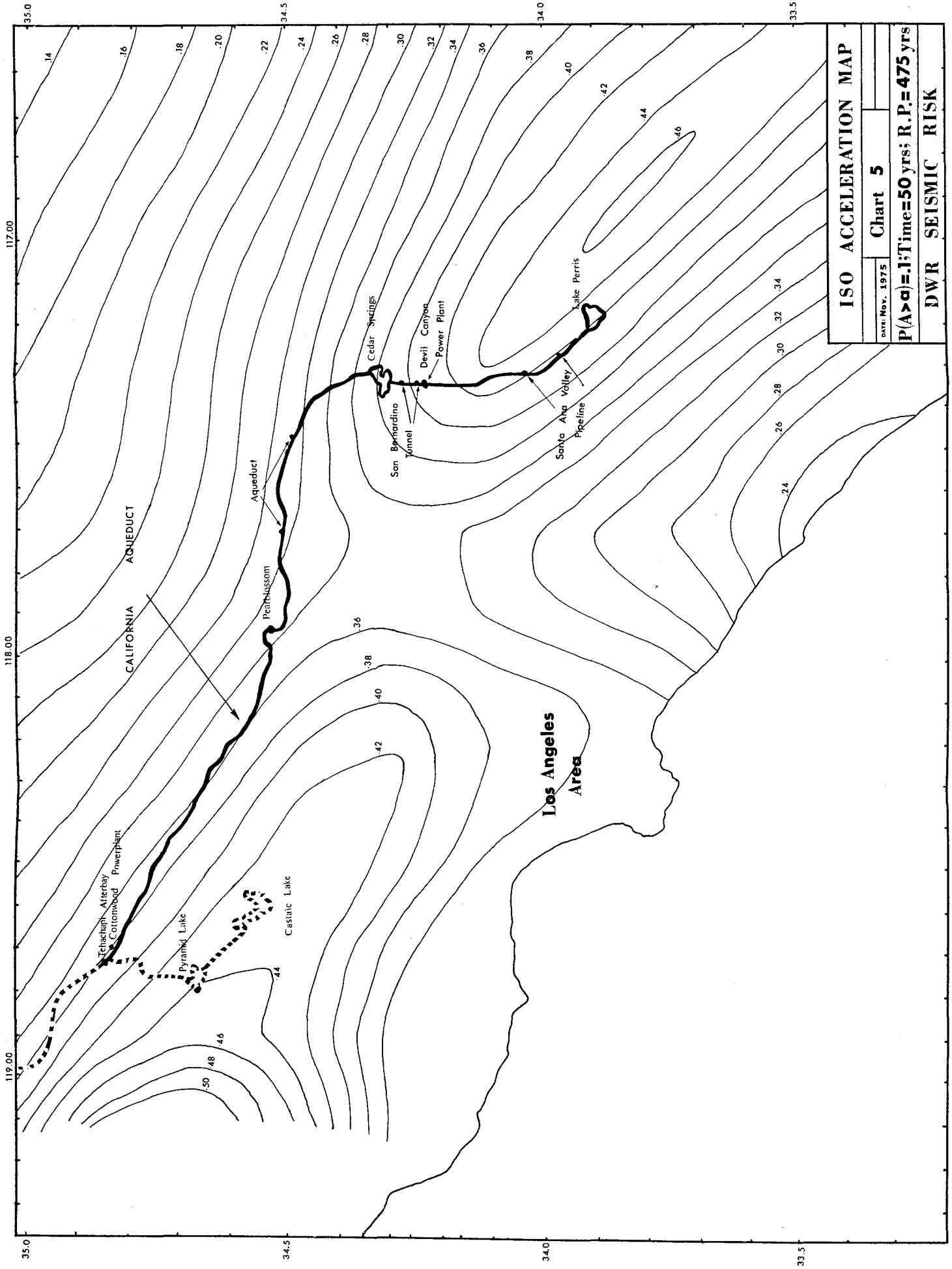
DATE NOV. 1975 **Chart 3**

P(A>a)=.1; Time 20 yrs; R.P.=190 yrs

DWR SEISMIC RISK







ISO ACCELERATION MAP	
DATE: Nov. 1975	Chart 5
P(A>α)=.1; Time=50 yrs; R.P.=475 yrs	
DWR SEISMIC RISK	

